

# Surface Geophysical Exploration of B, BX, and BY Tank Farms at the Hanford Site: Results of Background Characterization with Magnetics and Electromagnetics

Prepared by  
**D. Rucker**  
**M. Levitt**  
**B. Cabbage**  
hydroGEOPHYSICS, Inc.

**C. Henderson**  
Columbia Energy & Environmental Services, Inc.

Prepared for  
**CH2M HILL Hanford Group, Inc.**  
Richland, WA 99354  
U.S. Department of Energy Contract DE-AC27-99RL14047

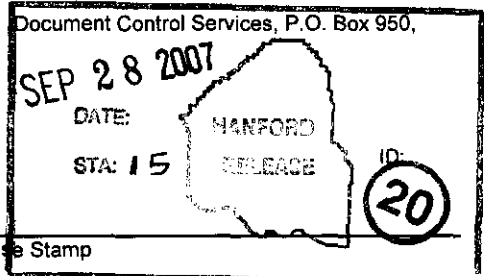
EDT/ECN: DRF UC:  
Cost Center: Charge Code:  
B&R Code: Total Pages: 76

Key Words: Waste Manatement Area B-BX-BY, 216-B trenches, 216-B cribs, 216-B tile field, electromagnetic indiction, magnetic gradiometry

Abstract: This report resents the results of the background characterization of the cribs, trenches, and tile fields within and around the B-BX-BY Waste Management Area.

TRADEMARK DISCLAIMER. Reference herein to any specific commercial product, process, or service by trade name, trademark, manufacturer, or otherwise, does not necessarily constitute or imply its endorsement, recommendation, or favoring by the United States Government or any agency thereof or its contractors or subcontractors.

Printed in the United States of America. To obtain copies of this document, contact: Mailstop H6-08, Richland WA 99352, Phone (509) 372-2420; Fax (509) 376-4989.



09/28/07 Janis Aardal  
Release Approval Date

Release Stamp

**Approved For Public Release**

## EXECUTIVE SUMMARY

This report documents the results of preliminary surface geophysical exploration activities performed between October and December 2006 at the B, BX, and BY tank farms (B Complex). The B Complex is located in the 200 East Area of the U.S. Department of Energy's Hanford Site in Washington State. The objective of the preliminary investigation was to collect background characterization information with magnetic gradiometry and electromagnetic induction to understand the spatial distribution of metallic objects that could potentially interfere with the results from high resolution resistivity survey.

Results of the background characterization show there are several areas located around the site with large metallic subsurface debris or metallic infrastructure.

Figure ES-1 shows the results of the vertical magnetic gradient in nanoTeslas/meter. Three main areas were covered for the survey, which included the western trenches, northern cribs and northeastern cribs, and tile field. The vertical magnetic gradient reveals some shallow ferrous materials primarily in the north, which are exhibited by the red and blue colors. Background is represented by yellow.

**Figure ES-1. Results of the Vertical Magnetic Gradient.**

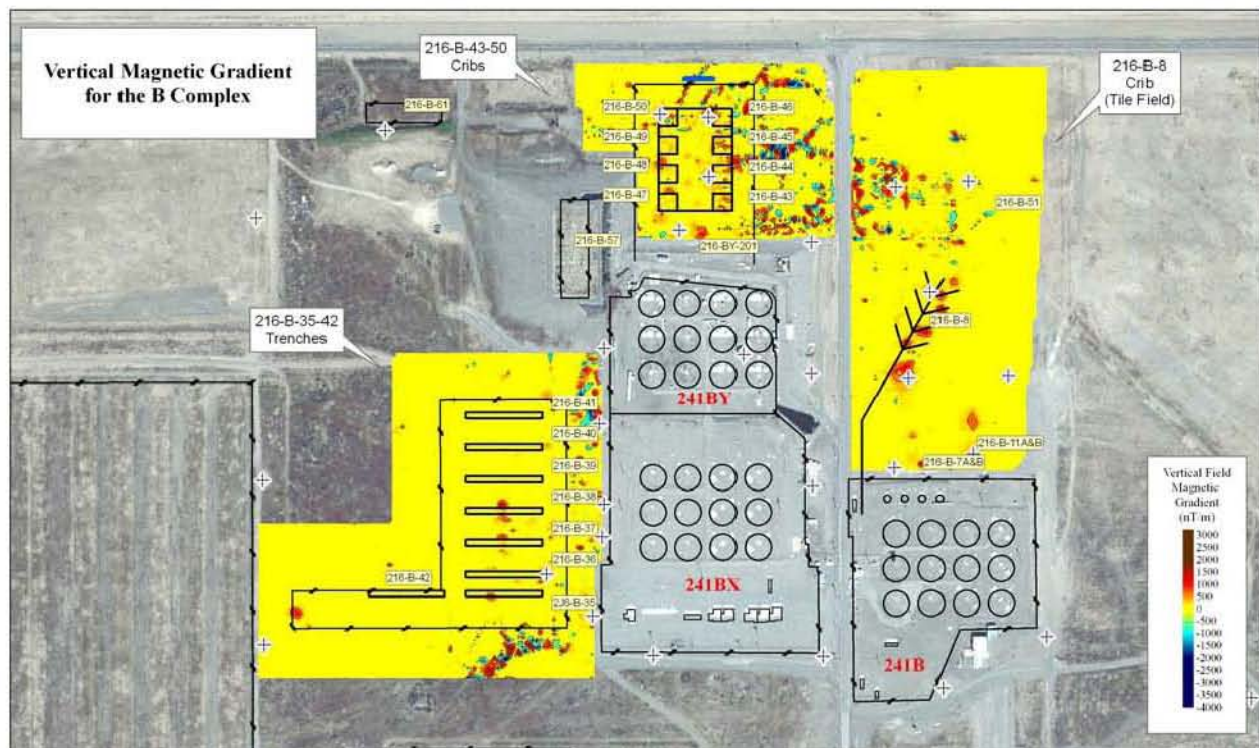
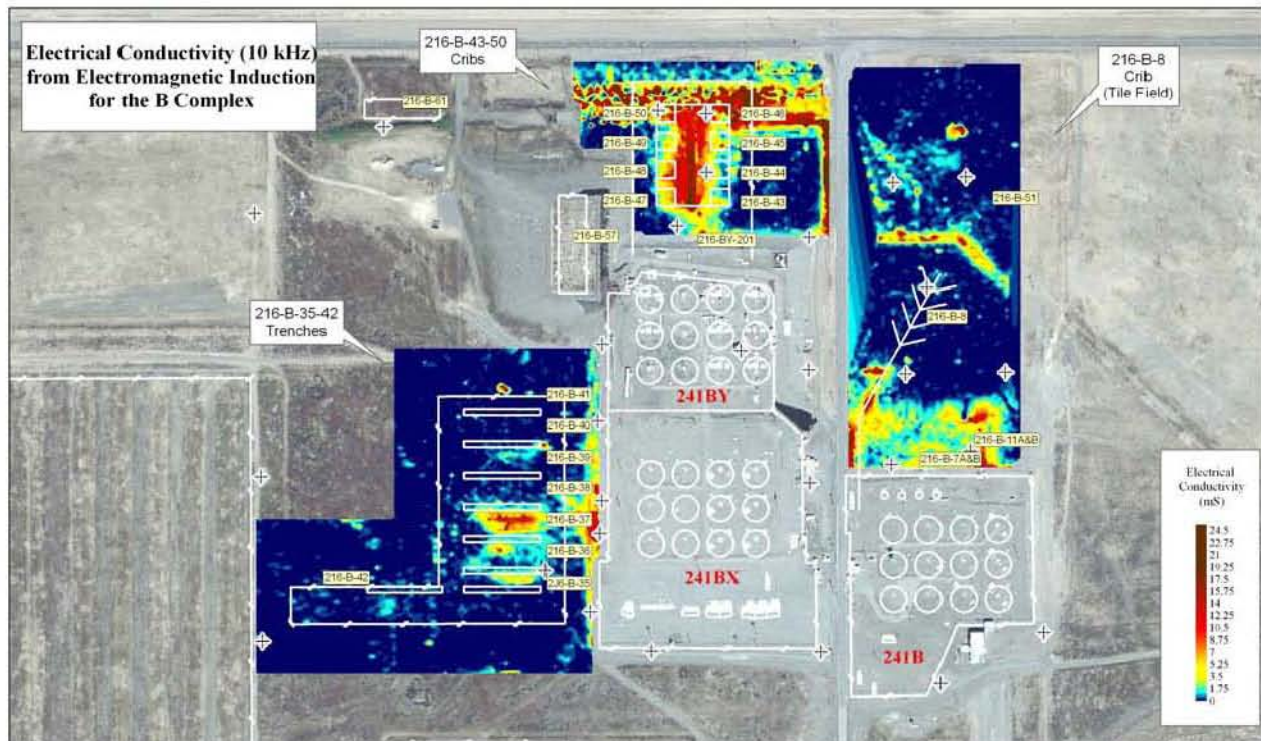


Figure ES-2 shows the results of the electrical conductivity collected from electromagnetic induction at 10 kHz. The color scale was developed to have background represented by blue, equivalent to electric conductivity less than 1 milliSiemen. The figure shows several high conductivity regions that could be indicative of subsurface metals, including stainless-steel pipes.

In the northern cribs, for example, there appears to be linear anomalies that could be interpreted as waste delivery pipes.

**Figure ES-2. Electrical Conductivity from the Electromagnetic Induction at 10 kHz.**



**TABLE OF CONTENTS**

1.0	INTRODUCTION .....	1
1.1	SCOPE.....	1
1.2	OBJECTIVES .....	1
1.3	REPORT LAYOUT .....	2
2.0	BACKGROUND .....	2
3.0	THEORY .....	5
3.1	MAGNETOMETRY .....	5
3.2	ELECTROMAGNETIC INDUCTION.....	7
4.0	METHODOLOGY .....	9
4.1	SURVEY AREA AND LOGISTICS .....	9
4.2	GEOPHYSICAL EQUIPMENT .....	11
4.2.1	Geophysical Operations Cart.....	11
4.2.2	Global Positioning Systems .....	11
4.2.3	Magnetometry .....	11
4.2.4	Electromagnetic Induction.....	11
4.3	PROCESSING .....	11
4.3.1	Downloading, Parsing, Quality Control – Onsite .....	11
4.3.2	Magnetometry Processing and Plotting. ....	13
4.3.3	Electromagnetic Processing and Plotting.....	16
5.0	ANALYSIS, RESULTS AND INTERPRETATION.....	16
5.1	MAGNETIC GRADIOMETRY .....	17
5.1.1	Total Magnetic Field.....	17
5.1.2	Vertical Magnetic Gradient.....	17
5.2	ELECTROMAGNETIC INDUCTION.....	19
5.2.1	In-Phase.....	19
5.2.2	Electrical Conductivity .....	22

6.0 CONCLUSIONS.....26  
7.0 REFERENCES .....27

**LIST OF APPENDICES**

A APPENDIX A..... A-i

**LIST OF FIGURES**

1. Location of B, BX, and BY Tank Farms .....3  
2. B-BX-BY Tank Farms with Characterization Activities, Surrounding  
Facilities, and Wells.....4  
3. Magnetic Anomalies for a Sphere at (A) Mid Latitude, (B) Equator, and  
(C) Near the North Pole .....6  
4. Depth Estimates for Magnetic Anomalies .....7  
5. Skin Depth Estimates for the GEM-2® at the Hanford Site.....8  
6. Geophysical Operations Cart Coverage.....10  
7. Geophysical Operations Cart Photo.....10  
8. Magnetic Base Station Data.....14  
9. Heading Error Associated with Magnetometer Readings for the Bottom  
Sensor.....15  
10. Heading Error Associated with Magnetometer Readings for the Top  
Sensor.....15  
11. Total Magnetic Field for the 241-B, BX, and BY Farms .....17  
12. Magnetic Anomaly Over a Pipe showing the Estimated Depth of the  
Target.....18  
13. Vertical Magnetic Gradient for the 241-B, BX, and BY Farms .....19

14.	In-Phase (5 kHz) from Electromagnetic Induction for the 241-B, BX, and BY Farm.....	20
15.	In-Phase (10 kHz) from Electromagnetic Induction for the 241-B, BX, and BY Farm.....	21
16.	In-Phase (20 kHz) from Electromagnetic Induction for the 241-B, BX, and BY Farm.....	22
17.	Electrical Conductivity (5 kHz) from Electromagnetic Induction for the 241-B, BX, and BY Farm .....	23
18.	Electrical Conductivity (10 kHz) from Electromagnetic Induction for the 241-B, BX, and BY Farm .....	24
19.	Electrical Conductivity (20 kHz) from Electromagnetic Induction for the 241-B, BX, and BY Farm .....	25
20.	Total Electrical Conductivity from Electromagnetic Induction for the 241-B, BX, and BY Farm .....	26

**LIST OF TABLES**

1.	Magnetic Data File Names and Locations of Coverage .....	12
2.	Electromagnetic Induction Data File Names and Locations of Coverage.....	13

## LIST OF TERMS

### Terms

Conductivity. The ability of a material to transmit or conduct an electric impulse; reciprocal of resistivity.

Inversion. Inversion, or inverse modeling, attempts to reconstruct subsurface features from a given set of geophysical measurements, and to do so in a manner that the model response fits the observations according to some measure of error.

Resistance. The opposition of a material to current passing through it; received voltage normalized by transmitted current.

### Abbreviations and Acronyms

B Complex	241-B, BX, and BY tank farms
EM	electromagnetic
G.O. Cart <sup>™</sup>	Geophysical Operations Cart <sup>™</sup>
GPS	Global-Positioning System
HRR <sup>™</sup>	High Resolution Resistivity <sup>™</sup>
MAG	magnetic gradiometry
WMA	waste management area

---

<sup>™</sup> G.O. Cart and Geophysical Operations Cart are trademarks of hydroGEOPHYSICS, Inc.

<sup>™</sup> HRR and High Resolution Resistivity are trademarks of hydroGEOPHYSICS, Inc.

## 1.0 INTRODUCTION

Beginning in November 2006 and ending in December 2006, a preliminary geophysical study was completed at the 241-B, BX, and BY tank farms (B Complex) at the U.S. Department of Energy's Hanford Site in eastern Washington State. Columbia Energy & Environmental Services, Inc. of Richland, Washington, and hydroGEOPHYSICS, Inc. of Tucson, Arizona, with support from CH2M HILL Hanford Group, Inc., conducted background geophysical surveys of the B Complex located in the 200 East Area of the Hanford Site. The geophysical surveys consisted of electromagnetic (EM) induction and magnetic gradiometry around the periphery of the tank farms.

This report is a companion document to the *Surface Geophysical Exploration of the B, BX, and BY Tank Farms at the Hanford Site* (RPP-34690). The purpose of this report is to document the findings of the EM and magnetic gradiometry survey of the areas surrounding the B, BX, and BY tank farms in an effort to identify the presence of buried infrastructure to aid in the interpretation of resistivity results. This information is intended to supplement existing information on buried infrastructure.

### 1.1 SCOPE

The scope of the geophysical surveying included data acquisition, processing, and visualization of EM induction and magnetic gradiometry from areas outside the tank farm fence lines in the B-BX-BY waste management area (WMA) to map buried subsurface infrastructure. Potential targets for the survey include buried pipelines, electrical conduits, and other metallic debris that may interfere with direct-current electrical resistivity imaging. The scope of this survey does not include the mapping of electrolytic targets that are a result of increased salt or moisture content from the direct disposal of liquid waste to the vadose zone.

The data acquisition was conducted by attaching the EM induction and magnetic gradiometry instruments to a Geophysical Operations Cart (G.O. Cart), which included an all-terrain vehicle and a fiberglass-towed trailer. The G.O. Cart was outfitted with a Global-Positioning System (GPS) for geo-referencing of data and to allow tracking of its location while traversing the area. Data coverage included a total of 56.7 line-kilometers over three main areas: the western trenches (216-B-37 through 216-B-42), northern cribs (216-B-43 through 216-B-50), and northeastern cribs and tile field (216-B-7 and 216-B-8). Total aerial coverage of the G.O. Cart survey was approximately 37 acres.

### 1.2 OBJECTIVES

The main objective for this geophysical investigation was to map the subsurface outside the tank farms with regards to the extent of metallic infrastructure and debris. The subsurface metal may interfere with High Resolution Resistivity (HRR) measurements, which is being conducted as the second phase of the surface geophysical exploration scope for the B-BX-BY WMA geophysical

characterization. The results of the HRR survey as well as in-farm mapping with ground penetrating radar are presented in subsequent reports RPP-34690 and *Surface Geophysical Exploration of B, BX, and BY Tank Farms at the Hanford Site: Results of Background Characterization with Ground Penetrating Radar* (RPP-34674).

### 1.3 REPORT LAYOUT

This report is divided into seven main sections.

- **Section 1.0, Introduction** – describes the scope and objectives of the investigation.
- **Section 2.0, Background** – describes the setting of the B tank farm and information regarding the metallic infrastructure in and around the tank farm.
- **Section 3.0, Theory** – discusses some of the theory behind EM induction and magnetic gradiometry.
- **Section 4.0, Methodology** – discusses the methodology and logistics of conducting the geophysical survey at the B Complex.
- **Section 5.0, Analysis, Results and Interpretation** – presents the results from the surveying effort.
- **Section 6.0, Conclusions** – provides conclusions drawn from the results, interpretations, and subsequent assessment of results.
- **Section 7.0, References** – lists reference documents cited in the report.

## 2.0 BACKGROUND

The B, BX, and BY tank farms comprise WMA B-BX-BY. These tank farms are located in the northern portion of the 200 East Area near B Plant (Figure 1).

The B tank farm comprises the following:

- 12 single-shell tanks each with 530,000-gallon (2,006,050-liter) capacity
- 4 single-shell tanks each with 55,000-gallon (208,175-liter) capacity
- Waste transfer lines
- Leak detection systems
- Tank ancillary equipment.

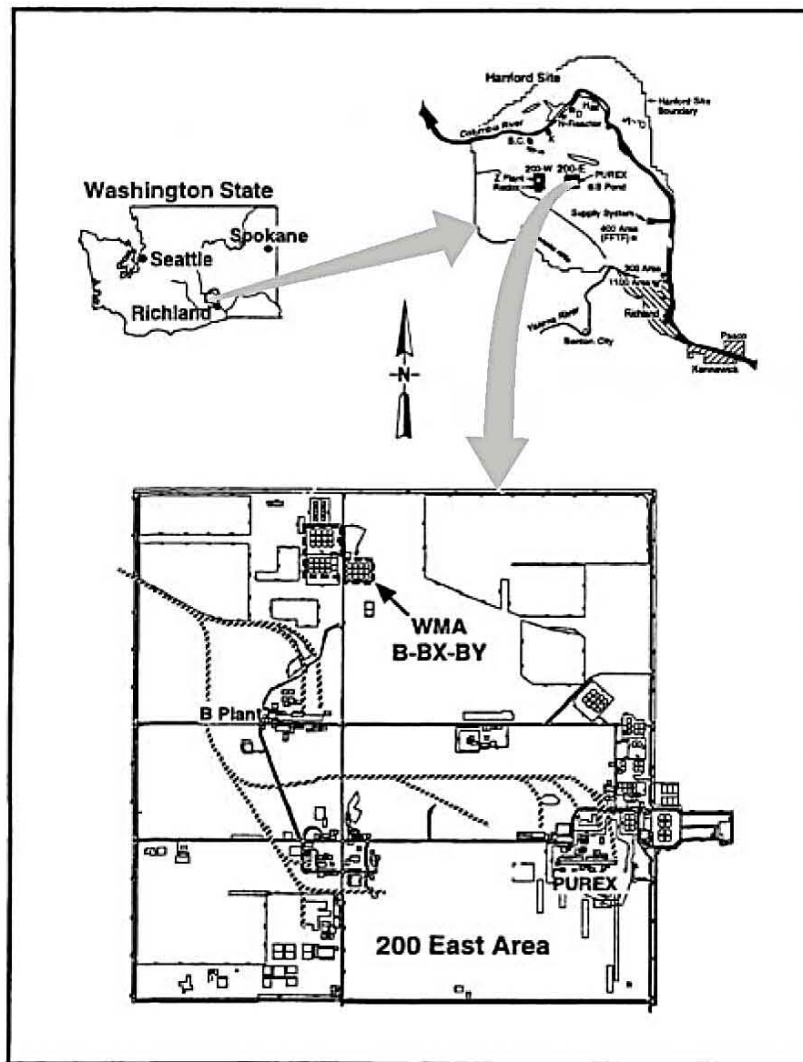
The BX tank farm comprises the following:

- 12 single-shell tanks each with 530,000-gallon (2,006,050-liter) capacity
- Waste transfer lines
- Leak detection systems
- Tank ancillary equipment.

The BY tank farm comprises the following:

- 12 single-shell tanks each with 758,000-gallon (2,869,030-liter) capacity
- Waste transfer lines
- Leak detection systems
- Tank ancillary equipment.

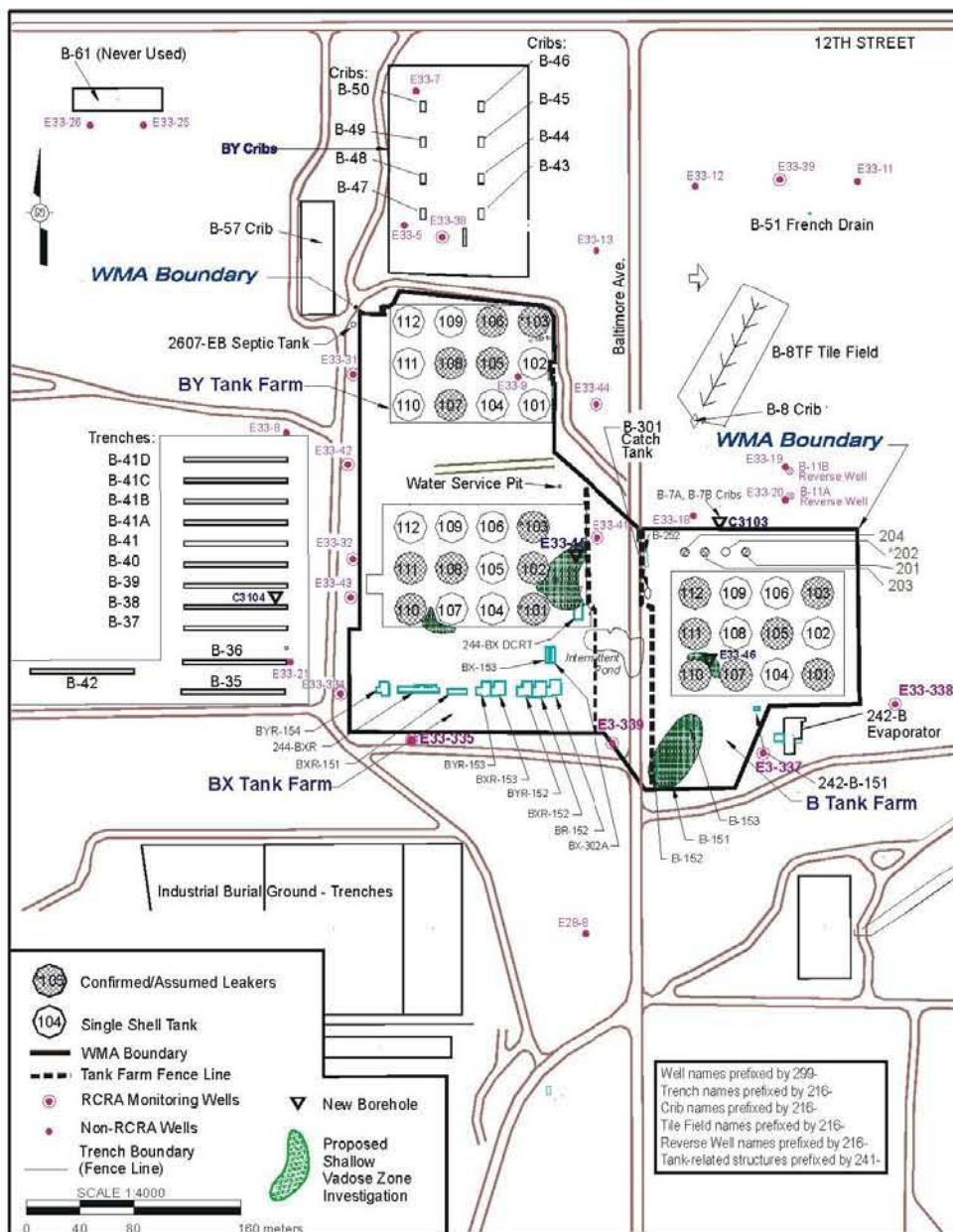
**Figure 1. Location of B, BX, and BY Tank Farms.**



Source: HNF-5507, 2000, *Subsurface Conditions for B-BX-BY Waste Management Area*, Rev. 0, Fluor Hanford, Inc., Richland, Washington..

Facilities of interest for magnetic and electromagnetic investigation within the WMA include the B-8 crib and tile field, BX trenches, and BY cribs. These facilities are down on Figure 2.

**Figure 2. B-BX-BY Tank Farms with Characterization Activities, Surrounding Facilities, and Wells.**



Note: All wells are preceded by 299-

Note: The intermittent pond between the B and BX tank farms has been addressed by interim measures.

Source: RPP-10098, 2003, *Field Investigation Report for Waste Management Area B-BX-BY*, Rev. 0, CH2M HILL Hanford Group, Inc., Richland, Washington.

### 3.0 THEORY

This chapter provides summary level descriptions for the theory behind different geophysical tools and methods used in the assessment.

#### 3.1 MAGNETOMETRY

Magnetic gradiometry (MAG) studies the Earth's magnetic field (*Applied Geophysics* [Telford et al. 1990]). The Earth's field is composed of three main parts:

- **Main Field** – internal to the Earth (i.e., from a source from within the Earth and varies slowly in time and space)
- **Secondary Field** – external to the Earth and varies rapidly in time
- **Small Internal Fields** – constant in time and space and are caused by local magnetic anomalies in the near-surface crust.

Localized magnetic anomalies are caused by magnetic minerals (mainly magnetite or pyrrhotite) or buried steel and contrast in the magnetic susceptibility ( $k$ ) with the background sediments. The average values for  $k$  are typically less than 1 for sedimentary formations and upwards to 20,000 for magnetite minerals.

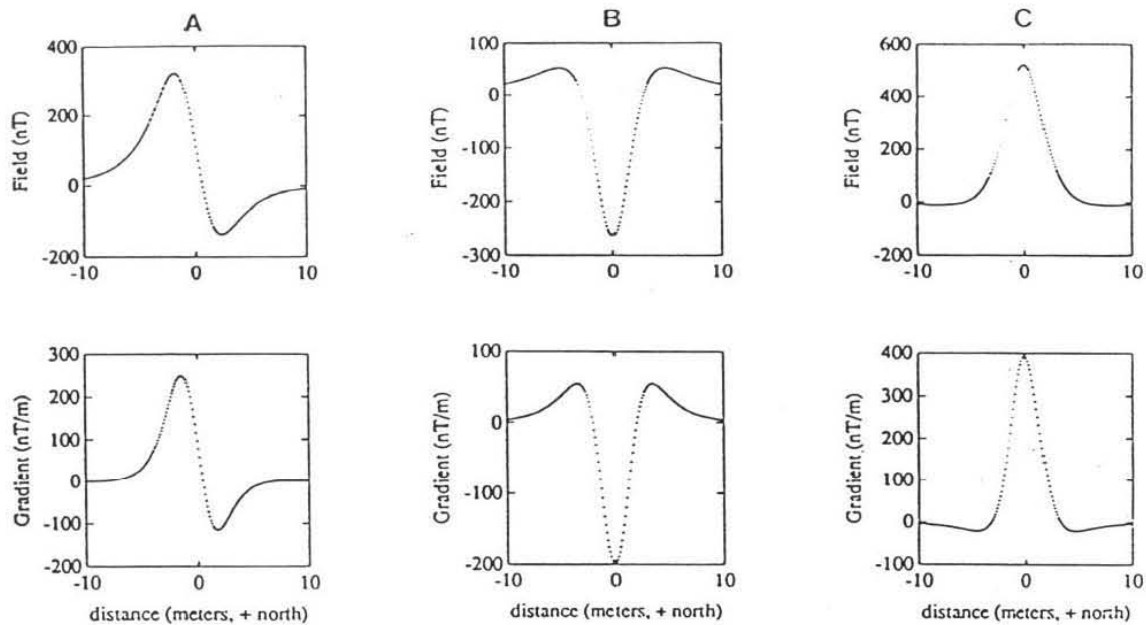
From basic magnetic field theory (*Interpretation Theory in Applied Geophysics* [Grant and West 1965]) the magnetic field due either to a point (dipole) source, or a three-dimensional finite volume of magnetized material, decays in proportion to  $r^3$  as we move away from the source, where  $r$  is the separation between the source and the magnetometer. However, the gradient of the field decays in proportion to  $r^4$ . By means of Fourier transform, it is possible to show that a signal proportional to  $r^4$  has more power at higher spatial frequencies relative to a signal proportional to  $r^3$  (the field itself). Consequently, the magnetic gradient signal due to a given three-dimensional source is more limited in spatial extent, making discrete near-surface bodies appearing more pronounced compared to background readings.

Schlenger (1990) (“Magnetometer and Gradiometer Surveys for Detection of Underground Storage Tanks”) showed the effects of a dipole source (i.e., a uniformly magnetized buried sphere on the geomagnetic field at several latitudes). The figure is reproduced here as Figure 3, where the anomaly is positioned at 0 feet (0 meters) at a depth of 6.5 feet (2 meters) below ground surface with the measurement at 6.5 feet (2 meters) above the ground surface. The figure shows the response of both total magnetic field and vertical magnetic gradient. Both plotting methods are sufficient at discriminating bodies in the near surface, but the total field is only useful for determining deeply buried bodies.

The presentation of magnetic data is accomplished with a contour map, where the magnitude of the magnetic field or vertical magnetic gradient data is represented by isopleths. In general, the

buried objects will appear as either a mono-polar or a dipolar anomalous response. For near-surface infrastructure mapping of steel objects, the values of the magnetic field can be several hundred to several thousand times higher than the background field. Linearly continuous anomalies observed along adjacently acquired data are interpreted as buried pipelines and singular anomalies that are not continuous are interpreted as discrete buried objects (tanks, drums, wells, or other metal that comprise the construction of tank farms).

**Figure 3. Magnetic Anomalies for a Sphere at (A) Mid Latitude, (B) Equator, and (C) Near the North Pole.**



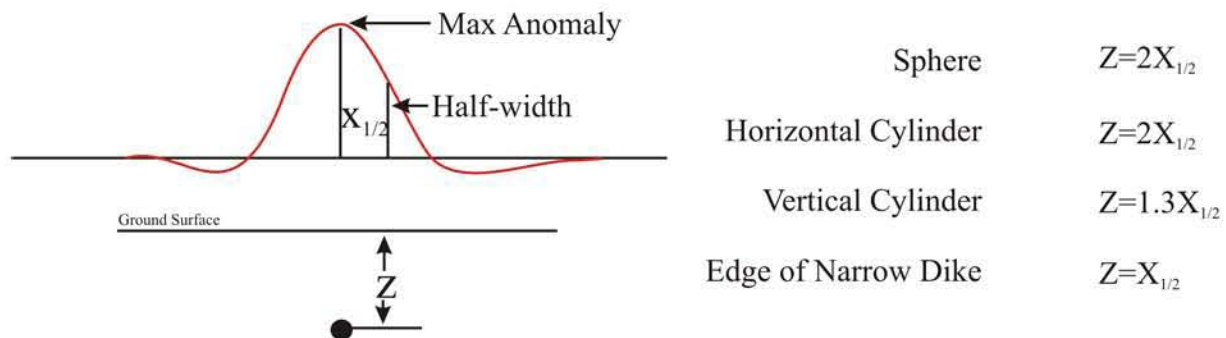
Source: Schlinger, C.M., 1990, "Magnetometer and Gradiometer Surveys for Detection of Underground Storage Tanks," *Bulletin of the Association of Engineering Geologists*, Vol. XXVII:37-50.

The magnetic field is measured with a magnetometer. Magnetometers permit rapid, non-contact surveys and were used outside the farm to locate buried metallic objects and features. Portable (one person) field units can be used virtually anywhere that a person can walk. Field-portable magnetometers may be single- or dual-sensor. Dual-sensor magnetometers are called gradiometers and measure gradient of the magnetic field; single-sensor magnetometers measure total field.

Magnetic surveys are typically run with two separate magnetometers. The first magnetometer is used as a base station to record the Earth's primary field and the diurnally changing secondary field. The second magnetometer is used as a rover to measure the spatial variation of the Earth's field. A residual magnetic field from local spatial variations is calculated by removing the temporal variation and, possibly the static value of the base station, from that of the rover.

The shortcoming with most magnetometers is that they only record the total magnetic field,  $F$ , and not the separate components of the vector field. This shortcoming can make the interpretation of magnetic anomalies difficult. Furthermore, the magnetic intensity or anomalies are highly variable in shape and amplitude. They are almost always asymmetrical, sometimes appear complex even from simple sources, and usually portray the combined magnetic effects of several sources (*Applications Manual for Portable Magnetometers* [Breiner 1973]). There are simplified depth estimation techniques based on graphical evaluation of data using the half-width rule. In magnetic fields, it can be shown for simple forms that the depth to the center of a buried object is related to the half-width of the measured anomaly. The half-width is the horizontal distance between the principal maximum (or minimum) of the anomaly (assumed to be over the center of the source) and the point where the value is exactly one-half the maximum value (see Figure 6). This rule is only valid for simple shaped forms such as a sphere, horizontal cylinder, vertical cylinder, and the edge of a narrow, nearly vertical dike.

**Figure 4. Depth Estimates for Magnetic Anomalies.**



Source: Breiner, S., 1973, *Applications Manual for Portable Magnetometers*, Geometrics, Inc., San Jose, California.

### 3.2 ELECTROMAGNETIC INDUCTION

Earth materials have the capacity to transmit electrical currents over a wide range depending on the material property of electrical conductivity. Electrical conductivity is a function of soil type, porosity, saturation, and dissolved salts. Electromagnetic induction identifies various earth materials by measuring their electrical characteristics and is used to identify buried infrastructure within the area where resistivity data are collected.

Electromagnetic induction methods use a transmitting coil and a receiving coil. The transmitting coil induces eddy currents in the Earth, which themselves generate magnetic fields that are affected by the earth materials within the excited zone. The receiving coil intercepts the field resulting in an output voltage that is proportional to the conductivity within the area. Moving these coils results in variations in conductivity that can be interpreted to find buried features or objects.

The transmitting coil frequency and electrical conductivity of the host material primarily determine the depth of investigation for EM techniques. Referred to as skin depth in the literature (Telford et al., 1990), it generally describes the decay of the EM field through a conductive medium. Formally, the skin depth ( $\delta$ ) is defined as the distance through which the field decays to  $e^{-1}$  (approximately 37 percent) of its original amplitude:

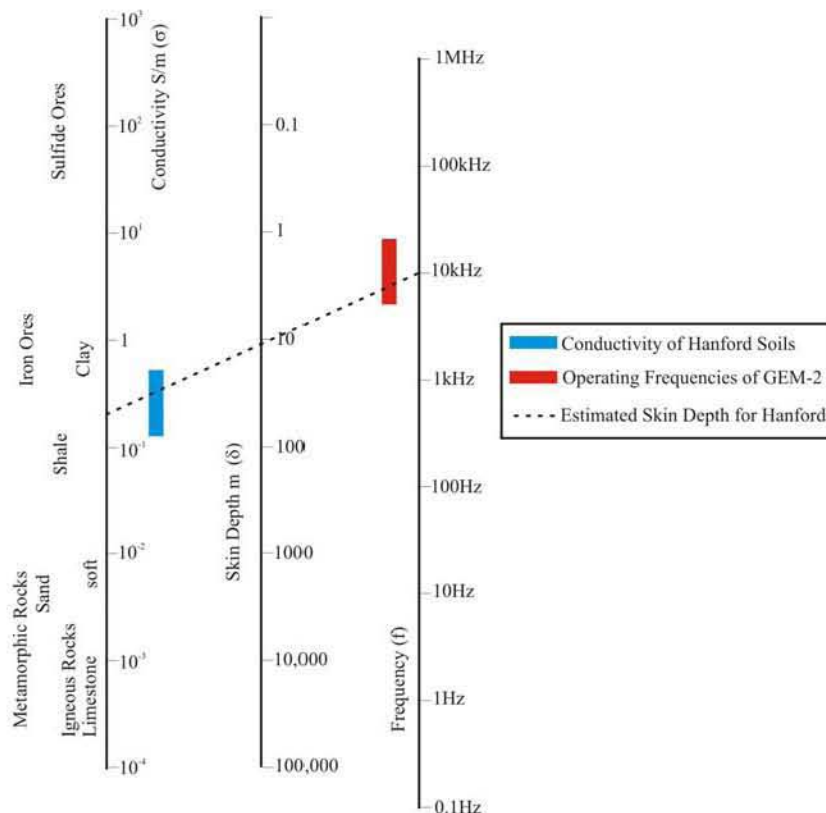
$$\text{Skin Depth: } \delta = \sqrt{\frac{2}{(\pi f)\mu\sigma}} \tag{1}$$

Where:

- $\sigma$  = the electrical conductivity of the host material
- $\mu$  = the magnetic permeability
- $f$  = the operating frequency of the instrument.

Graphically, Won (1980) (“A wideband electromagnetic exploration method – Some theoretical and experimental results”) developed a nomogram, from which the skin depth may be determined from a given frequency. Figure 5 shows the nomogram and an example of skin depth for Hanford-specific soils. For the 10 kHz frequency, it is expected that the skin depth is approximately 33 feet (10 meters).

**Figure 5. Skin Depth Estimates for the GEM-2® at the Hanford Site.**



Source: Won, L.J., 1980, “A wideband electromagnetic exploration method – Some theoretical and experimental results,” *Geophysics*, 45 (3):928-940.

® GEM-2 is a registered trademark of Geophex, Ltd.

There are several advantages of using a broadband, multi-frequency EM sensor. Since conductivity and permeability of the host material cannot be manipulated, the skin depth can be changed by changing frequencies. In theory, scanning through a frequency window is equivalent to depth sounding, where the results from multiple frequencies can be presented to understand the layering of earth materials. However, in practice hydroGEOPHYSICS, Inc. has observed that a fixed object of high conductivity (such as a metal pipe) will appear in all frequencies, eliminating the possibility of depth-specific estimations for individual targets.

## **4.0 METHODOLOGY**

### **4.1 SURVEY AREA AND LOGISTICS**

This section describes the equipment and methodology used to collect, manage, and process geophysical data around the B Complex. A summary of the survey coverage area can be viewed in Figure 6.

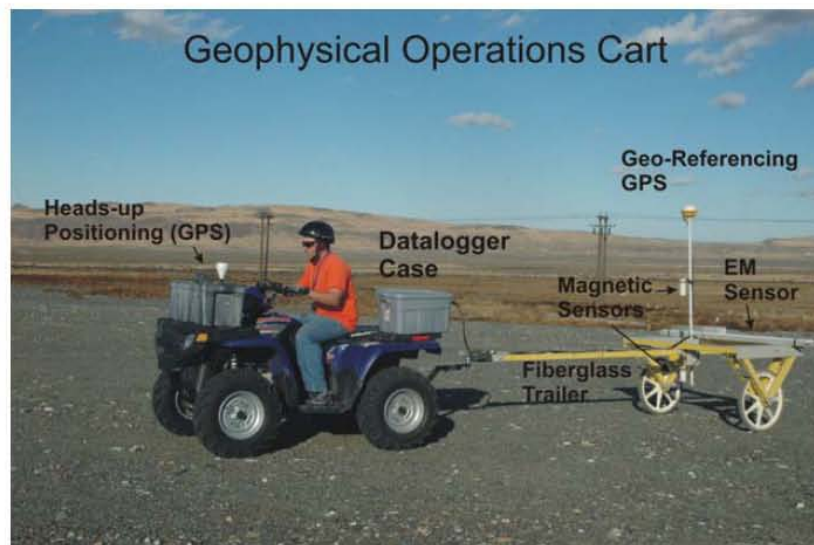
Data acquisition commenced on November 9, 2006, by establishing a magnetic base station. The magnetic base station was used to remove diurnal variations of the magnetic field from data acquired using the roving magnetometer attached to the G.O. Cart.

The G.O. Cart was equipped with two cesium-vapor magnetic sensors spaced 3.3 feet (1 meter) apart in a vertical orientation, a broadband electromagnetic conductivity meter, a differential GPS for geo-referencing of geophysical data, and a heads-up GPS display for navigation along the survey lines (Figure 7).

Figure 6. Geophysical Operations Cart Coverage.



Figure 7. Geophysical Operations Cart Photo.



## **4.2 GEOPHYSICAL EQUIPMENT**

Five different geophysical methods were deployed at the B Complex. The different geophysical instruments are described in the following sections.

### **4.2.1 Geophysical Operations Cart**

The complexity of site characterization required information about multiple physical properties that could be combined to enhance characterization efforts. Recent technological advances in mobile computing and geophysical instrumentation have greatly improved surveying. The G.O. Cart provides the ability to simultaneously deploy multiple survey instruments.

### **4.2.2 Global Positioning Systems**

A Trimble Ag-132 GPS was used to establish the physical location of magnetic and EM data. The accuracy of the system is based partly on the G.O Cart speed and was within 3.3 feet (1 meter) for this survey.

### **4.2.3 Magnetometry**

Two Geometrics, Inc. magnetometers were used to monitor variations within the Earth's magnetic field. A model G-856 proton precession magnetometer was used as a base station and a model G-858G cesium vapor magnetometer was used as a roving magnetic gradiometer. The G-858G was set up with two sensors oriented vertically, spaced one meter apart with the lowest sensor approximately 1.6 feet (0.5 meters) from the ground surface.

### **4.2.4 Electromagnetic Induction**

Electromagnetic data were collected using a GEM-2<sup>®</sup> unit. The GEM-2 is a broadband multi-frequency meter (from 300Hz to 96kHz) with bistatic transmitter and receiver coils. The coils have a separation of 5.3 feet (1.6 meters).

## **4.3 PROCESSING**

### **4.3.1 Downloading, Parsing, Quality Control – Onsite**

The rover and base magnetic data were downloaded to a field laptop computer through MagMap2000<sup>®</sup>. The data were saved in binary format, with the instrument type, date stamp, and

---

<sup>®</sup> GEM-2 is a registered trademark of Geophex, Ltd.

<sup>®</sup> MagMap2000 is a registered trademark of Geometrics, Inc.

location as part of the naming structure. Table 1 lists the data files for the magnetic data and Table 2 lists the files for the EM data.

**Table 1. Magnetic Data File Names and Locations of Coverage.**

<b>Date</b>	<b>Location</b>	<b>MAG Rover File Names</b>	<b>MAG Base File Names</b>
November 9, 2006	Trenches	mag 110906 Trenches1.bin mag 110906 Trenches1a.bin mag 110906 Trenches2.bin	base 11.09.06.stn
November 13, 2006	Trenches	mag 111306 Trenches1a.bin	base 11.13.06.stn
November 14, 2006	Trenches	mag 111406 Trenches.bin	base 11.14.06.stn
November 15, 2006	Trenches	mag 111506 Trenches.bin	base 11.15.06.stn
November 16, 2006	Tile Field	mag 111606 Tile.bin mag 111606 Tile2.bin	base 11.16.06.stn
November 27, 2006	Tile Field	mag 112706 Tile.bin mag 112706 Tile2.bin	base 11.27.06.stn
Dec 7, 2006	Crib	mag 12.07.06 Crib.bin mag 12.07.06 Crib2.bin	base 12.07.06.stn
December 8, 2006	Crib	mag 12.08.06 Calibration Crib.bin mag 12.08.06 Part 1 Crib.bin mag 12.08.06 Part 2 Crib.bin mag 12.08.06 Part 3 Crib.bin	base 12.08.06.stn
December 11, 2006	Soil Contamination Area	mag 121106 SCA.bin	base 12.11.06.stn
December 12, 2006	Heading Correction	mag 121206 Rose Diagram.bin	12.12.06 Rose Diagram base.stn

**Table 2. Electromagnetic Induction Data File Names and Locations of Coverage.**

Date	Location	EM File Names
November 9, 2006	Trenches	em 110906 trenches1a.gbf em 110906 trenches2.gbf
November 13, 2006	Trenches	em 111306 Trenches1a.gbf
November 14, 2006	Trenches	em 111406 Trenches.gbf
November 15, 2006	Trenches	em 111506 trenches.gbf
November 16, 2006	Tile Field	em 111606 Tile.gbf em 111606 Tile2.gbf
November 27, 2006	Tile Field	em 112706 Tile.gbf em 112706 Tile2.gbf
December 7, 2006	Crib	em 12.0706 Crib.gbf em 12.0706 Crib2.gbf
December 8, 2006	Crib	em 12.08.06 Crib.gbf
December 11, 2006	Soil Contamination Area	em 12.11.06 SCA.gbf

Onsite quality control included plotting the GPS locations of the G.O. Cart on the B Complex base map. The plotting ensured that spatial coverage for the day met expectations, and off-normal situations (e.g., full data logger or dead battery) did not result in the loss of data. All binary files were uploaded daily for processing and evaluation of data quality statistics (i.e., low noise, sufficient data density, low drop-out rate). Onsite quality control also included plotting the magnetic field versus time to observe the diurnal changes in the base station data.

#### 4.3.2 Magnetometry Processing and Plotting.

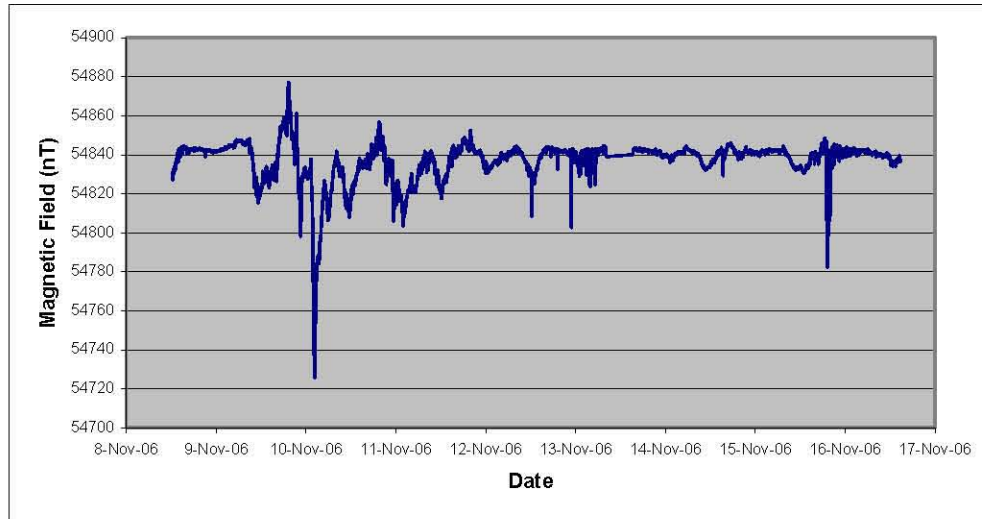
Processing the MAG data required a multi-step process. After downloading the data, the MagMap2000 software was used to make diurnal corrections. The diurnal correction was applied by subtracting the coincident time readings of the base station from the rover magnetic data. Subtracting the diurnal field from the total field resulted in a relative magnetic field for both the upper and lower magnetic sensors. Figure 8 shows the results of the diurnal magnetic field from November 8 through November 16, 2006.

After diurnal corrections to the data, each data point was geo-referenced with the GPS data. Since the GPS data were recorded every second and the magnetometer data were recorded five times per second, the GPS data were associated with every magnetic reading using linear interpolation.

After geo-referencing the data set, data spikes were removed. This was the first step of data rejection. The total field magnetic data were typically around 54,000 nanoTeslas before diurnal corrections and ranged between -1,500 and 1,500 after diurnal corrections depending on items

buried in the ground. A data spike had a value outside the range of  $-2,000$  to  $2,000$  nanoTeslas. Other rejection criteria included removal of data when the instrument did not move. Data were rejected if the position had not moved more than  $0.13$  feet ( $0.04$  meters) between successive data points.

**Figure 8. Magnetic Base Station Data.**



After data removal, the heading error was removed. Heading error in the magnetic data results from the preferential alignment of the magnetic sensors with the Earth's magnetic field. Breiner (1973) discusses the heading error problem more thoroughly. Heading errors cause anomalous readings unrelated to any response from buried metallic debris. The error associated with heading was calculated from the magnetic data collected in eight distinct directions. Data were collected every 45 degrees from a northerly heading. A curve was fit for the direction of travel versus field strength for each sensor (Figures 9 and 10), which was subtracted from the data.

The last step of processing before plotting involved filtering the data to smooth out high frequency noise. A 17-point sinc filter was applied to each day separately to avoid overlap between days. The files were gridded in Surfer8<sup>®</sup> using a spatial interpolation algorithm. The gridding and interpolation allowed a contour plot of data to be placed over the B Complex base map and interpretation of linear or discrete objects.

It should be noted that the International Geomagnetic Reference Field was not subtracted from the magnetic data. The International Geomagnetic Reference Field allows the removal of large-scale trends present in magnetic data that covers large areas. For the B Complex, the International Geomagnetic Reference Field varies by  $2.2$  nanoTeslas, an insignificant variation.

<sup>®</sup> Surfer is a registered trademark of Golden Software, Inc.

**Figure 9. Heading Error Associated with Magnetometer Readings for the Bottom Sensor.**

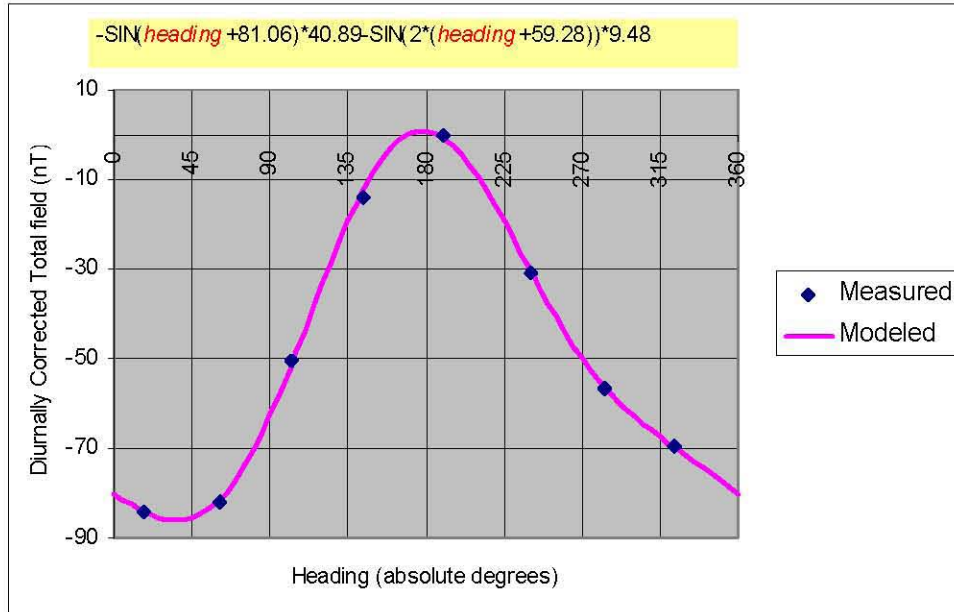
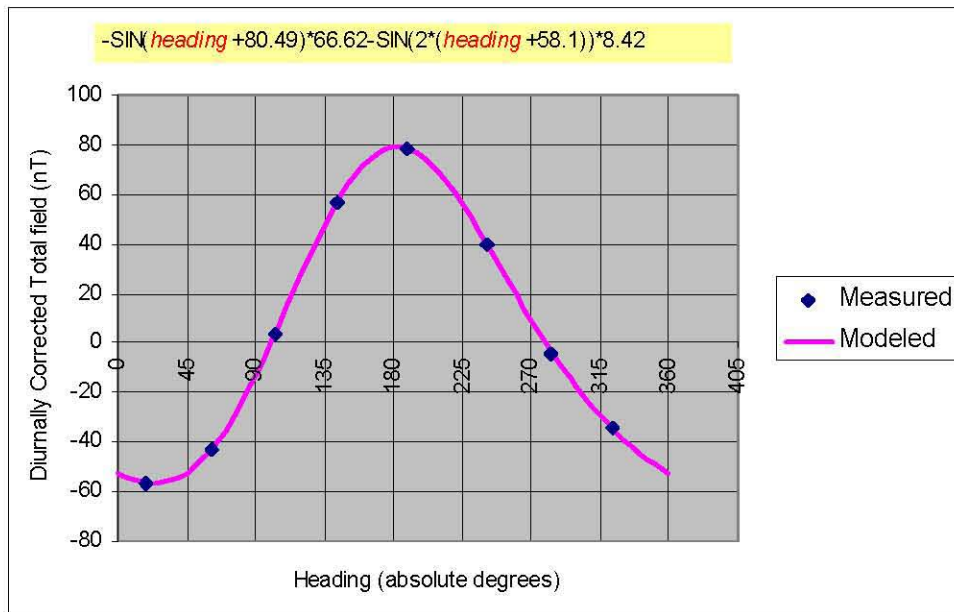


**Figure 10. Heading Error Associated with Magnetometer Readings for the Top Sensor.**



### **4.3.3 Electromagnetic Processing and Plotting**

Electromagnetic data processing was similar to magnetic processing. Processing occurred in discretely separate steps so that all data from a previous step could be recovered. The first step in processing was to geo-reference with the GPS data. Electromagnetic data were recorded with a higher sampling frequency than the GPS data. The GPS data were linearly interpolated to the EM data locations, based on the time stamp of each data point.

The survey collected both in-phase and quadrature data for the electromagnetic signal. Typically, the in-phase data relates to magnetic susceptibility, and quadrature data relates to electrical conductivity. Each are a function of signal frequency, vertical distance of the coils to the ground, coil orientation (horizontal or vertical), and coil separation. The in-phase and quadrature data were subjected to an inversion algorithm provided by Geophex, Ltd. The inversion algorithm converted the measured quadrature data to electrical conductivity. The total electrical conductivity was calculated by equally weighting the individual frequencies in order to produce an average, frequency-independent electrical conductivity.

After inversion, the data were shifted for the day-to-day changes. The day-to-day changes were calculated from a coincident data collection run at the beginning of each collection day. Slight differences in the daily data records occurred due to environmental or instrument setup changes. The first run of the day was collected by overlapping at least one line from the previous day.

After correcting the EM data for each of the time-series issues, the data were compiled spatially and passed through a low-pass, one-dimensional spatial filter to remove high frequency noise. The filter was a simple 17-point sinc function. Additionally, coincident data points (within 0.13 feet [0.04 meters]) were removed to eliminate redundancy.

After filtering, the data were combined to a single data file for each frequency and type (in-phase or electrical conductivity) and location (tile field, crib, or trenches). A total of six plots were created for the EM data by gridding and interpolating the data for contouring purposes. The contours for each of the plots were overlain on the B Complex base map and interpreted for linear or discrete objects.

## **5.0 ANALYSIS, RESULTS AND INTERPRETATION**

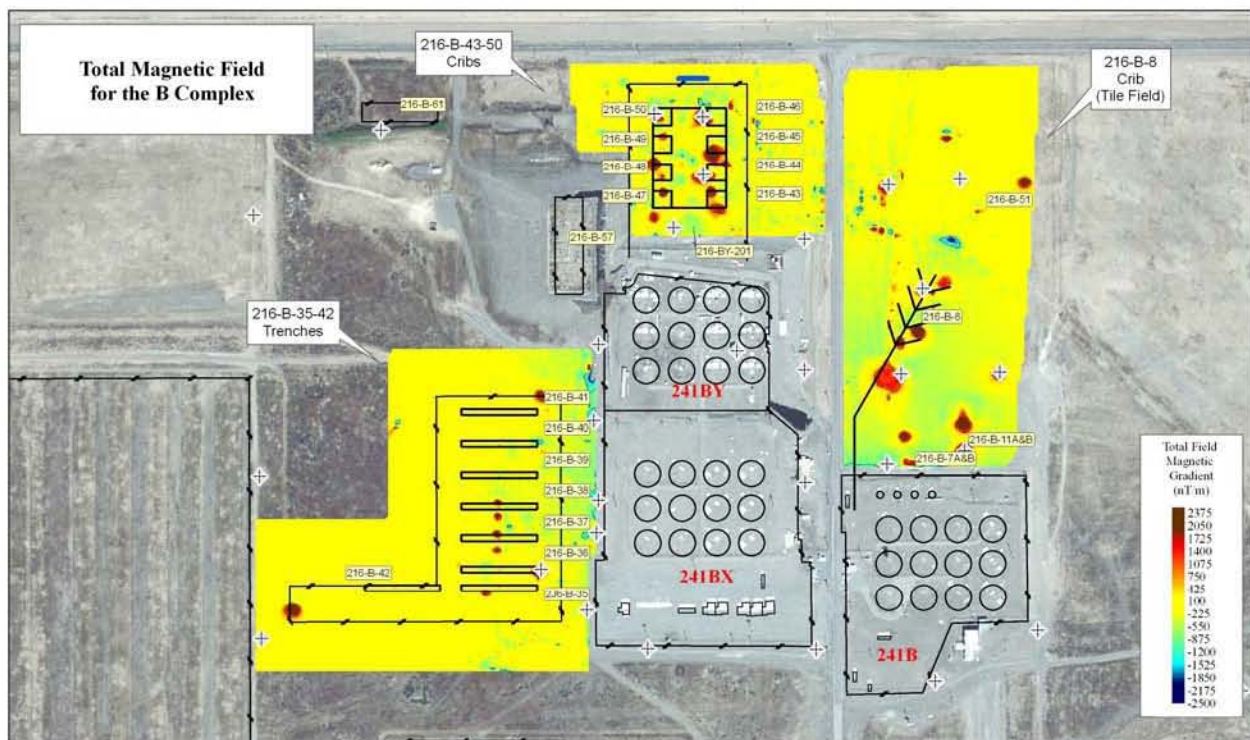
This section contains figures created from the magnetic and electromagnetic surveying effort. These figures and the results within are discussed in the subsequent sections. Engineering drawings of the results are shown in Appendix A.

## 5.1 MAGNETIC GRADIOMETRY

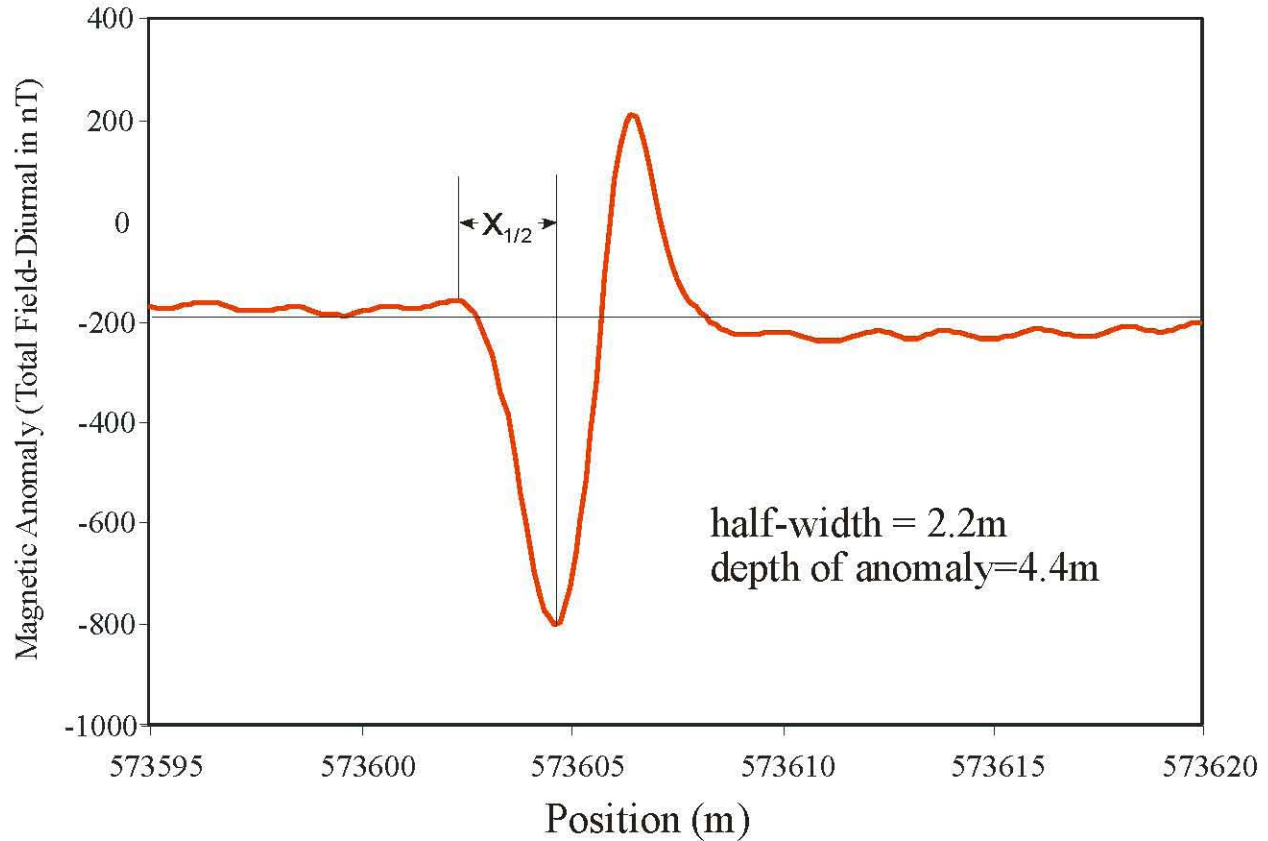
### 5.1.1 Total Magnetic Field

The results of the total magnetic field are shown in Figure 11. Localized monopolar features appear as an extreme positive response in the total magnetic field. Ferrous metallic objects that extend deeply into the subsurface account for these responses, where one pole is near the surface and the other pole is buried deeply within the subsurface. For infrastructure mapping, these responses usually correlate to well casings.

**Figure 11. Total Magnetic Field for the 241-B, BX, and BY Farms.**

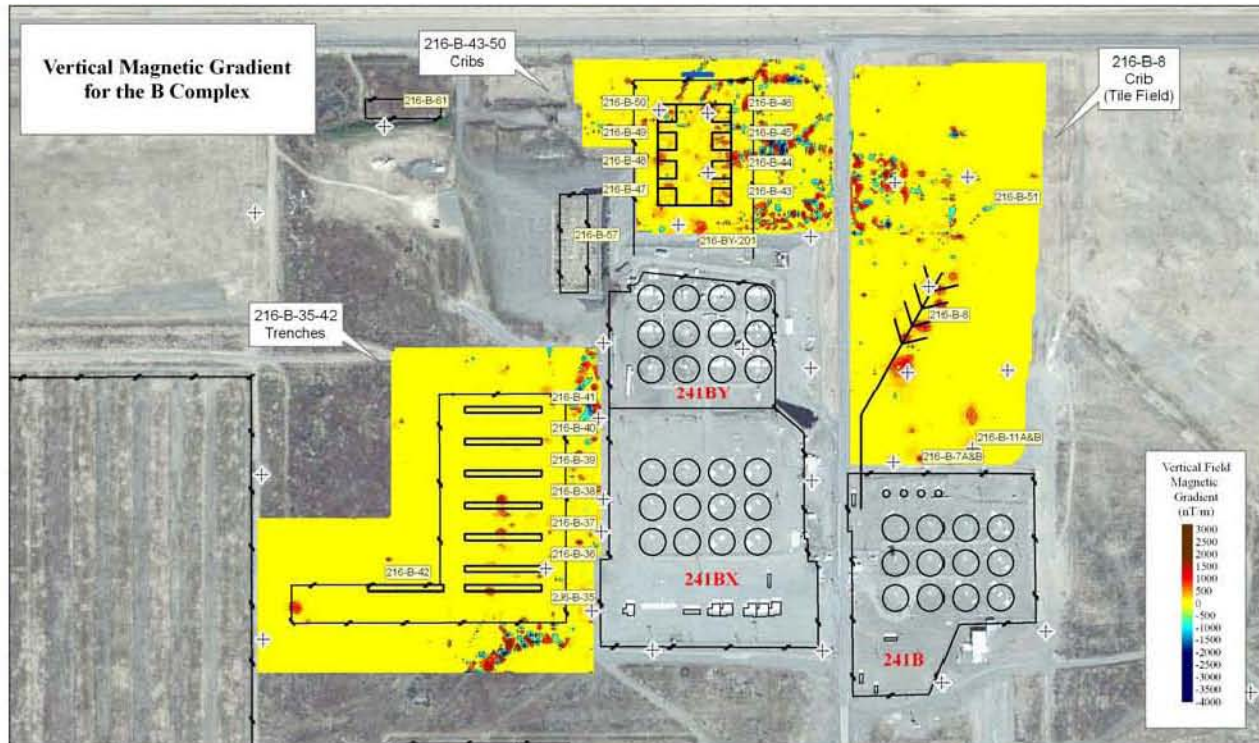


The depth to anomalies can be estimated from the half-width of the magnetic anomaly. An example of a half-width calculation for data near the BY cribs is shown in Figure 12 with the spatial location of the data for the analysis shown in Figure 11. The calculation for the depth shows the pipe is approximately 14 feet (4.4 meters) below ground surface.

**Figure 12. Magnetic Anomaly Over a Pipe showing the Estimated Depth of the Target.**

### 5.1.2 Vertical Magnetic Gradient

The results of the vertical magnetic gradient are shown in Figure 13. The vertical magnetic gradient is the difference between the magnetic field of the bottom sensor and the top sensor, divided by the separation distance of 3.3 feet (1 meter). This calculation provides a tool for mapping near-surface objects. Features closer to the surface (e.g., pipes) stand out prominently compared to deep objects (e.g., wells). Several linear anomalies appear in the data, and are confined mainly to the northern crib area.

**Figure 13. Vertical Magnetic Gradient for the 241-B, BX, and BY Farms.**

## 5.2 ELECTROMAGNETIC INDUCTION

### 5.2.1 In-Phase

The results of the in-phase measurements from electromagnetic induction for the frequencies of 5, 10, and 20 kHz are shown in Figures 14 through 16. The data were contoured to show the spatial representation of relevant subsurface features. The figures show sporadic in-phase responses over the western trenches area. These responses are likely noise due to subtle differences within the soil, and the limitations of the survey instrument. Additionally, the monitoring wells produce little response because the EM sensor was not placed directly over top of their locations.

**Figure 14. In-Phase (5 kHz) from Electromagnetic Induction for the 241-B, BX, and BY Farm.**

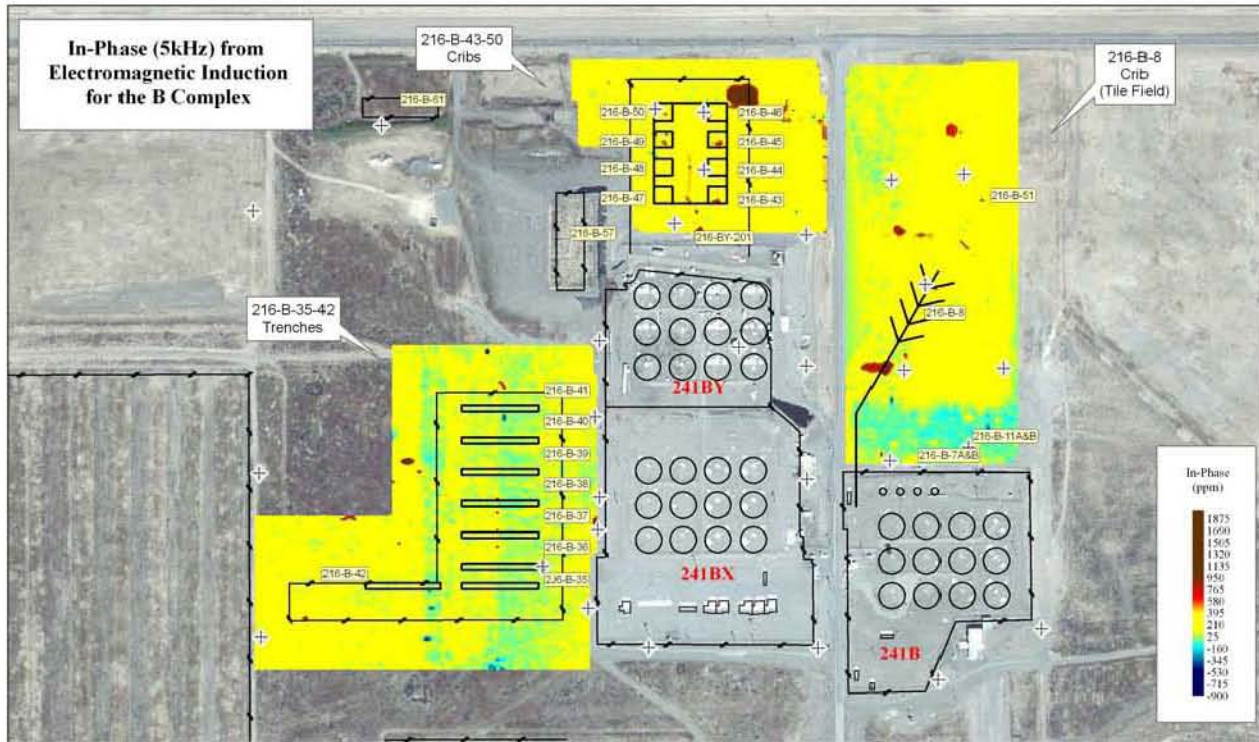


**Figure 15. In-Phase (10 kHz) from Electromagnetic Induction for the 241-B, BX, and BY Farm.**

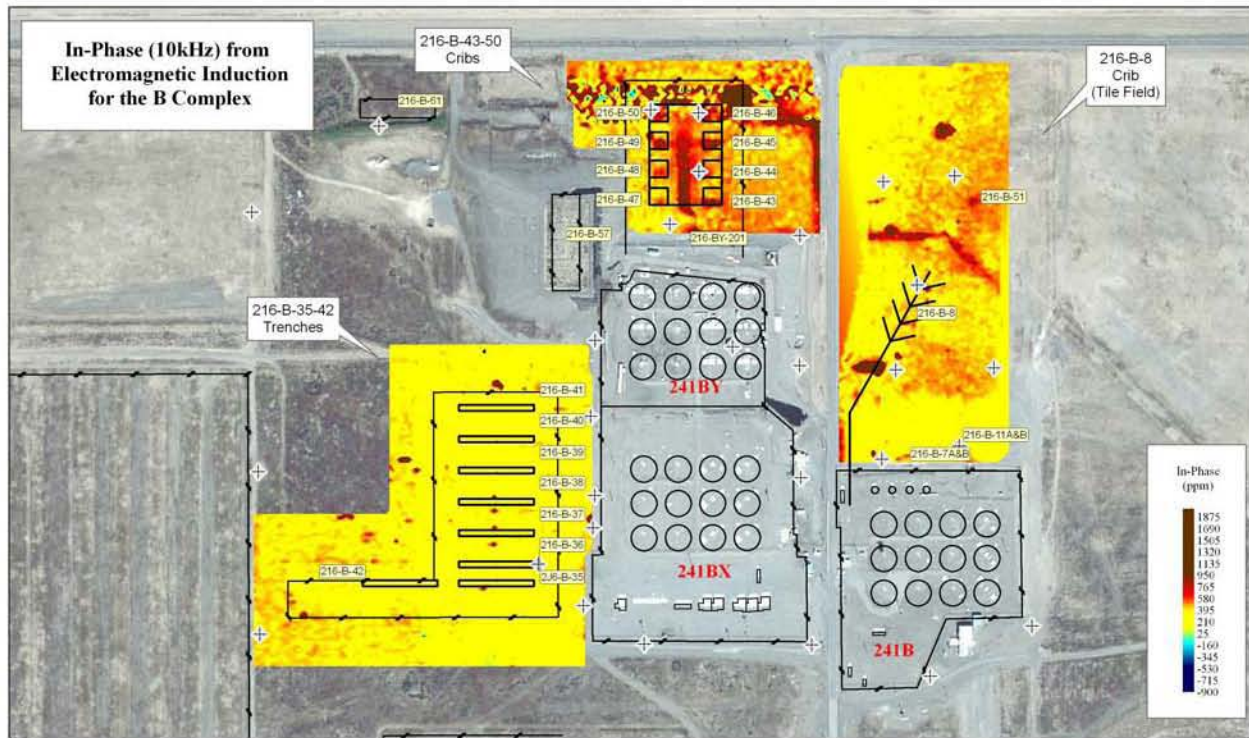
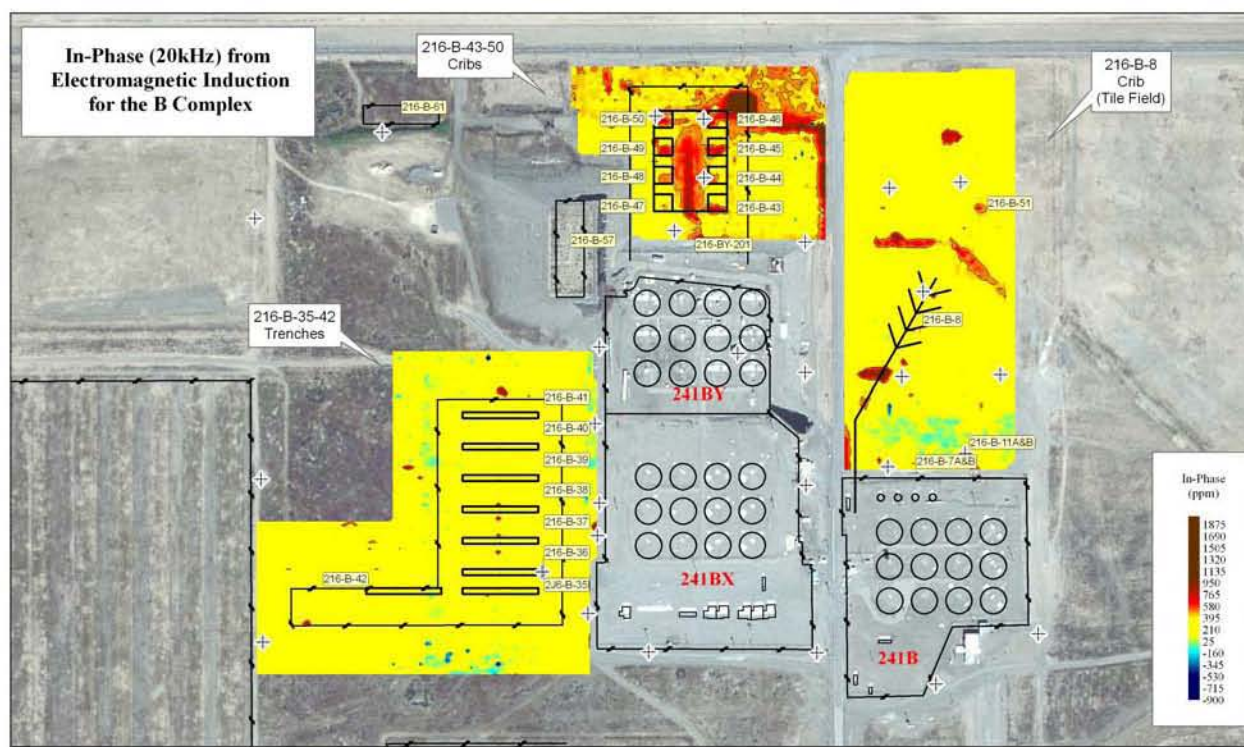


**Figure 16. In-Phase (20 kHz) from Electromagnetic Induction for the 241-B, BX, and BY Farm.**



The northern cribs and northeastern tile fields shows some coherency among the high- and low-value anomalies. These anomalies could be related to a subsurface liquid waste delivery system.

### 5.2.2 Electrical Conductivity

The results of the electrical conductivity measurements from electromagnetic induction for the frequencies of 5, 10, and 20 kHz and total electrical conductivity are shown in Figures 17 through 20. Unlike the MAG and EM in-phase data, anomalous responses in the electrical conductivity could result from increased soil moisture or salt deposits, in addition to the presence of ferrous and non-ferrous metals.

The figures use a color scheme that represents variations in the data. Hues ranging from brown to red to yellow represent high electrical conductivity. Green, light blue, and dark blue hues represent low electrical conductivity.

In general, the figures show linear anomalies that could be indicative of a subsurface liquid waste delivery system. The high electrical conductivity areas generally form linear anomalies that could be interpreted as pipes.

**Figure 17. Electrical Conductivity (5 kHz) from Electromagnetic Induction for the 241-B, BX, and BY Farm.**

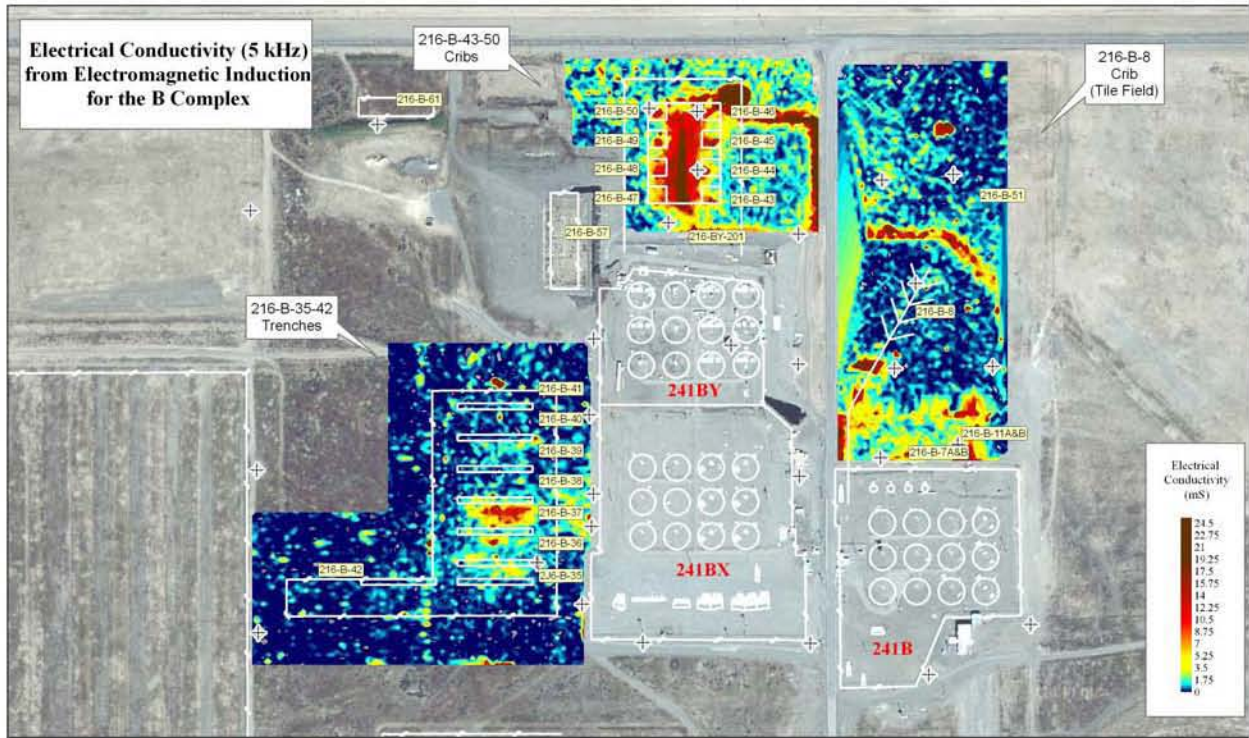


**Figure 18. Electrical Conductivity (10 kHz) from Electromagnetic Induction for the 241-B, BX, and BY Farm.**

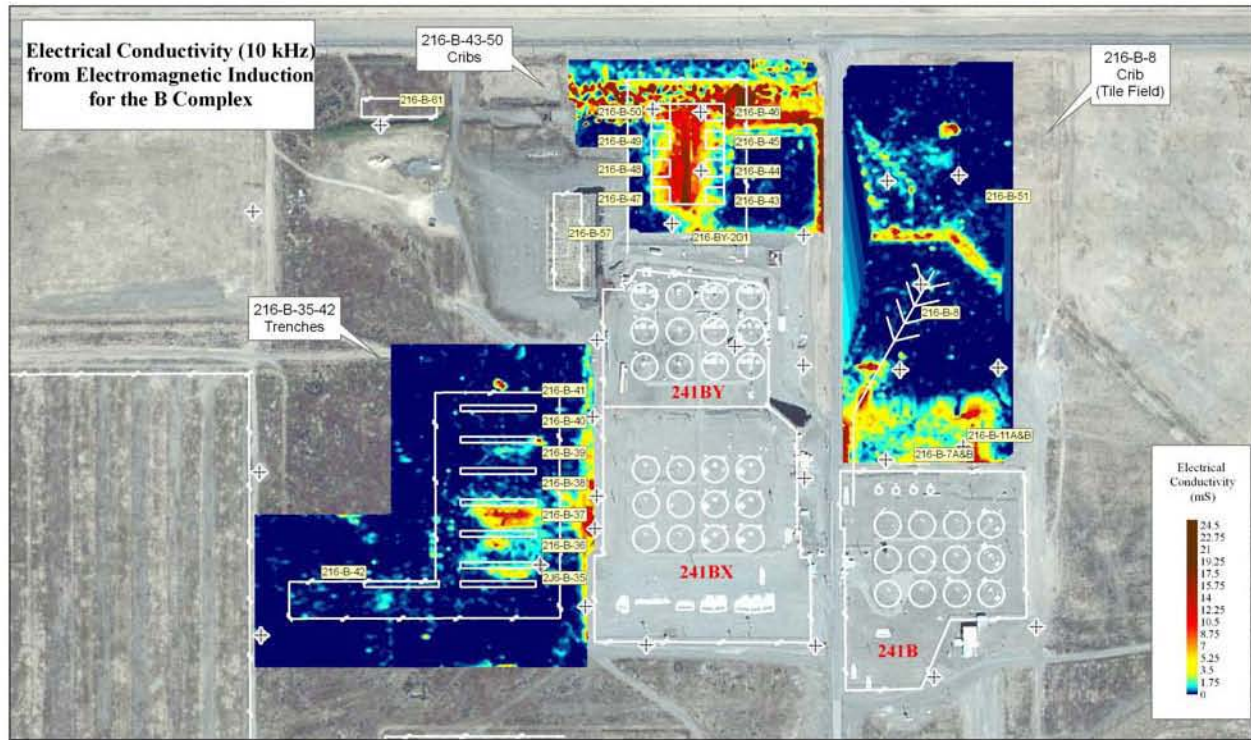


**Figure 19. Electrical Conductivity (20 kHz) from Electromagnetic Induction for the 241-B, BX, and BY Farm.**

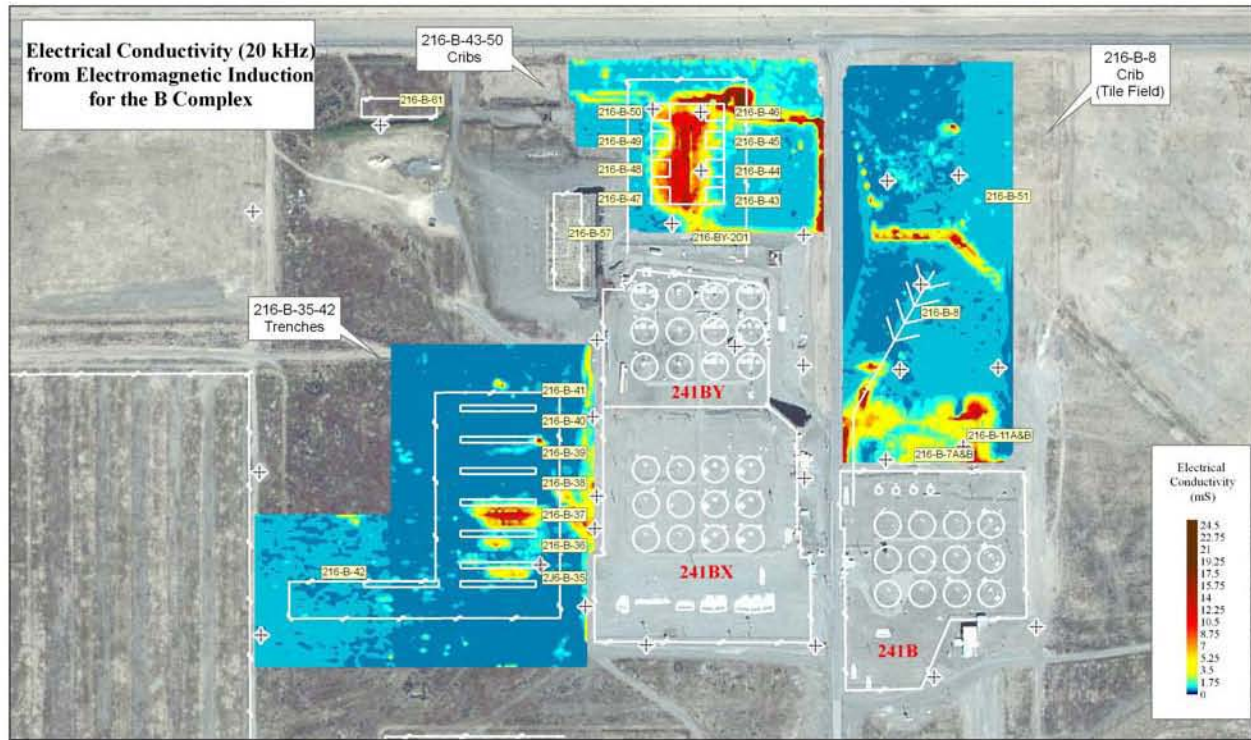
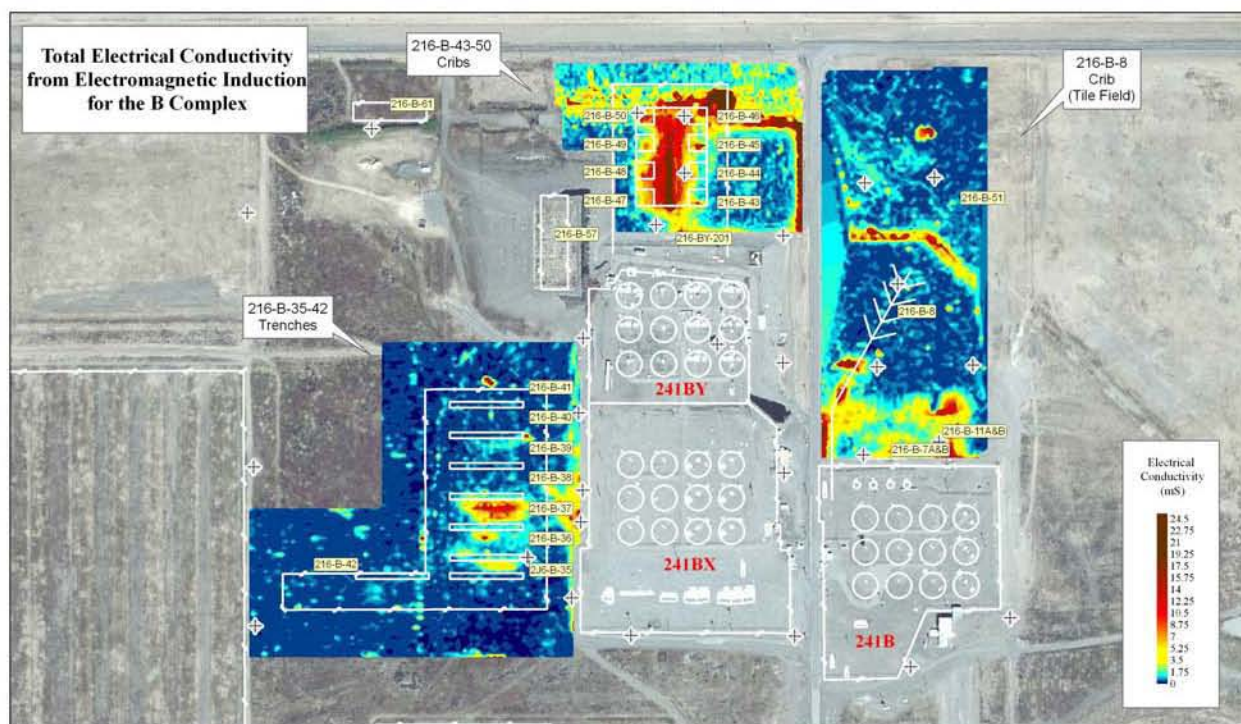


**Figure 20. Total Electrical Conductivity from Electromagnetic Induction for the 241-B, BX, and BY Farm.**



## 6.0 CONCLUSIONS

Magnetic gradiometry and EM induction surveys were conducted around the periphery of the B, BX, and BY tank farms to map the location of metal objects that may interfere with HRR measurements. The surveys were part of the broad application of subsurface geophysical exploration that is being conducted at the B Complex.

Results of the surveying revealed several subsurface features that could be interpreted as pipes. The contoured data from the vertical magnetic gradient as well as the in-phase and electrical conductivity showed linear anomalies near the cribs and north of the tile field. These are likely locations for pipelines and they could have an impact of HRR measurements.

## 7.0 REFERENCES

- Breiner, S., 1973, *Applications Manual for Portable Magnetometers*, Geometrics, Inc., San Jose, California. ([www.geometrics.com/Literature/Magnetics/magnetics.html](http://www.geometrics.com/Literature/Magnetics/magnetics.html))
- Grant F.S. and G.F. West, 1965, *Interpretation Theory in Applied Geophysics*, McGraw-Hill Book Co., New York, New York.
- HNF-5507, 2000, *Subsurface Conditions for B-BX-BY Waste Management Area*, Rev. 0, Fluor Hanford, Inc., Richland, Washington.
- RPP-10098, 2003, *Field Investigation Report for Waste Management Area B-BX-BY*, Rev. 0, CH2M HILL Hanford Group, Inc., Richland, Washington.
- RPP-34674, 2007, *Surface Geophysical Exploration of B, BX, and BY Tank Farms at the Hanford Site: Results of Background Characterization with Ground Penetrating Radar*, Rev. 0, CH2M HILL Hanford Group, Inc., Richland, Washington.
- RPP-34690, 2007, *Surface Geophysical Exploration of the B, BX, and BY Tank Farms at the Hanford Site*, Rev. 0, Rev. 0, CH2M HILL Hanford Group, Inc., Richland, Washington.
- Schlinger, C.M., 1990, "Magnetometer and Gradiometer Surveys for Detection of Underground Storage Tanks," *Bulletin of the Association of Engineering Geologists*, Vol. XXVII:37-50.
- Telford, W.M., L.P. Geldart, and R.E. Sherriff, 1990, *Applied Geophysics*, Cambridge University Press, Cambridge, United Kingdom.
- Won, I.J., 1980, "A wideband electromagnetic exploration method – Some theoretical and experimental results," *Geophysics*, 45 (3):928-940.

**APPENDIX A**

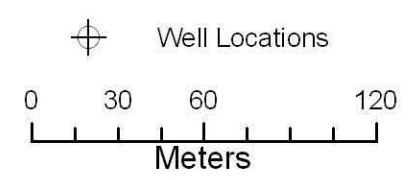
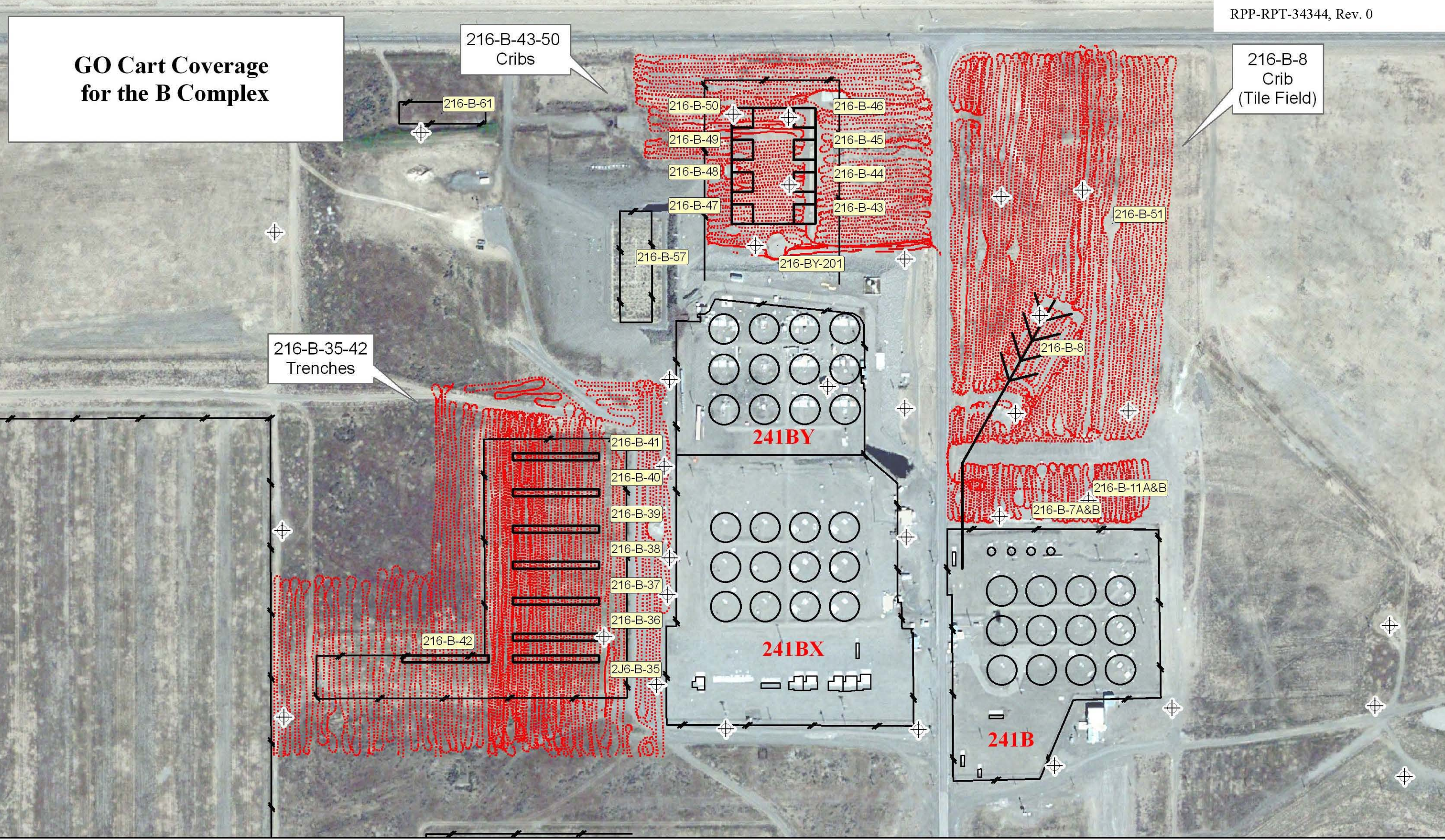
**ENGINEERING DRAWING RESULTS**

# GO Cart Coverage for the B Complex

216-B-43-50  
Cribs

216-B-8  
Crib  
(Tile Field)

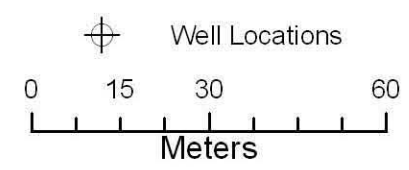
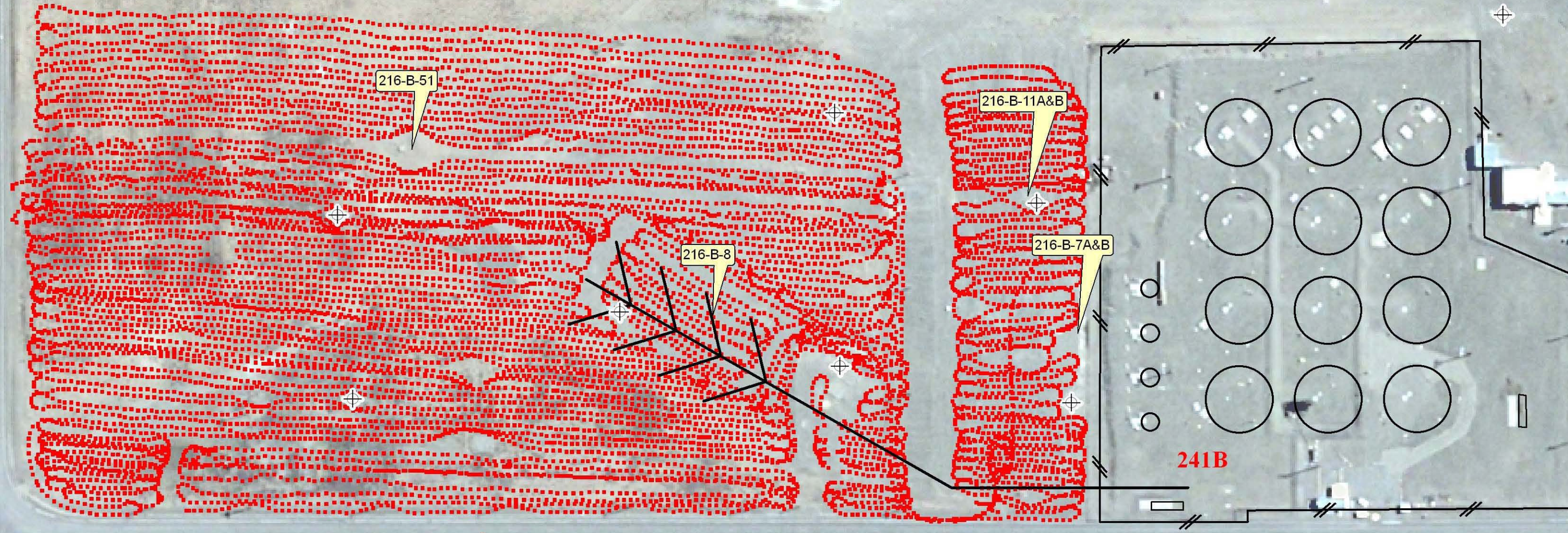
216-B-35-42  
Trenches



A-1

<b>Geophysical Survey</b>	
Date: February 2007	Figure A-1
2302 North Forbes Blvd.	Tucson, AZ 85745 (520) 647-3315

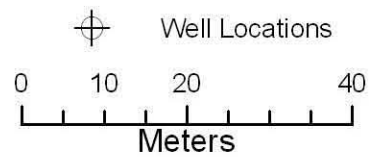
**GO Cart Coverage  
for the 216-B-35-42  
Trenches  
B Complex**



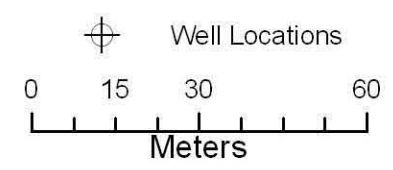
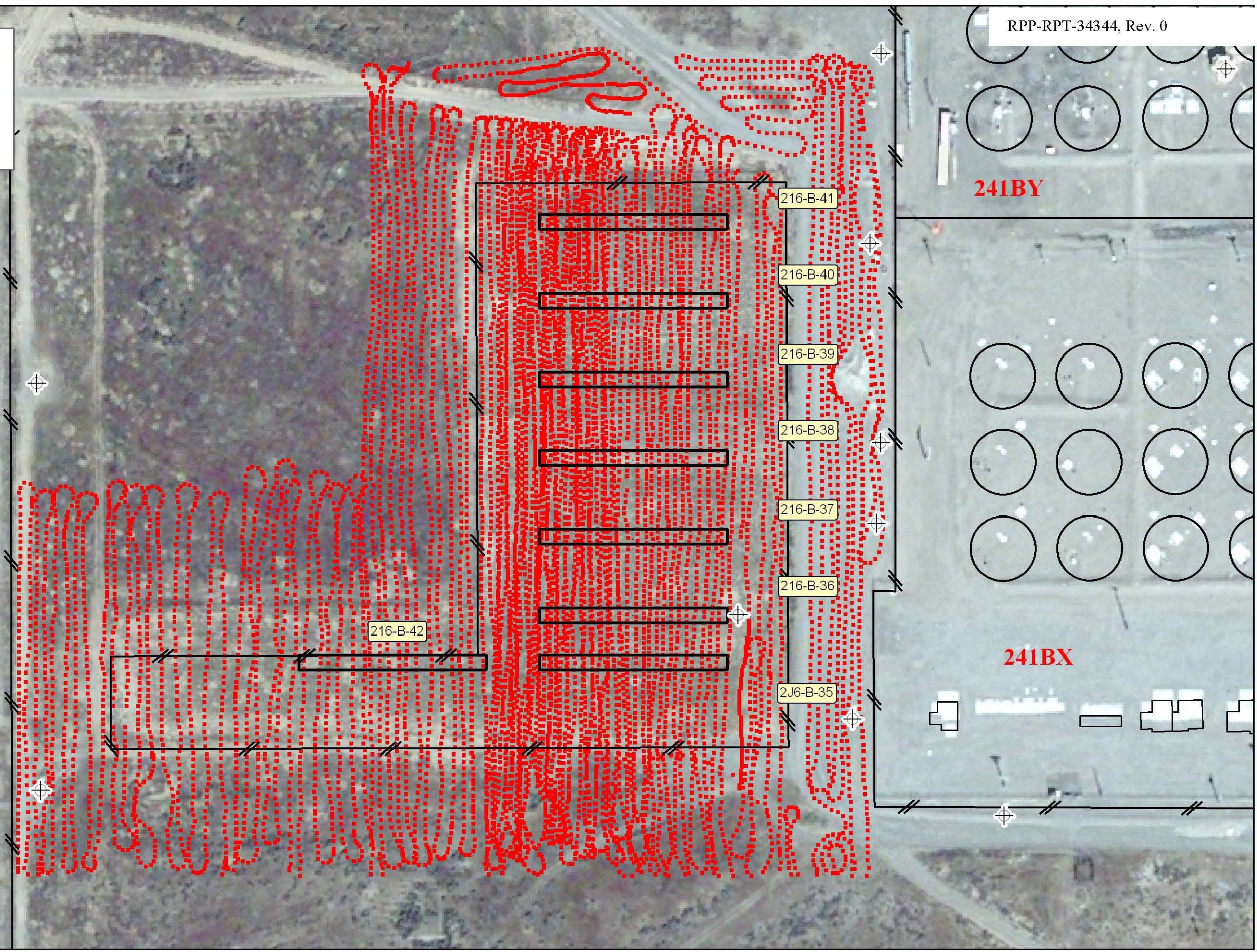
A-2

<b>Geophysical Survey</b>	
<i>Date: February 2007</i>	<i>Figure A-2</i>
2302 North Forbes Blvd.	Tucson, AZ 85745 (520) 647-3315

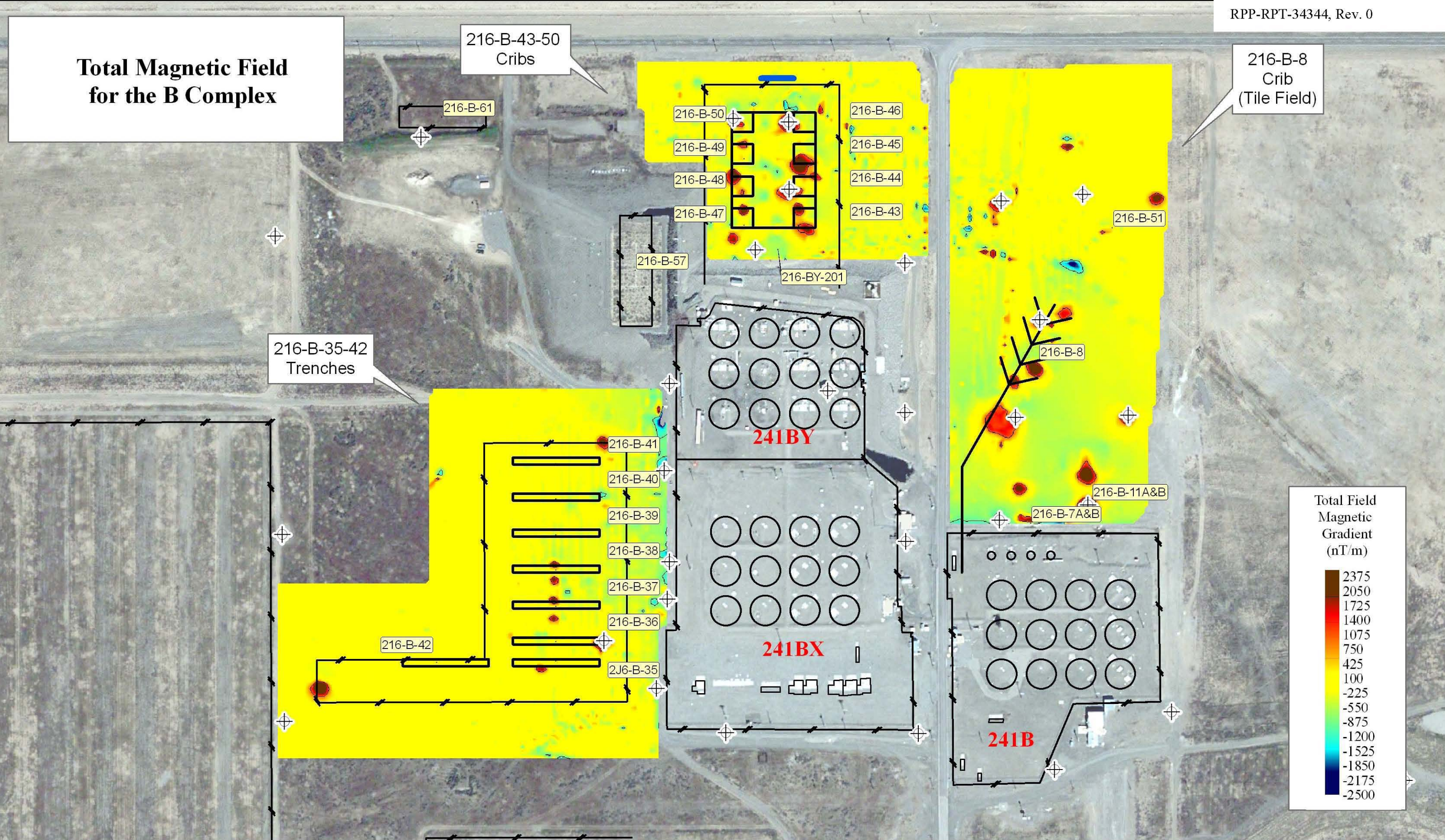
**GO Cart Coverage  
for the 216-B-43-50  
Cribs  
B Complex**



**GO Cart Coverage  
for the 216-B-35-42  
Trenches  
B Complex**



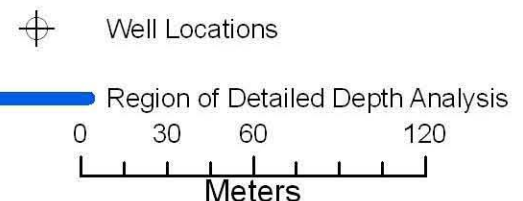
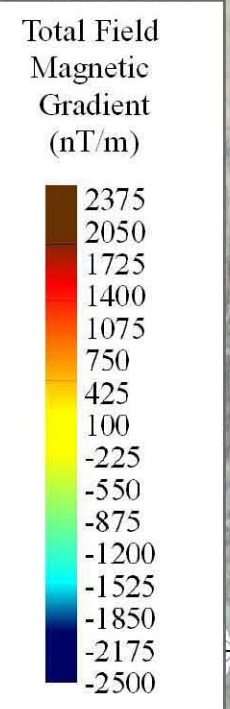
# Total Magnetic Field for the B Complex



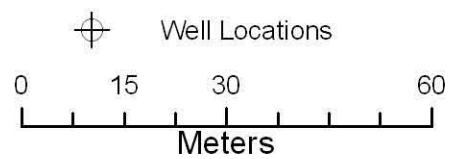
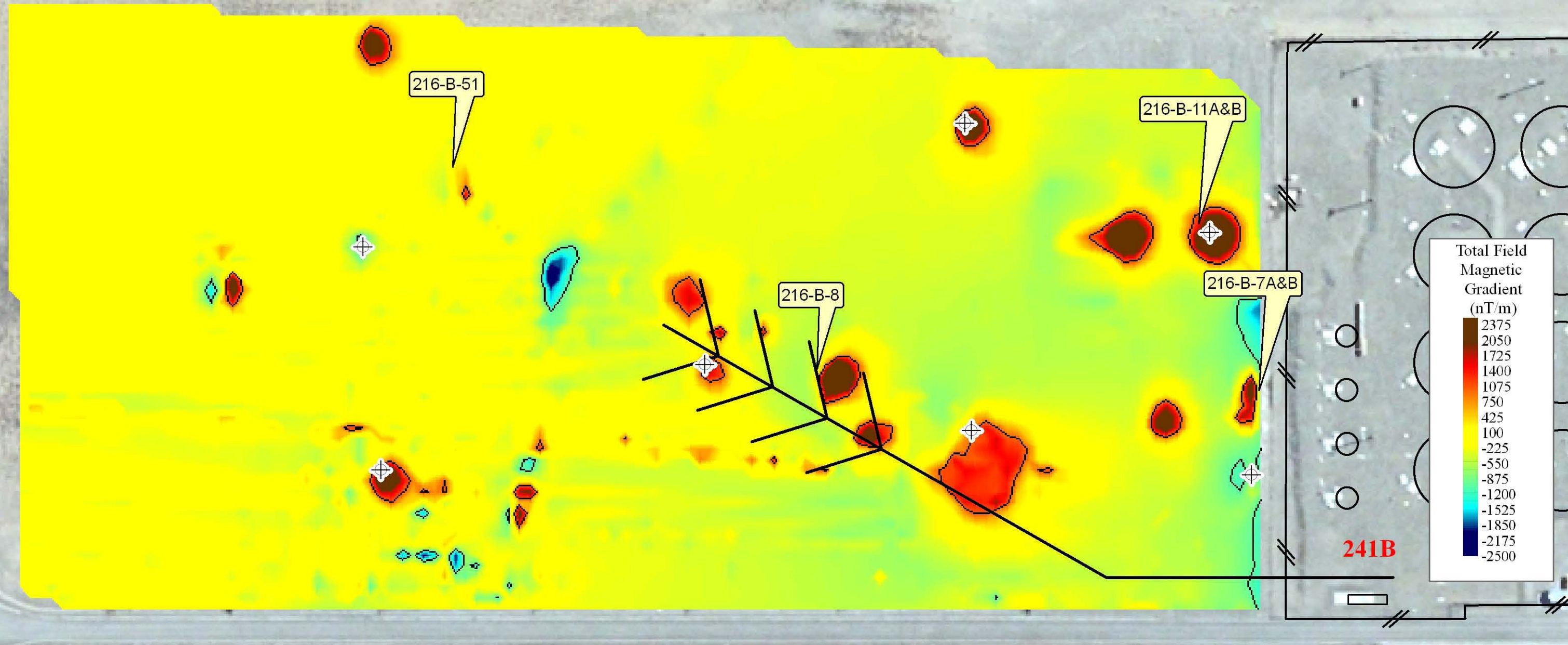
216-B-8 Crib (Tile Field)

216-B-43-50 Cribs

216-B-35-42 Trenches



**Total Magnetic Field  
for the 216-B-8  
(Tile Field)  
B Complex**

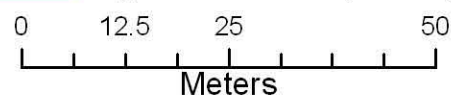


# Total Magnetic Field for the 216-B-43-50 Cribs B Complex



⊕ Well Locations

— Region of Detailed Depth Analysis



A-7

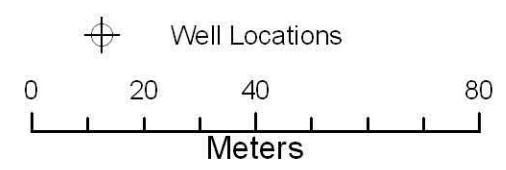
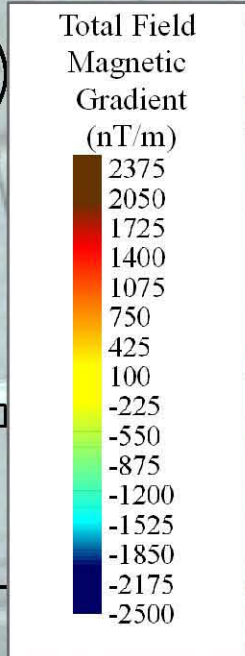
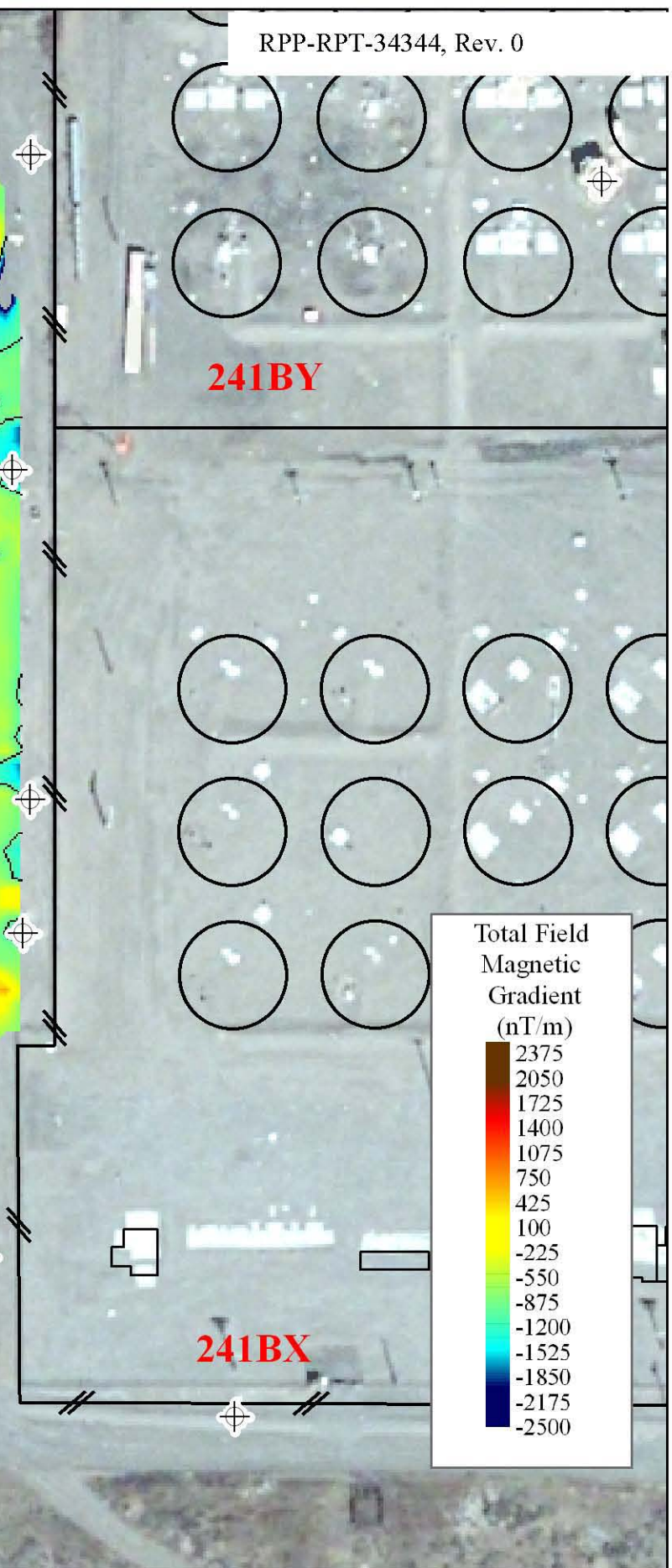
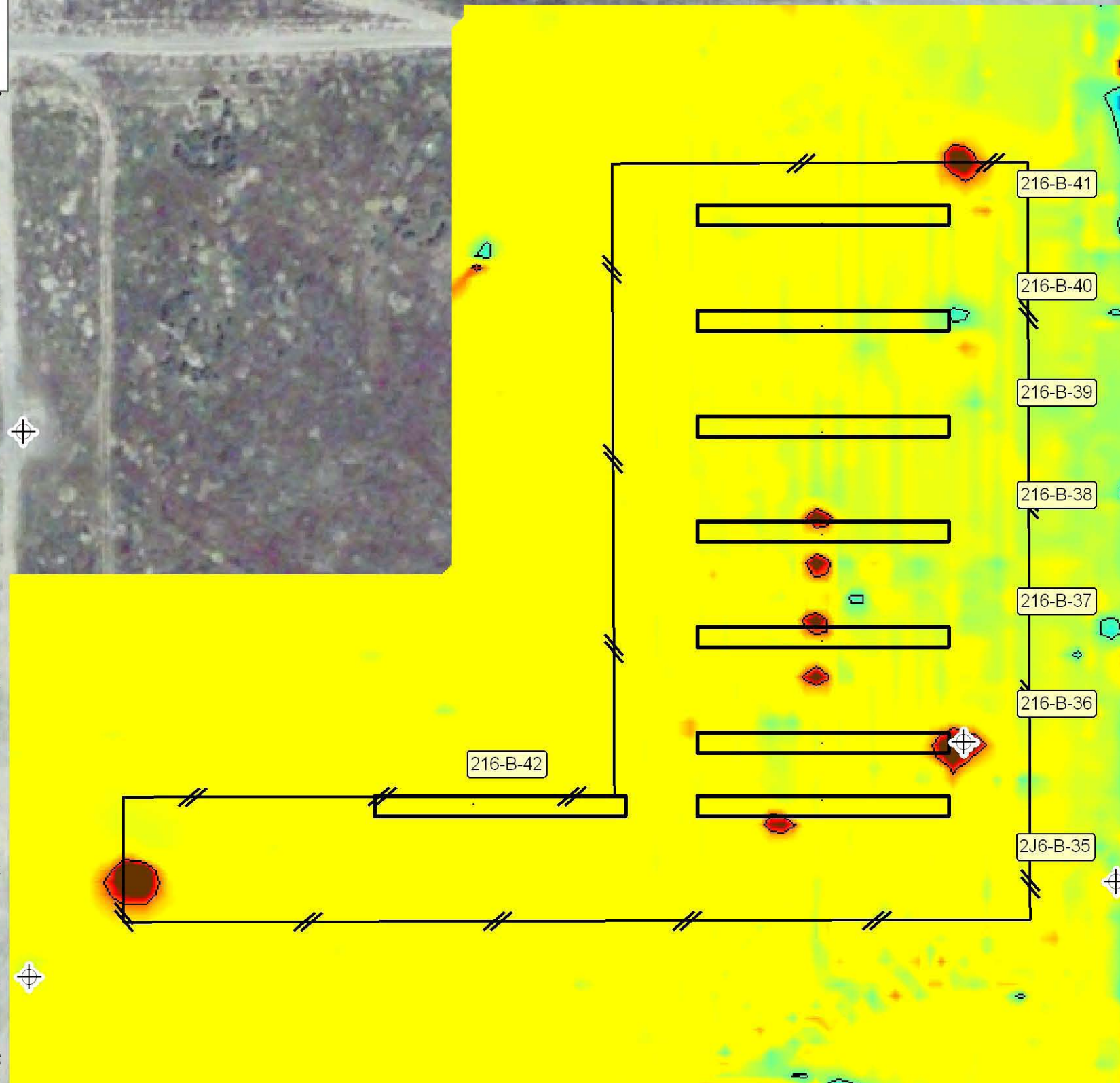
## Geophysical Survey

Date: February 2007

Figure A-7

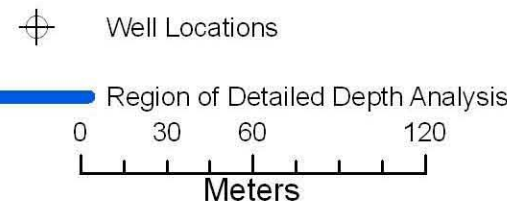
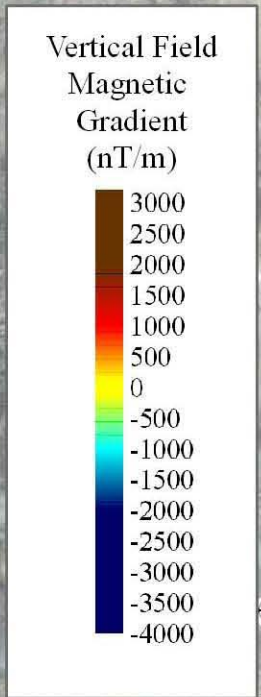
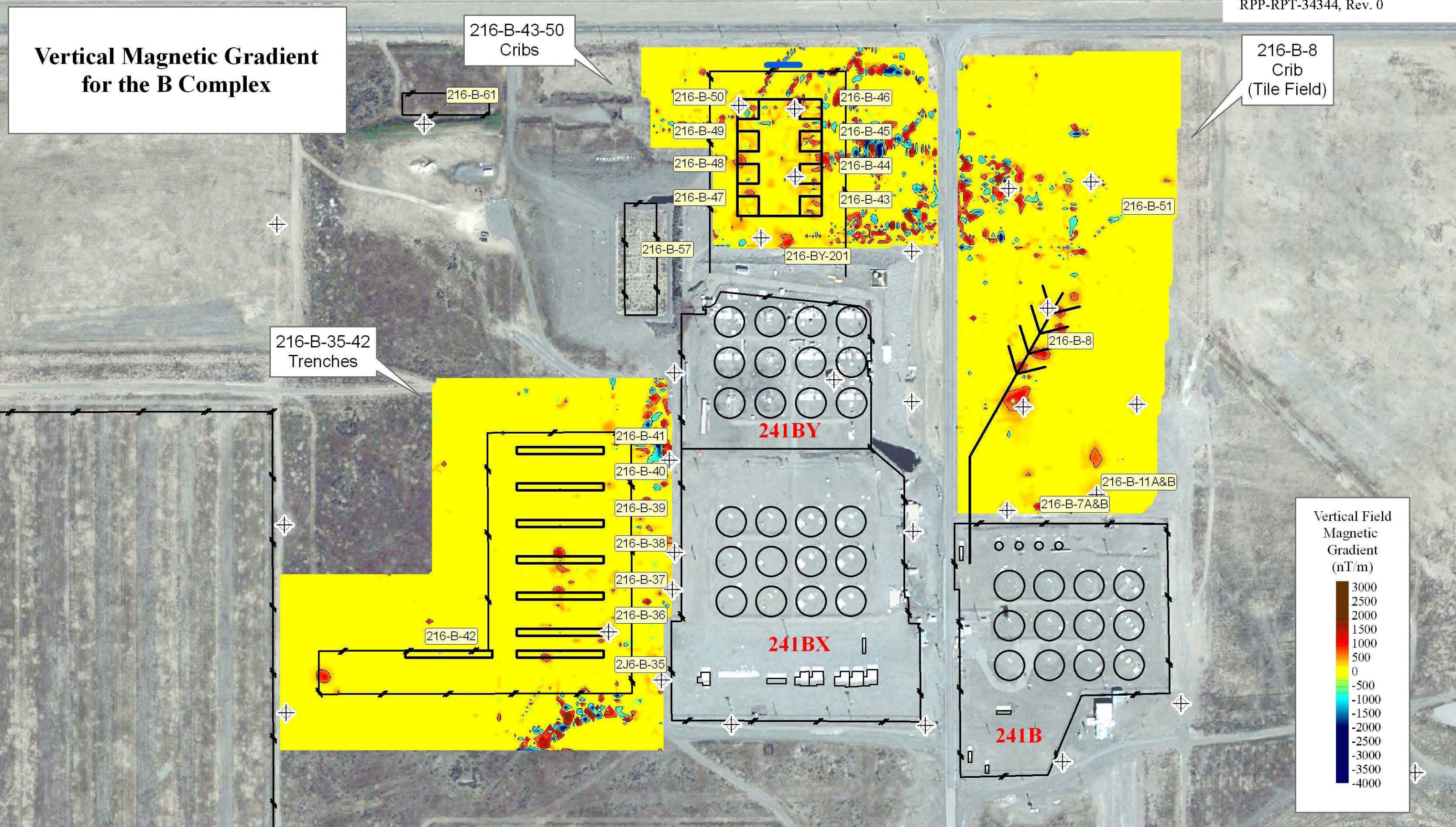
2302 North Forbes Blvd. Tucson, AZ 85745 (520) 647-3315

# Total Magnetic Field for the 216-B-35-42 Trenches B Complex

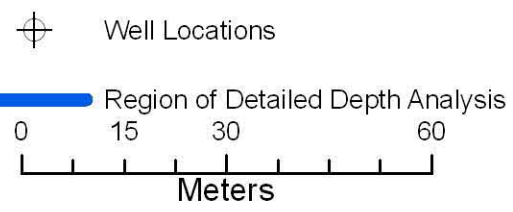
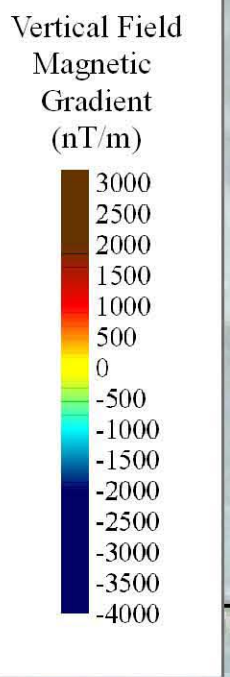
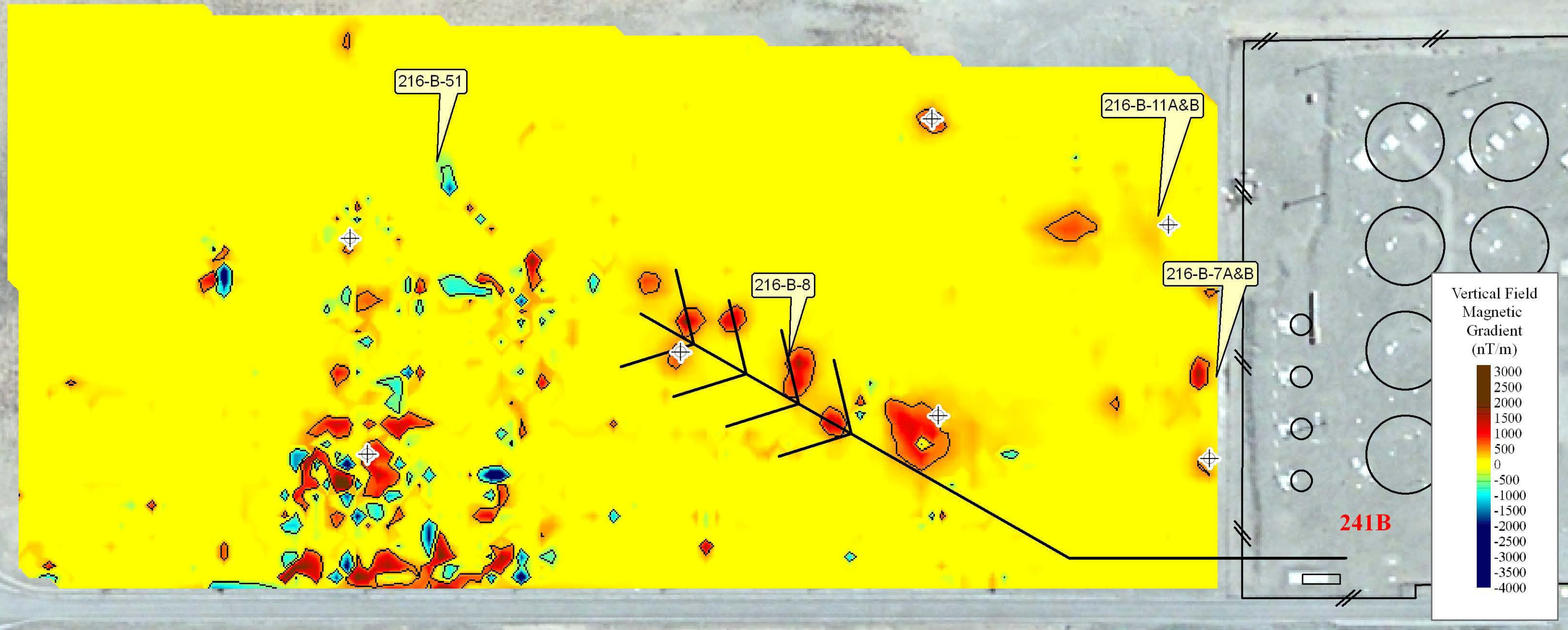


A-8

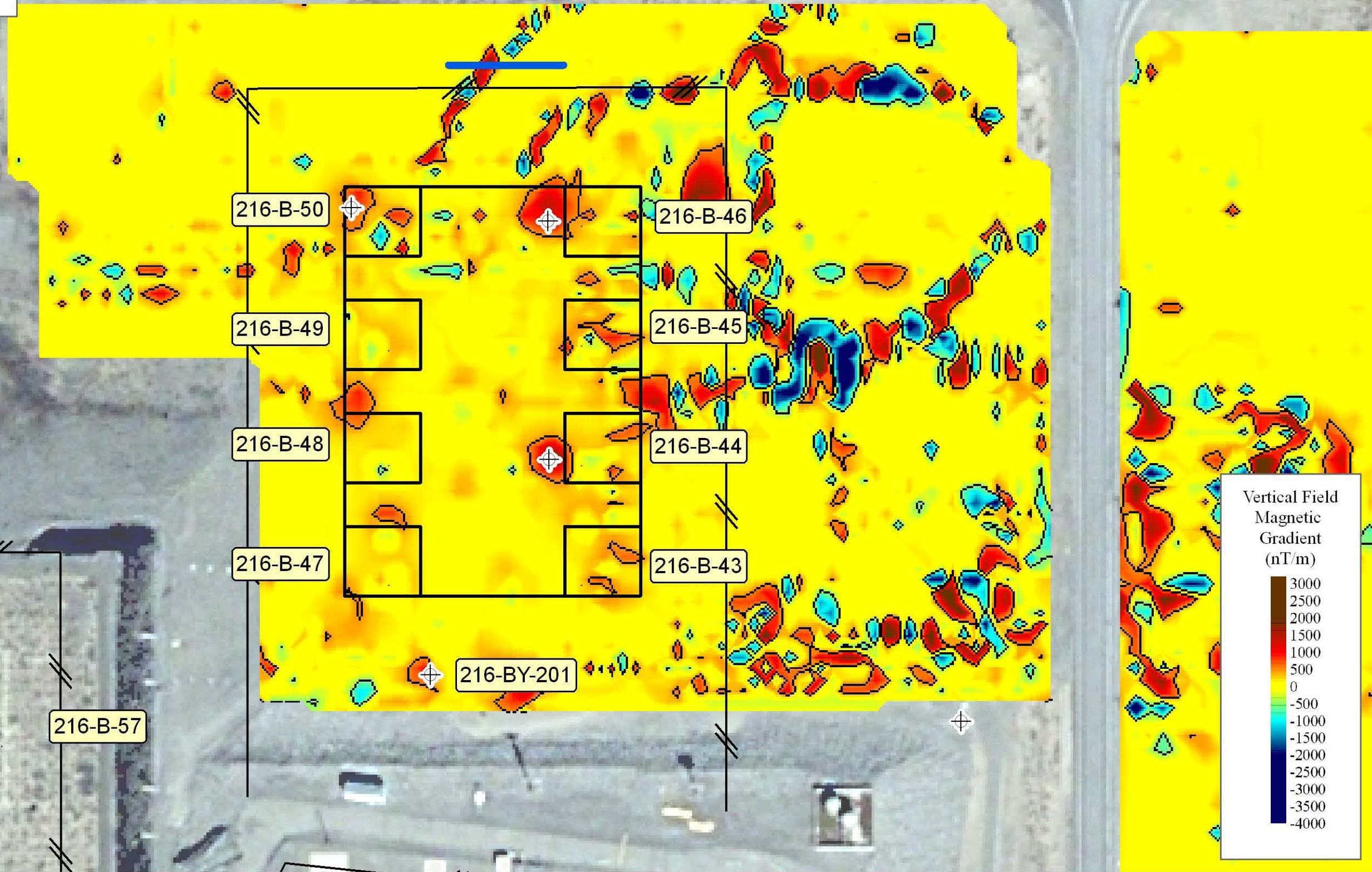
# Vertical Magnetic Gradient for the B Complex



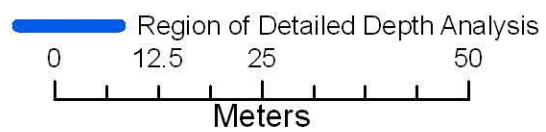
**Vertical Magnetic Gradient  
for the 216-B-8  
(Tile Field)  
B Complex**



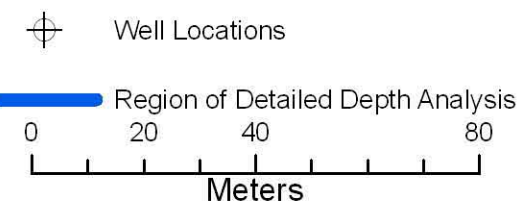
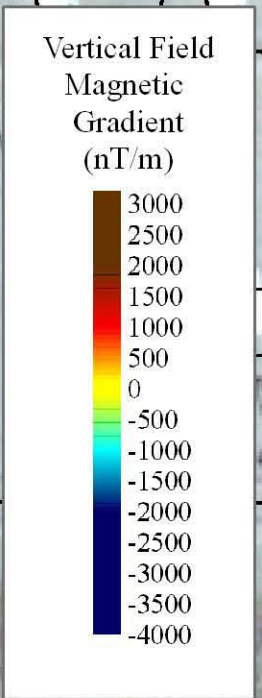
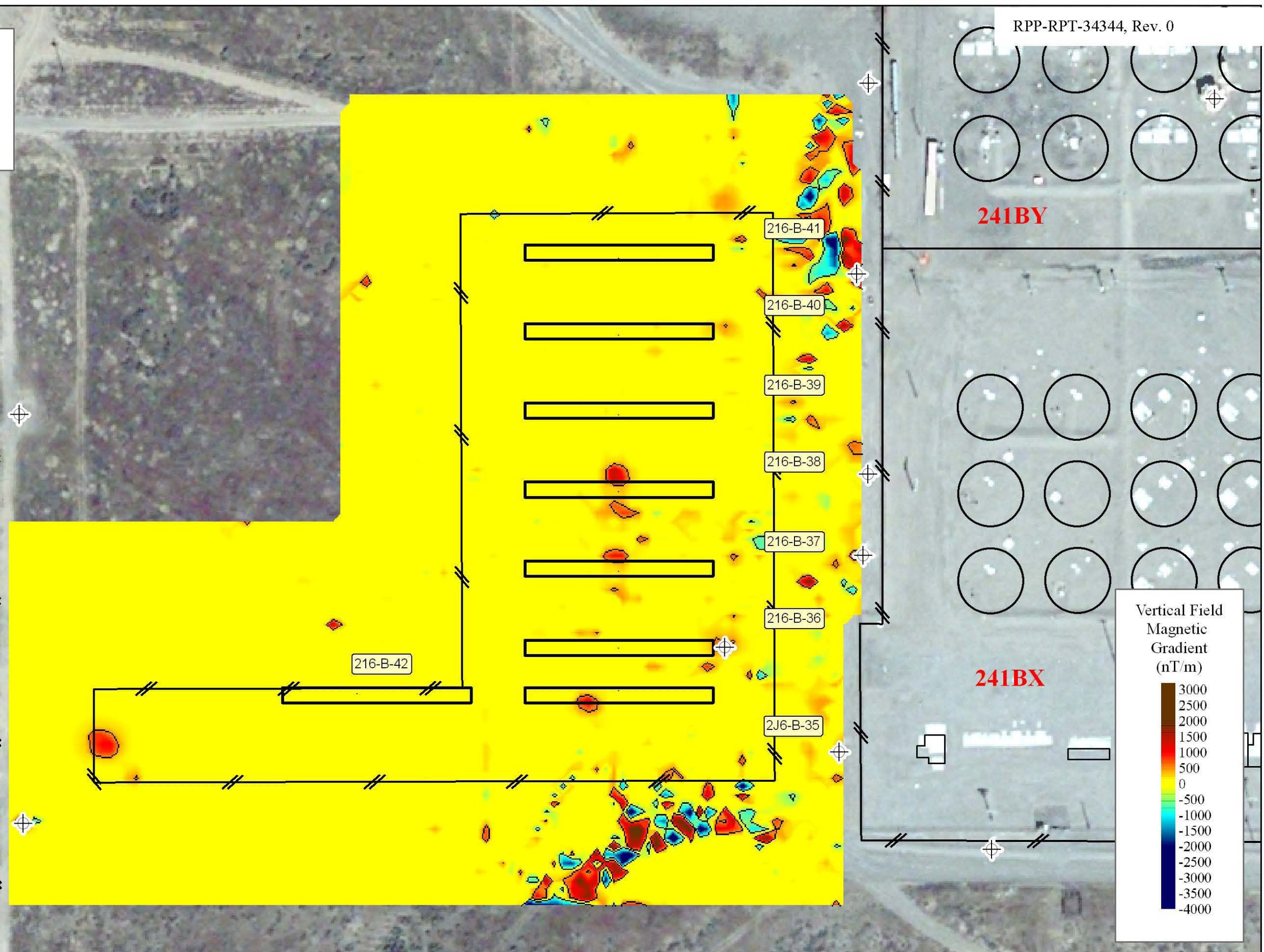
# Vertical Magnetic Gradient for the 216-B-43-50 Cribs B Complex



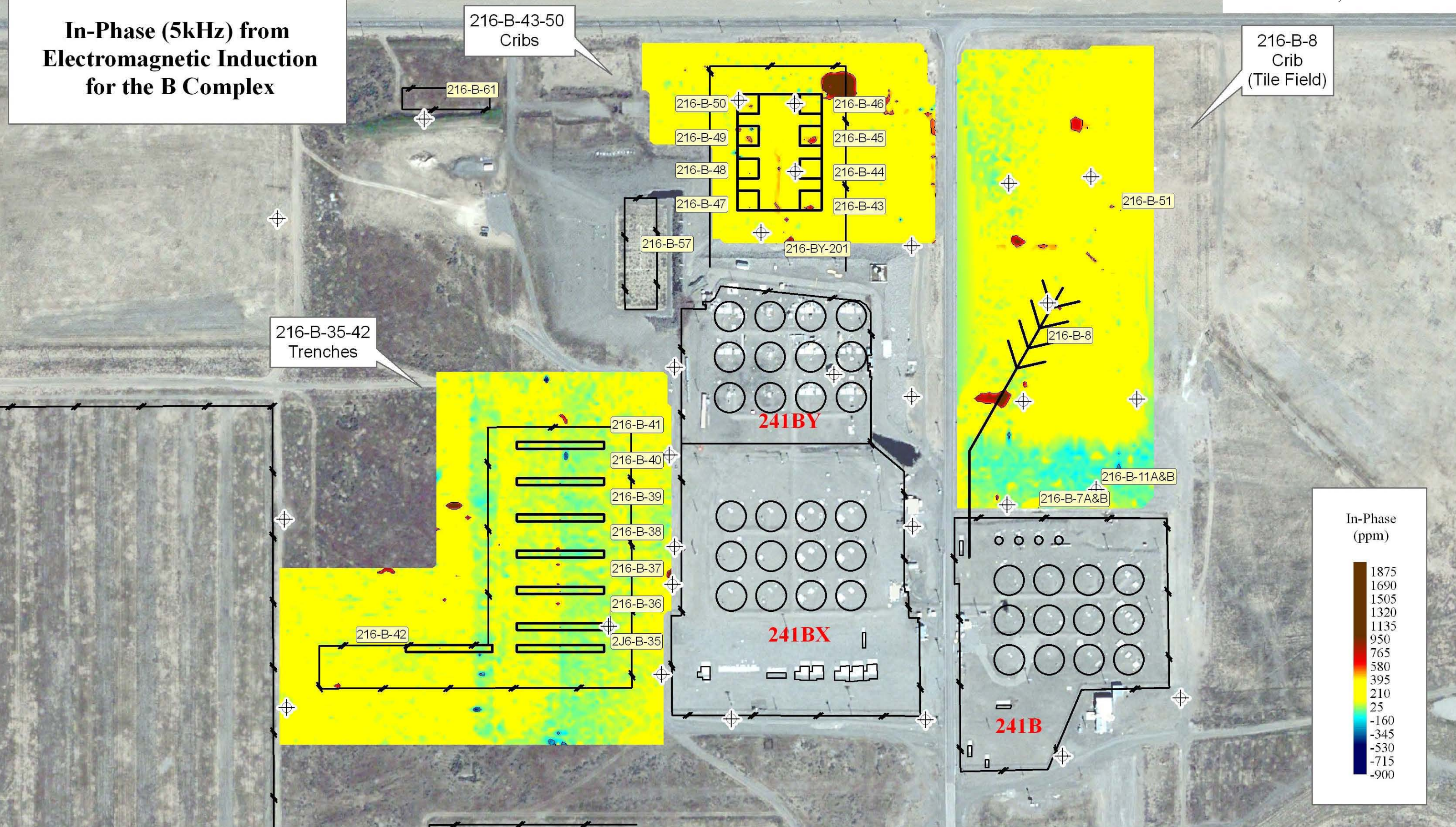
⊕ Well Locations



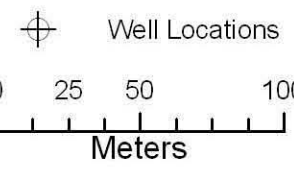
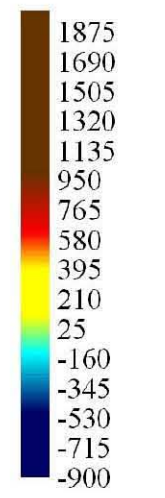
# Vertical Magnetic Gradient for the 216-B-35-42 Trenches B Complex



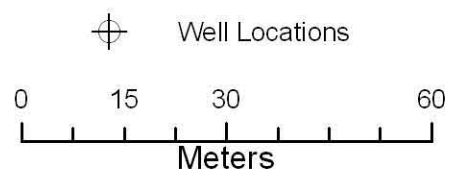
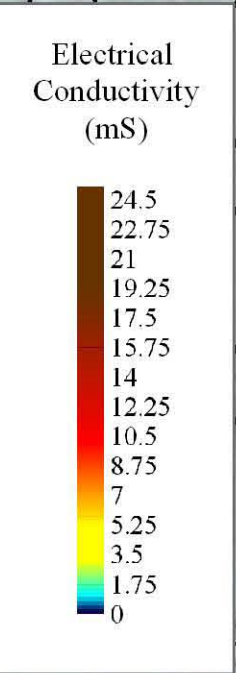
# In-Phase (5kHz) from Electromagnetic Induction for the B Complex



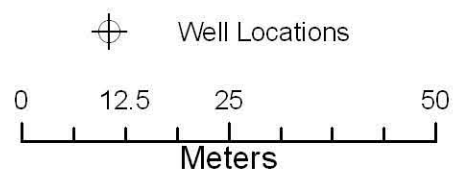
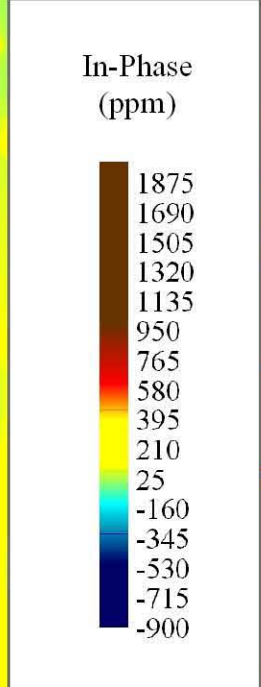
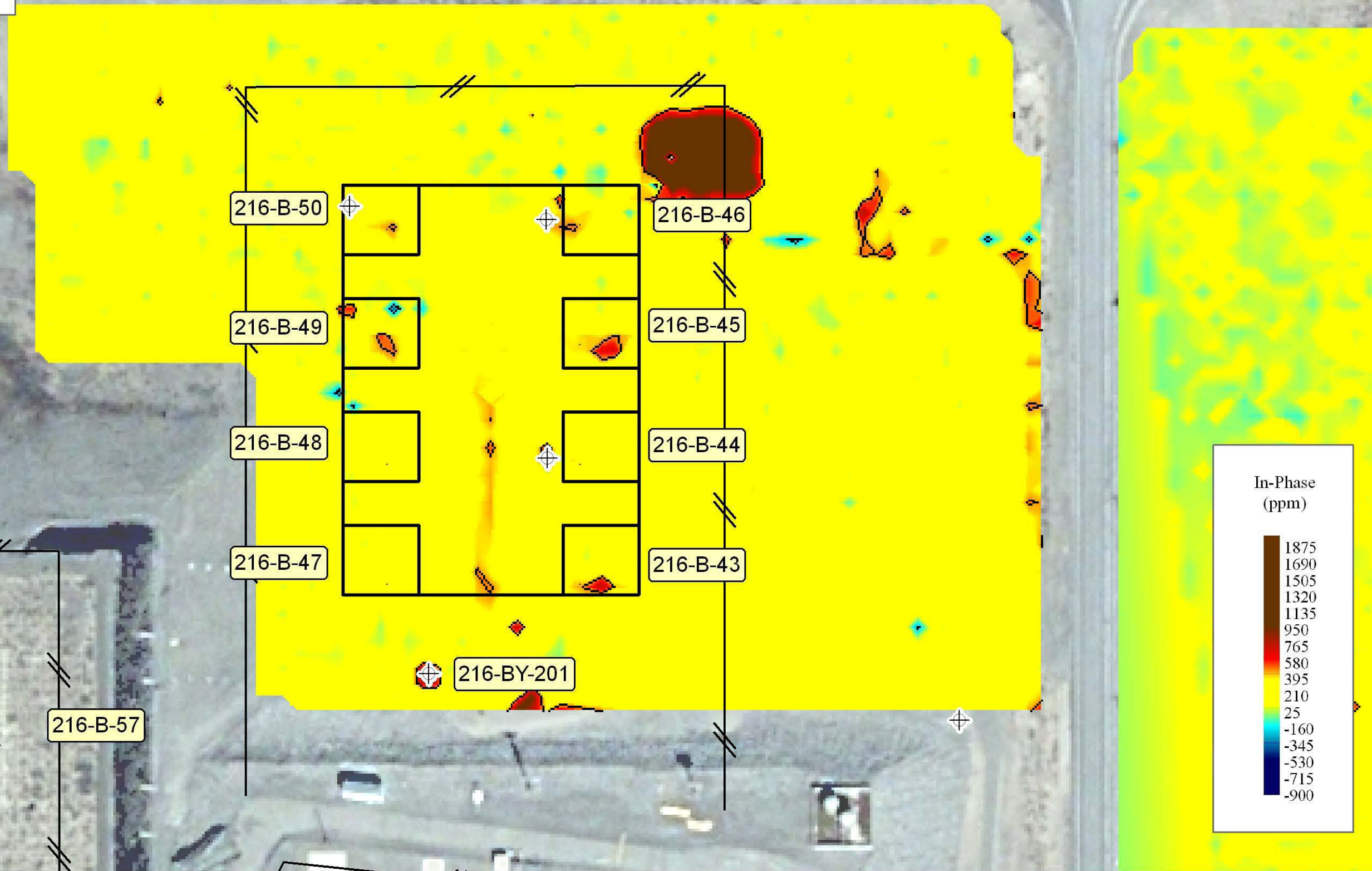
In-Phase  
(ppm)



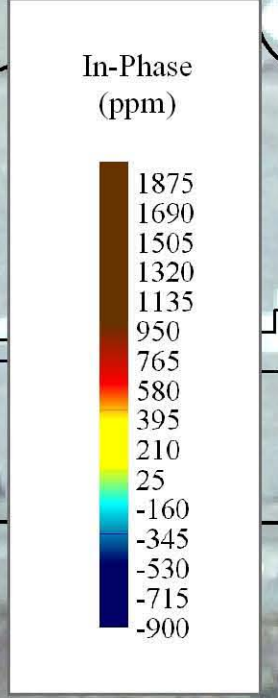
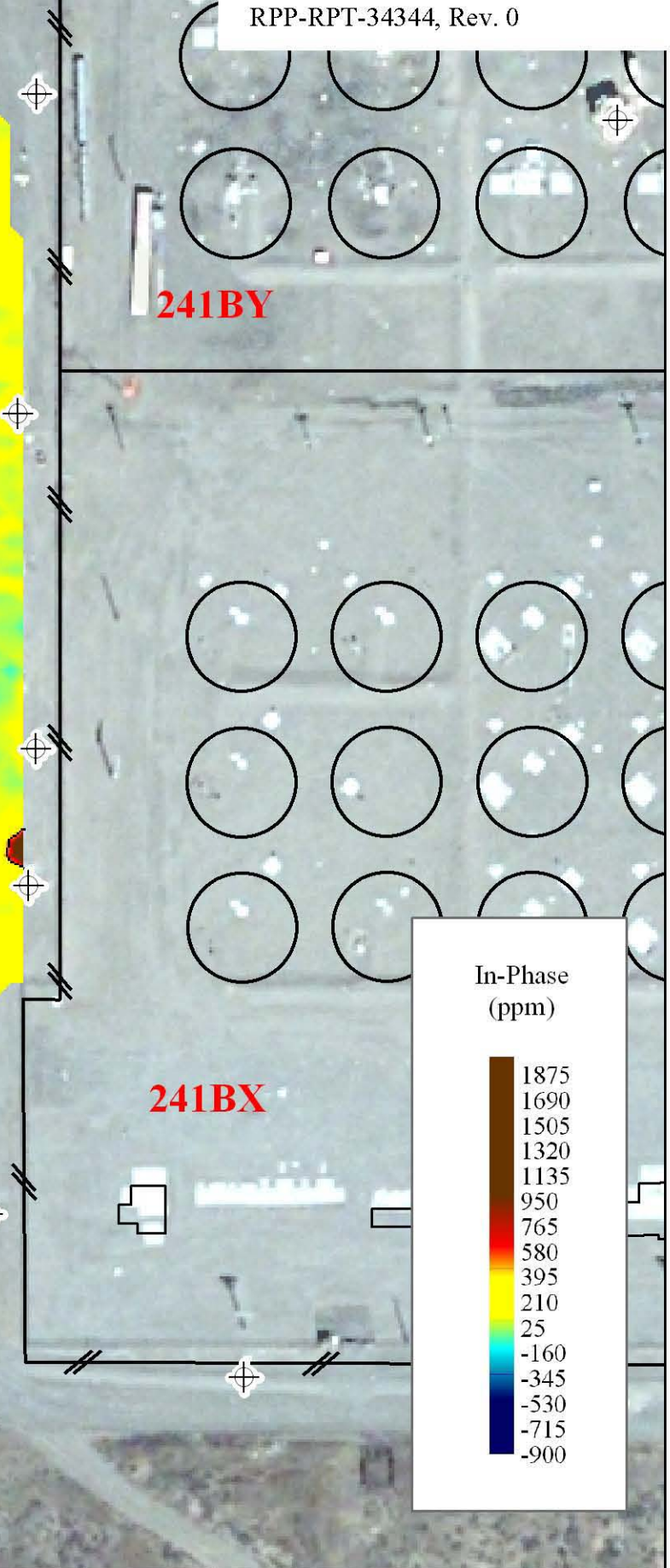
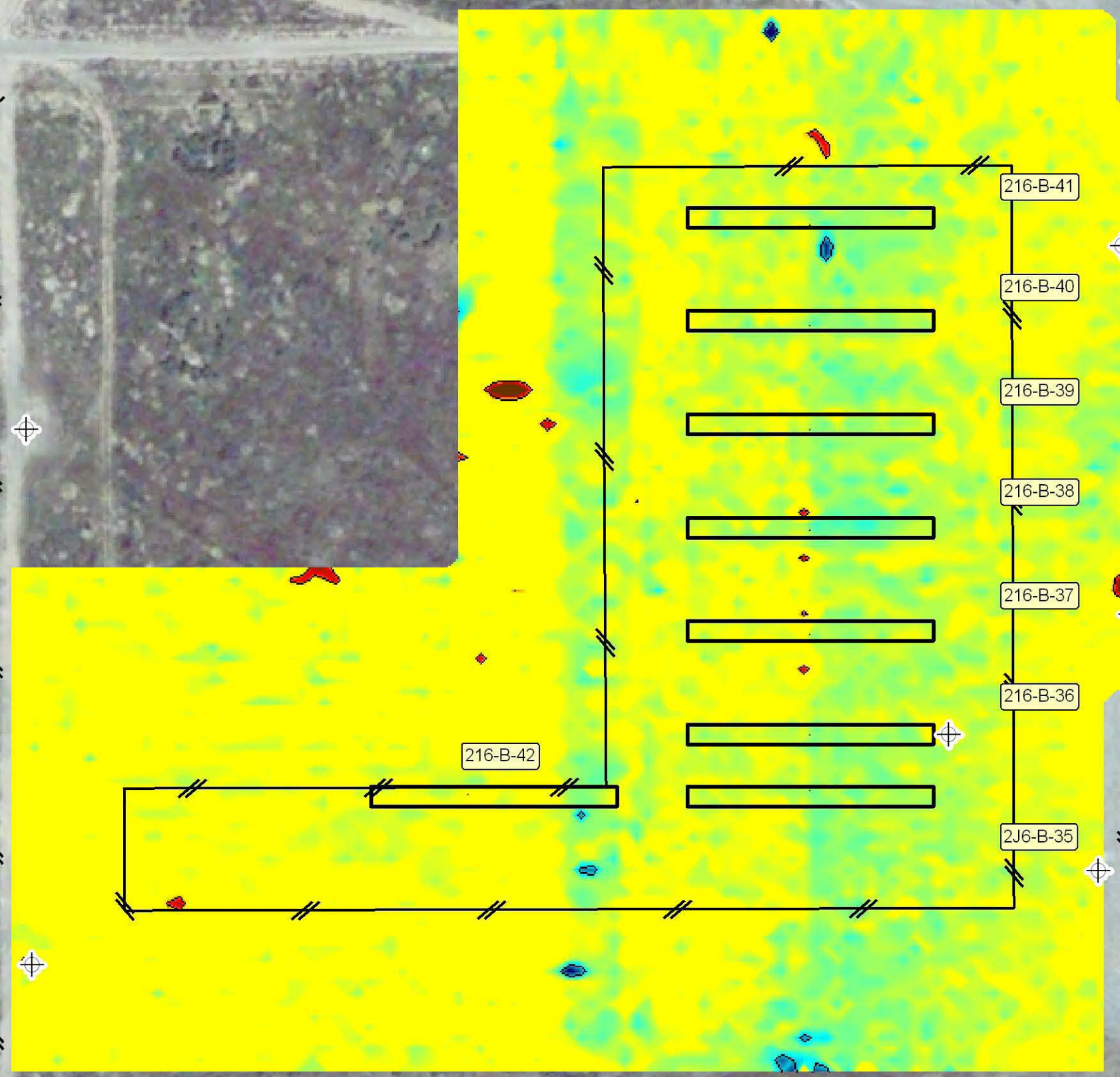
**In-Phase (5kHz) from  
Electromagnetic Induction  
216-B-8 Crib (Tile Field)  
B Complex**



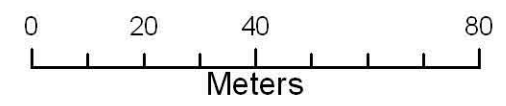
**In-Phase (5kHz) from  
Electromagnetic Induction  
216-B-43-50 Cribs  
B Complex**



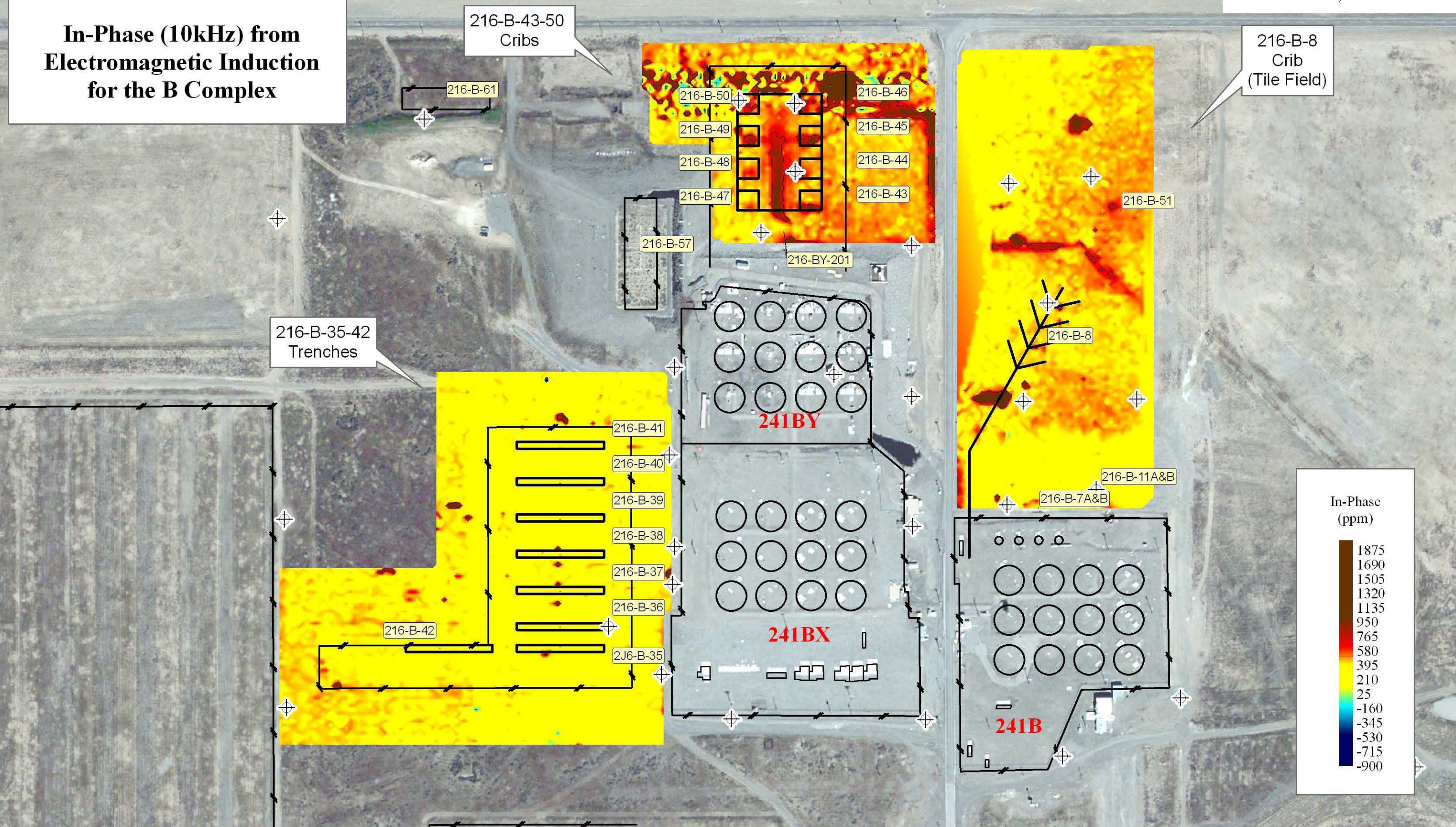
# In-Phase (5kHz) from Electromagnetic Induction 216-B-35-42 Trenches B Complex



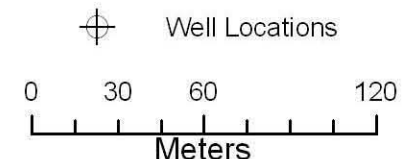
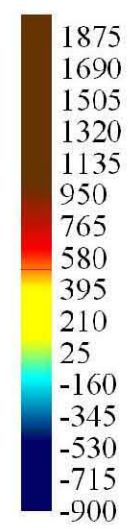
Well Locations



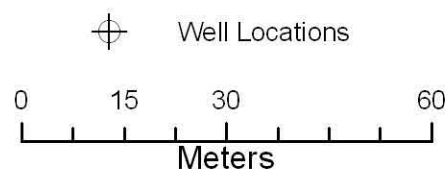
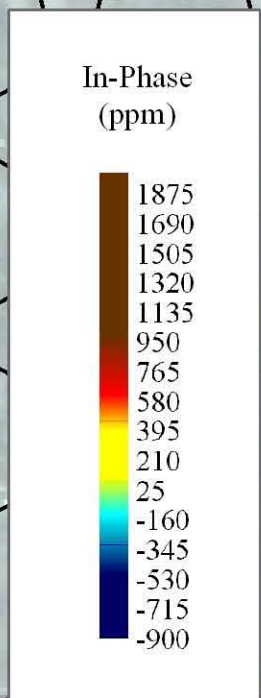
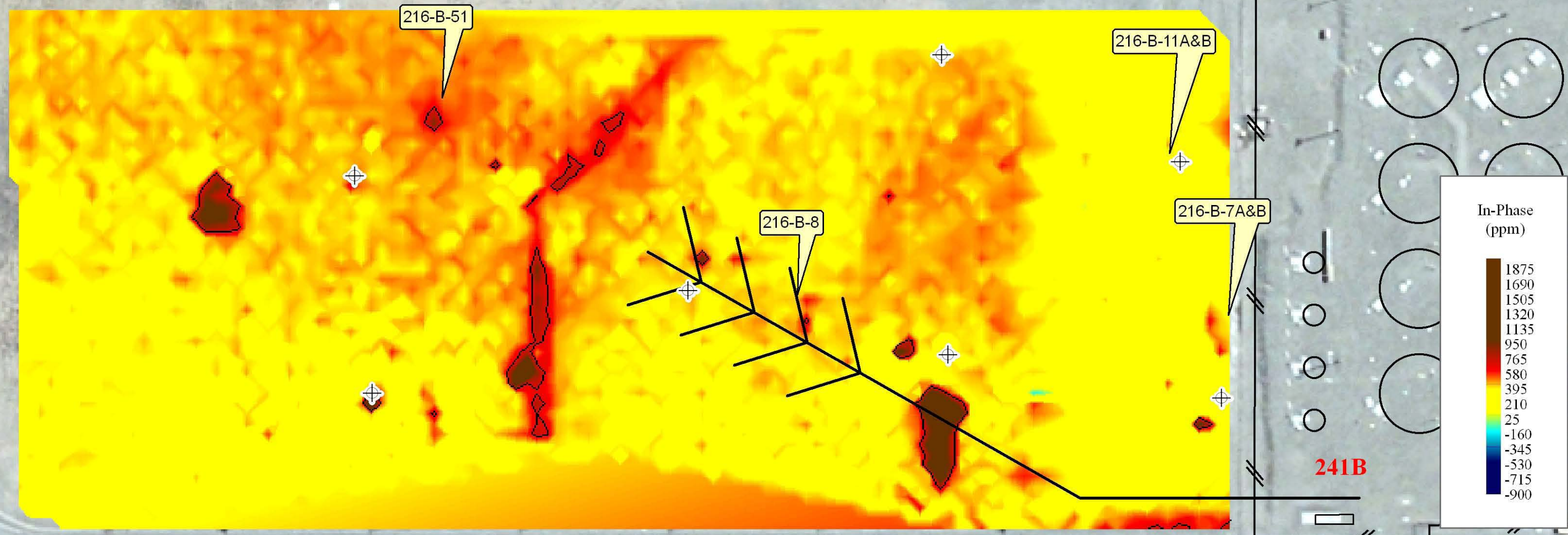
# In-Phase (10kHz) from Electromagnetic Induction for the B Complex



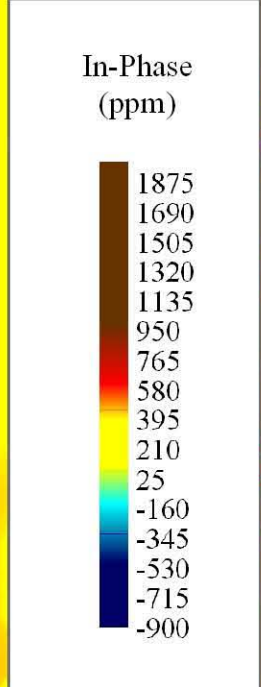
In-Phase (ppm)



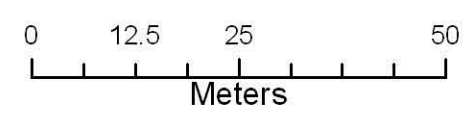
**In-Phase (10kHz) from  
Electromagnetic Induction  
216-B-8Crib (Tile Field)  
B Complex**



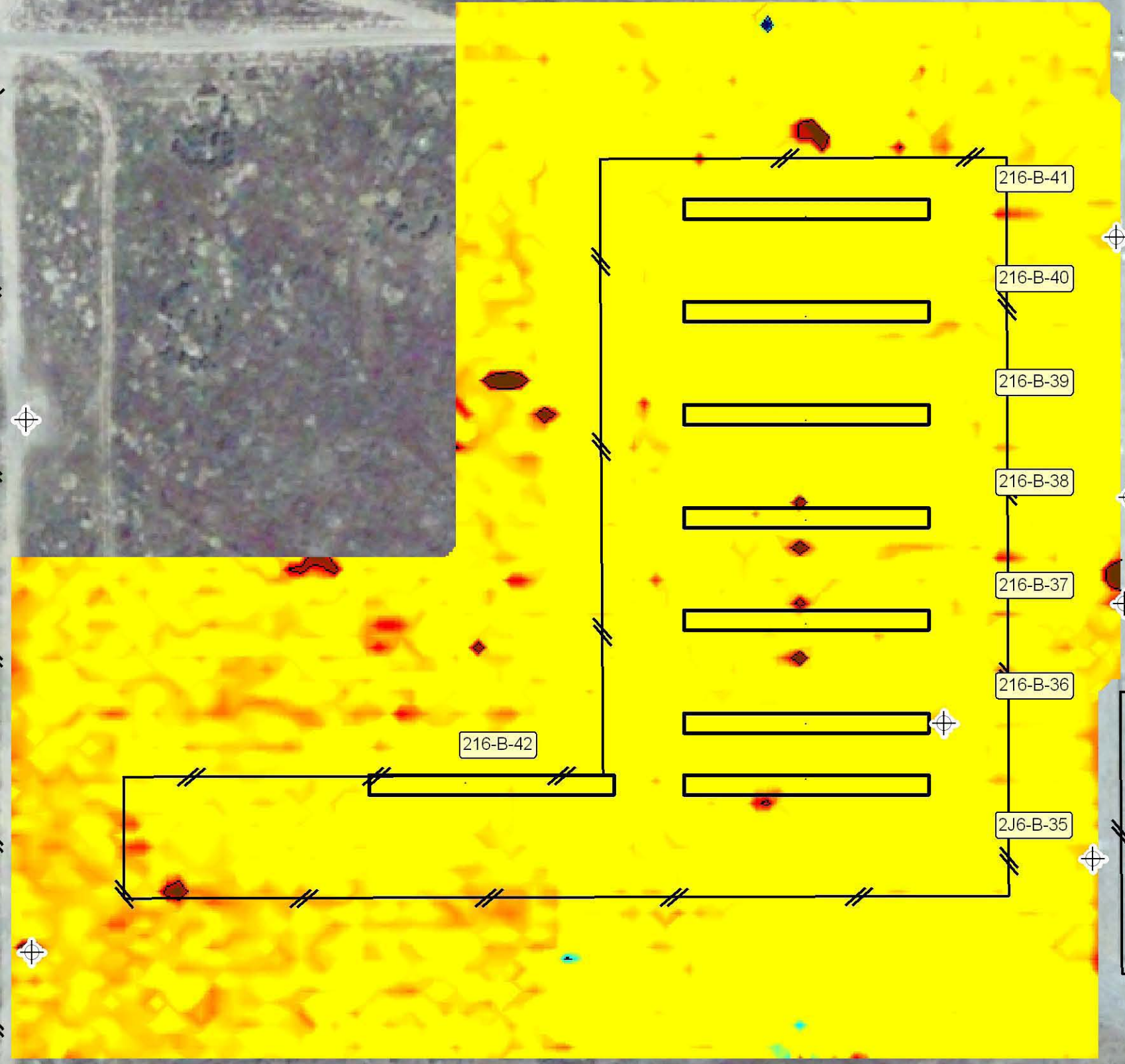
**In-Phase (10kHz) from  
Electromagnetic Induction  
216-B-43-50 Cribs  
B Complex**



⊕ Well Locations

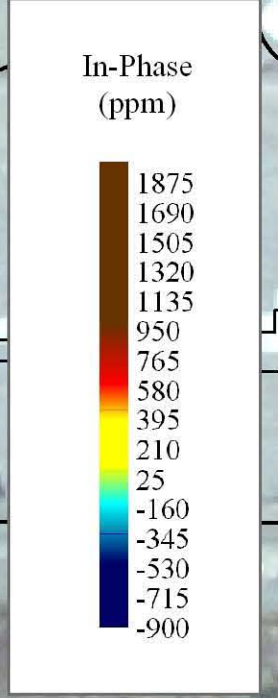


**In-Phase (10kHz) from  
Electromagnetic Induction  
216-B-35-42 Trenches  
B Complex**

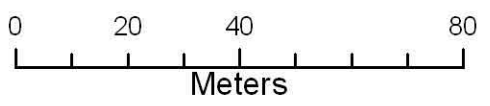


**241BY**

**241BX**

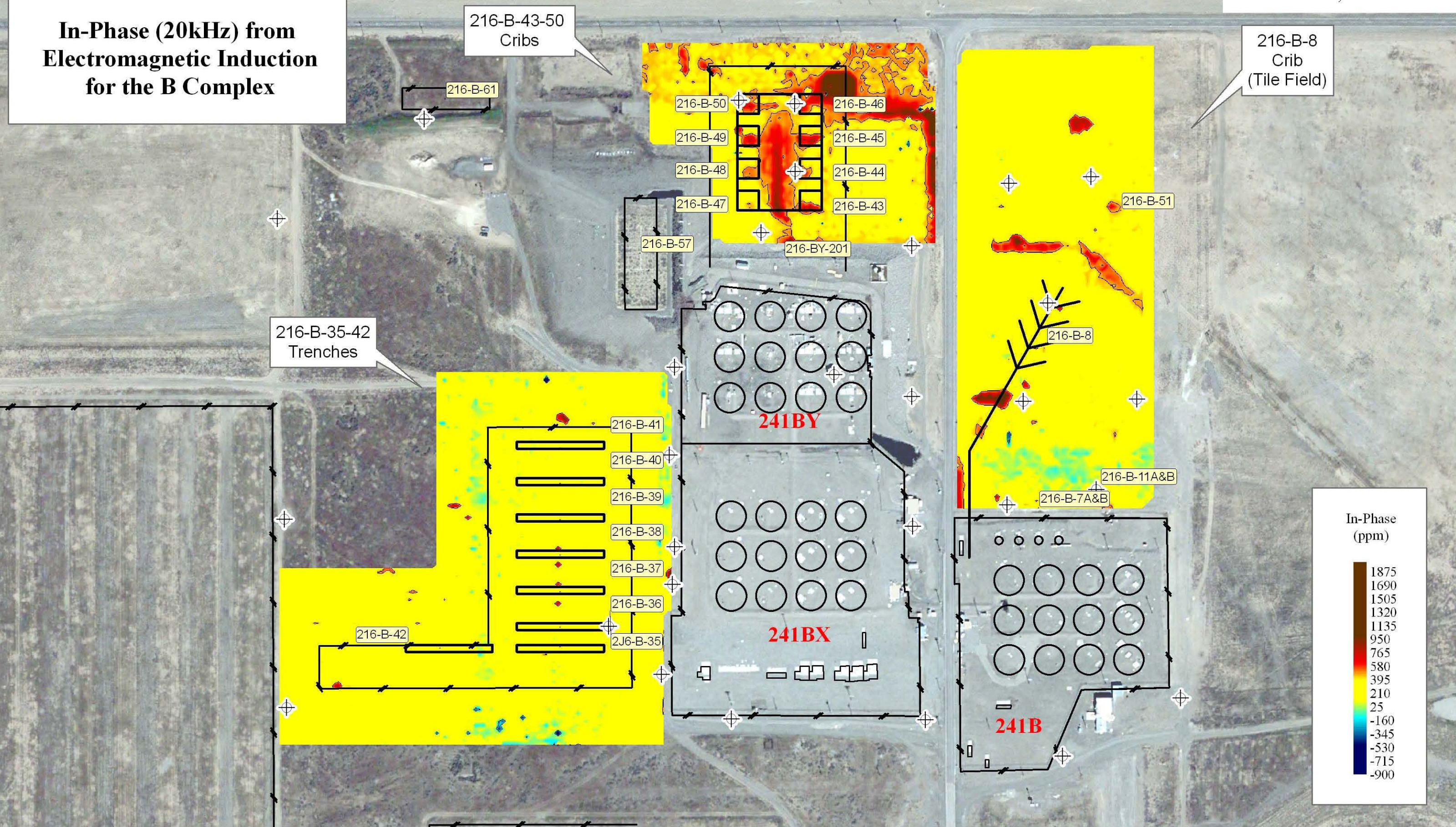


Well Locations

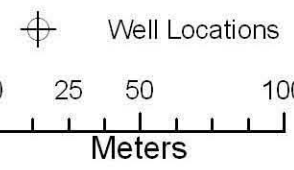
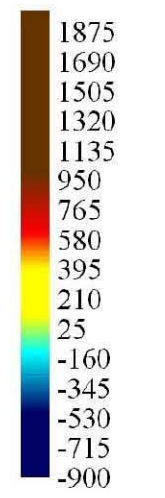


A-20

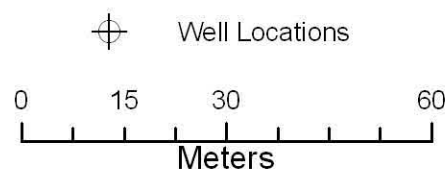
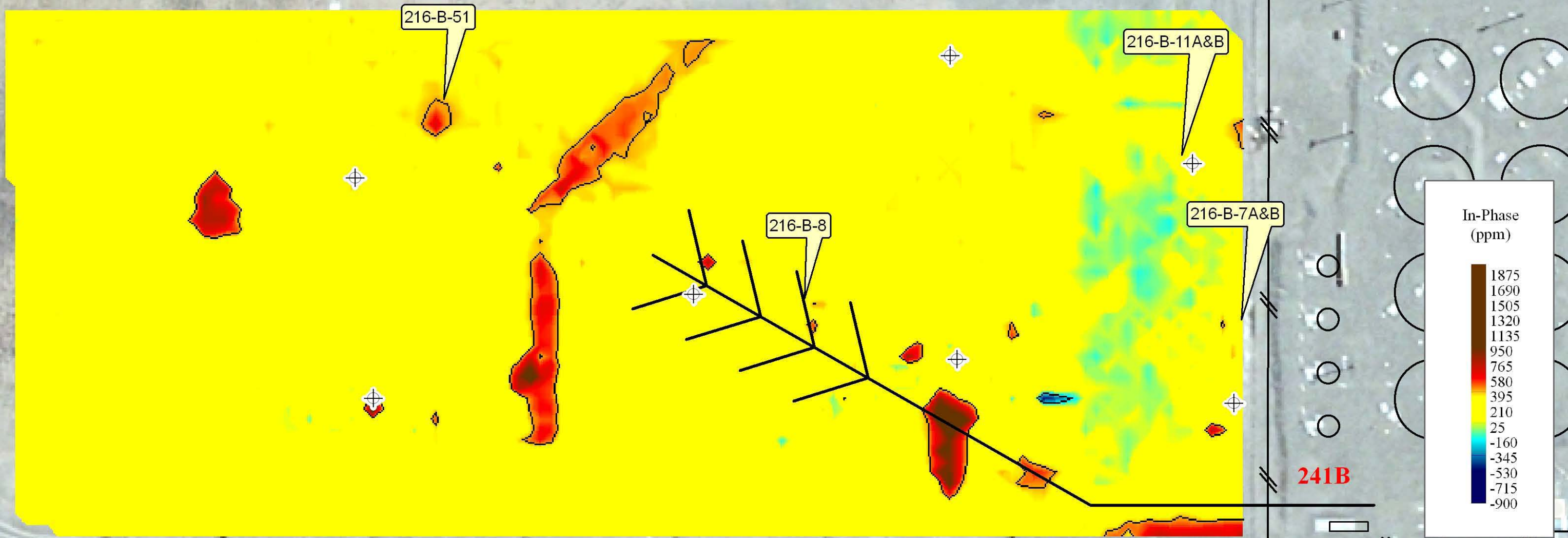
# In-Phase (20kHz) from Electromagnetic Induction for the B Complex



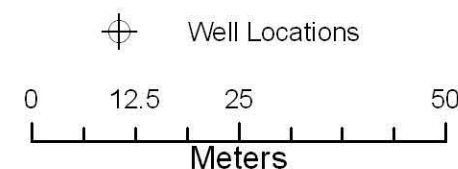
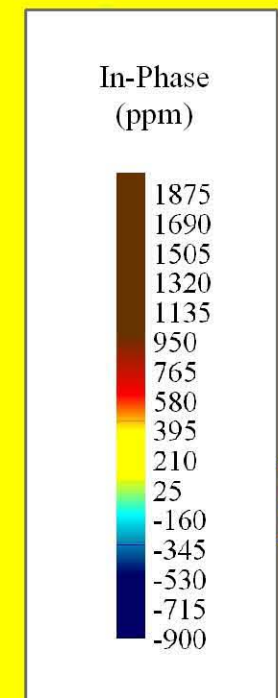
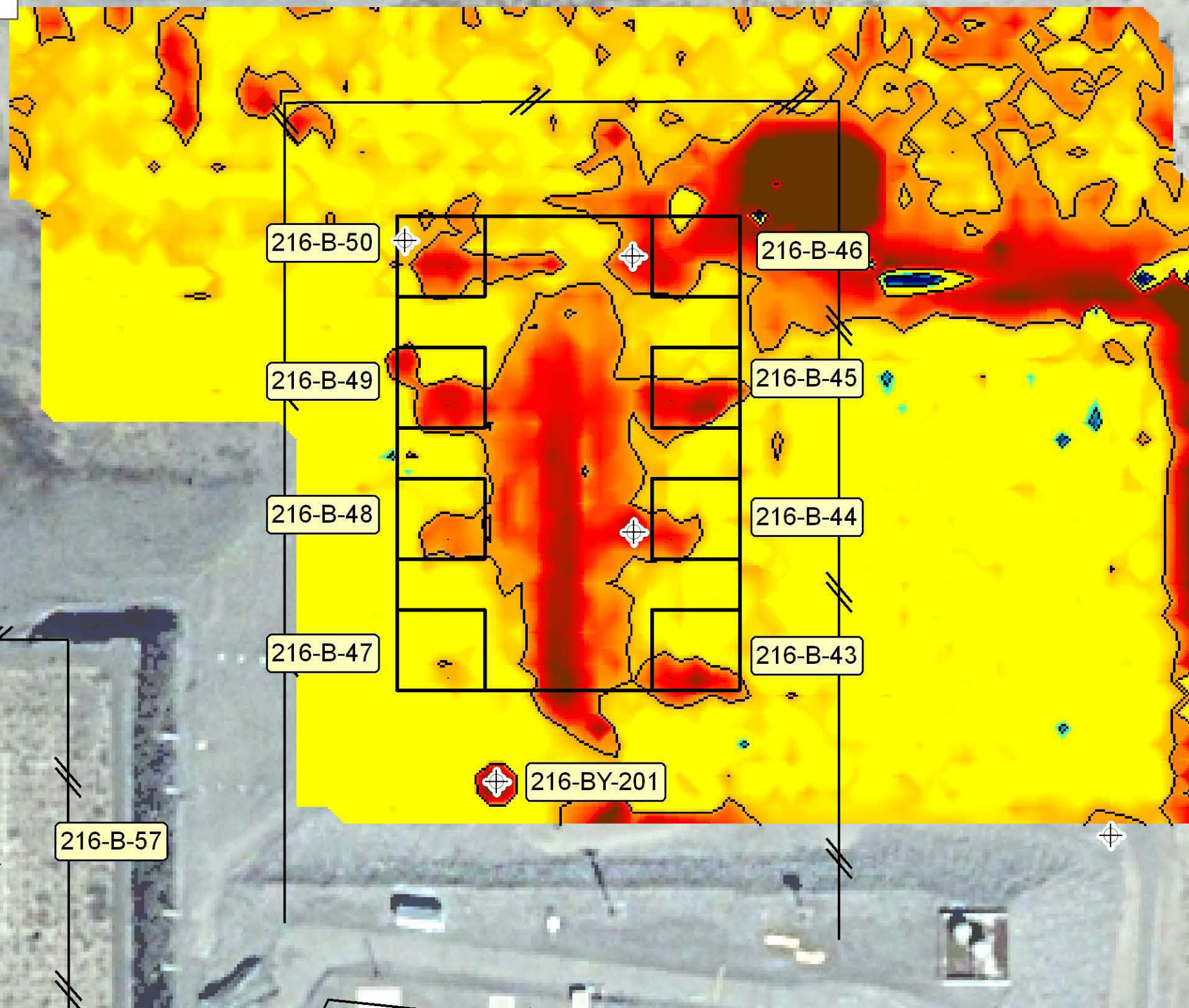
In-Phase  
(ppm)



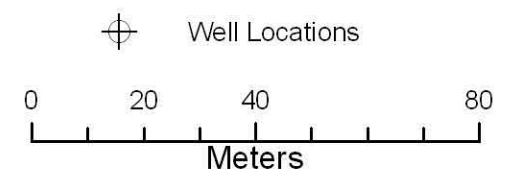
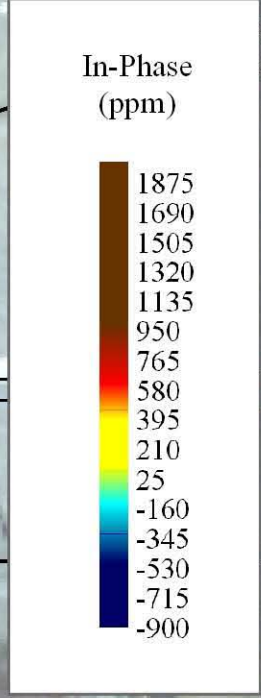
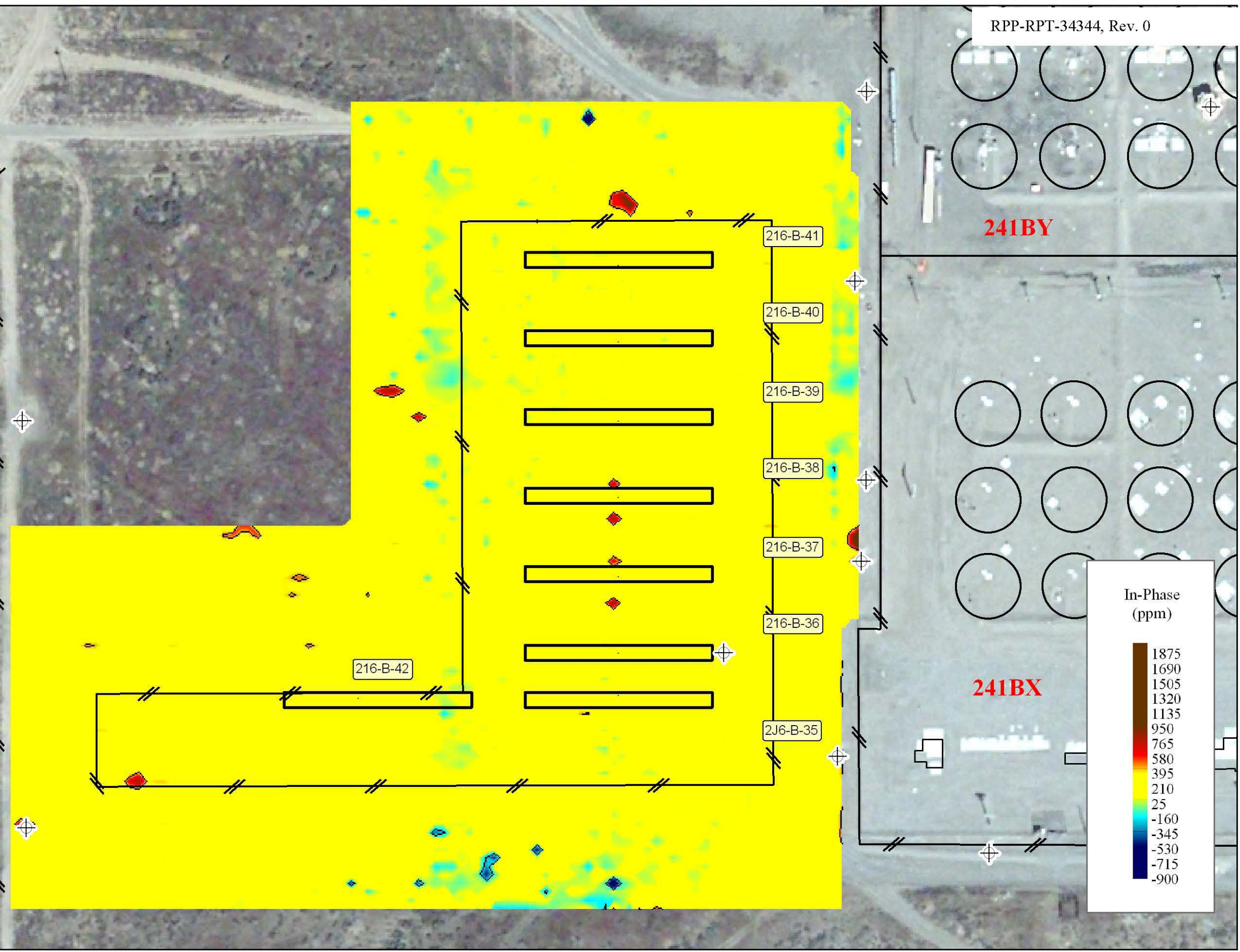
**In-Phase (20kHz) from  
Electromagnetic Induction  
216-B-8Crib (Tile Field)  
B Complex**



**In-Phase (20kHz) from  
Electromagnetic Induction  
216-B-43-50 Cribs  
B Complex**

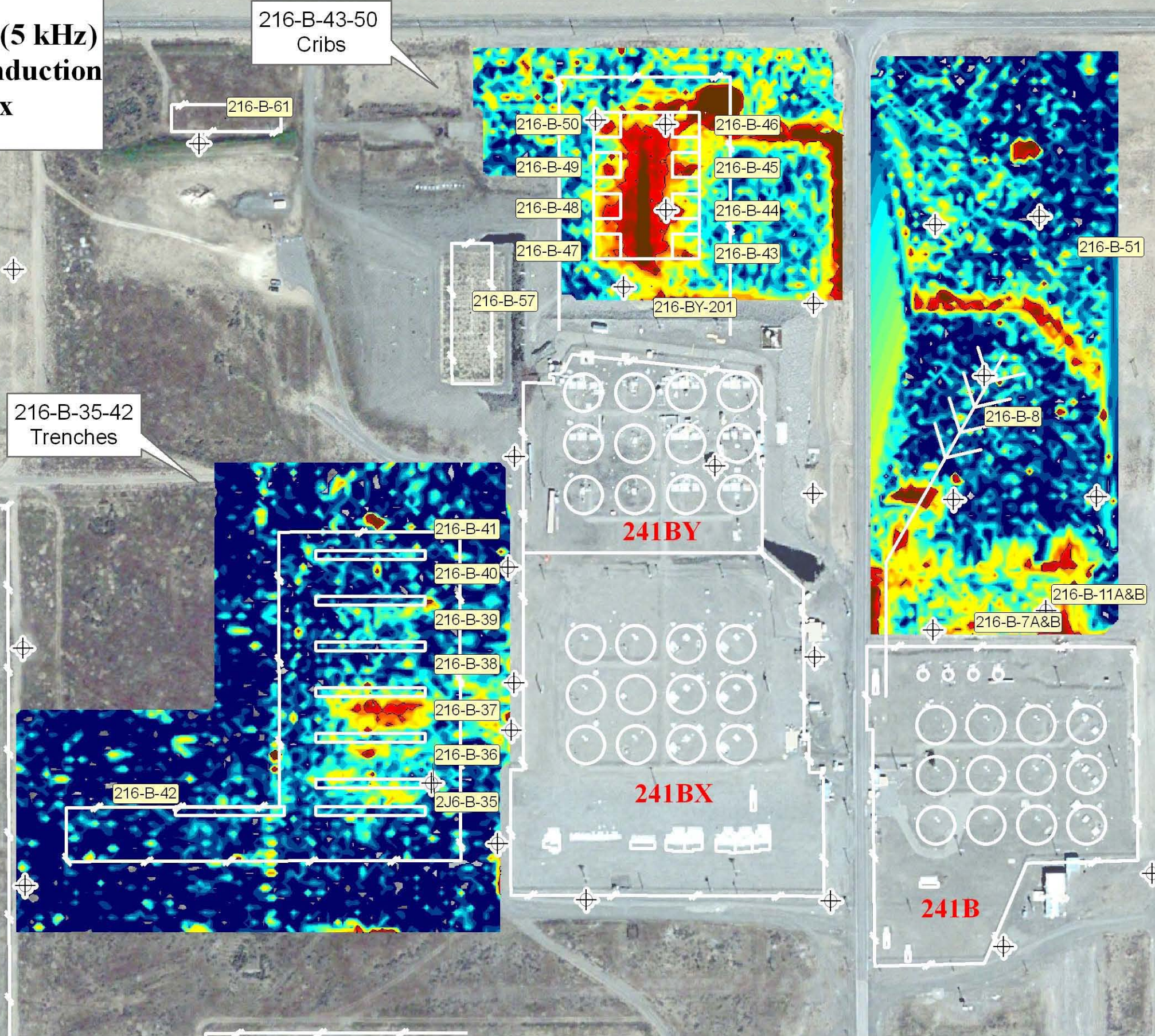


**In-Phase (20kHz) from  
Electromagnetic Induction  
216-B-35-42 Trenches  
B Complex**



A-24

# Electrical Conductivity (5 kHz) from Electromagnetic Induction for the B Complex

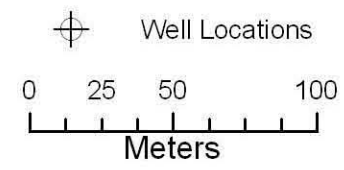
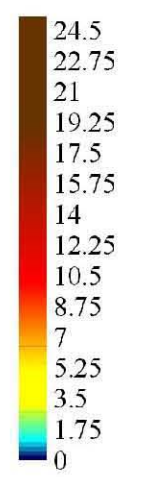


216-B-35-42  
Trenches

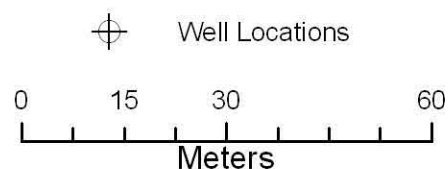
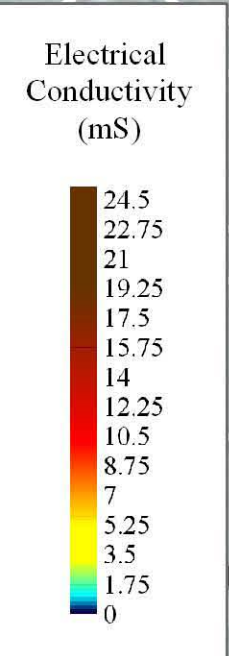
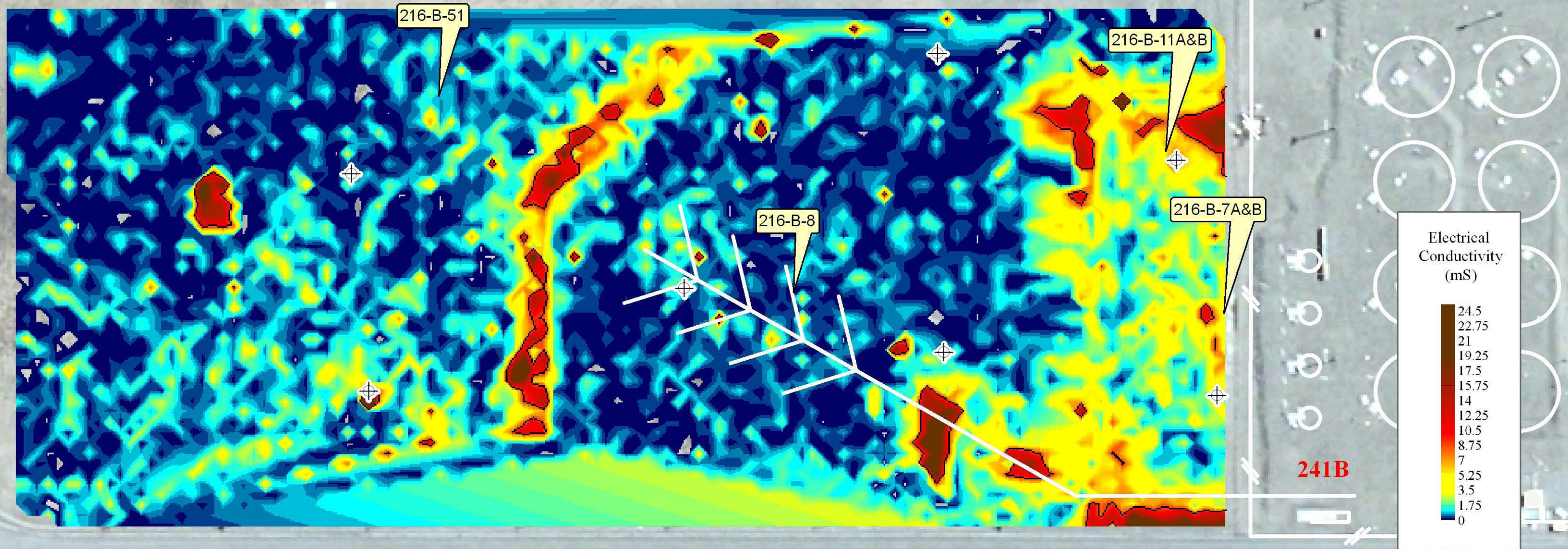
216-B-43-50  
Cribs

216-B-8  
Crib  
(Tile Field)

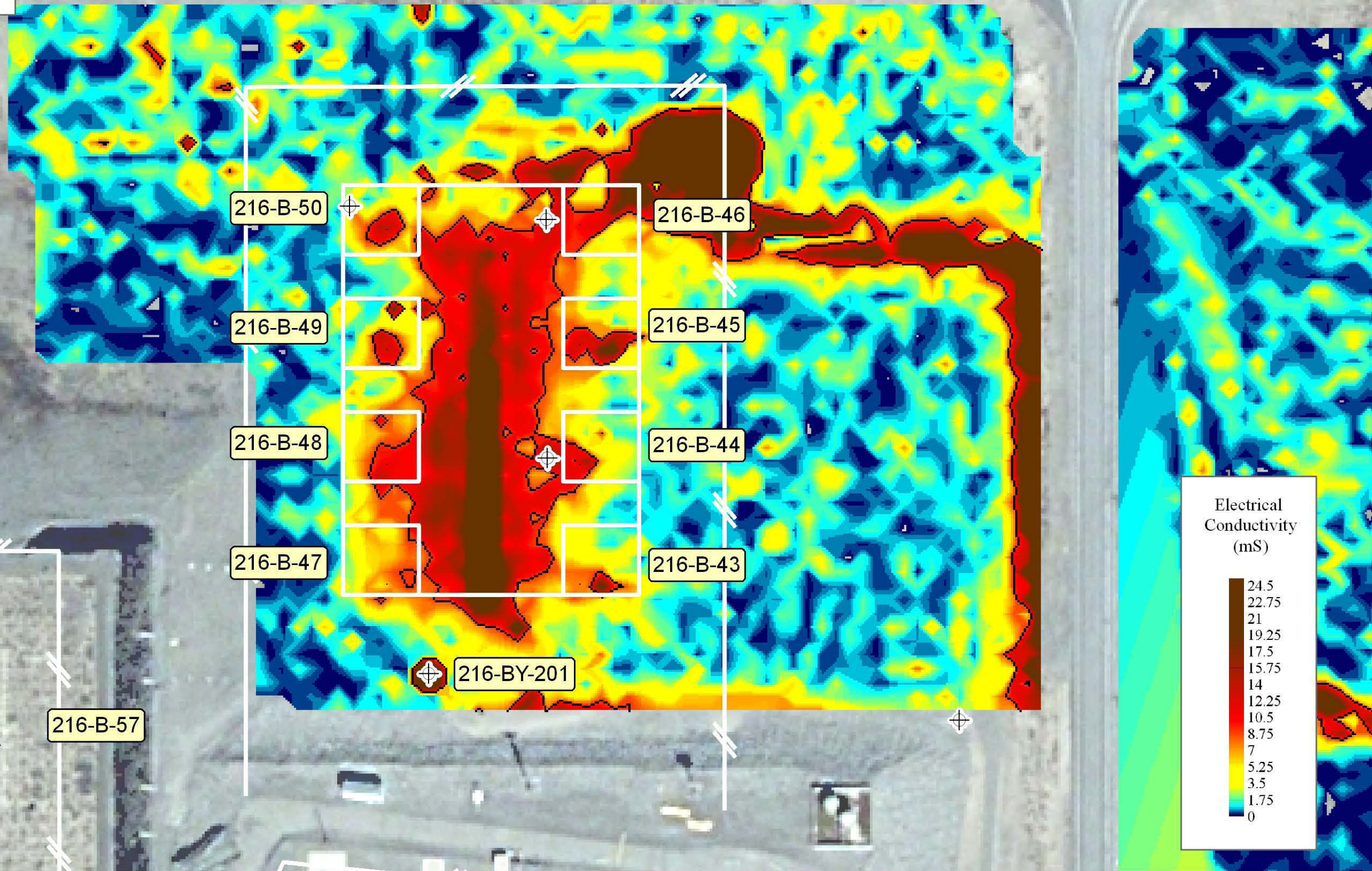
Electrical  
Conductivity  
(mS)



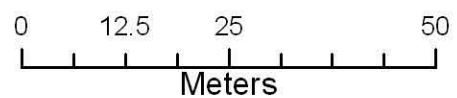
**In-Phase (5kHz) from  
Electromagnetic Induction  
216-B-8 Crib (Tile Field)  
B Complex**



**In-Phase (5kHz) from  
Electromagnetic Induction  
216-B-43-50 Cribs  
B Complex**



⊕ Well Locations

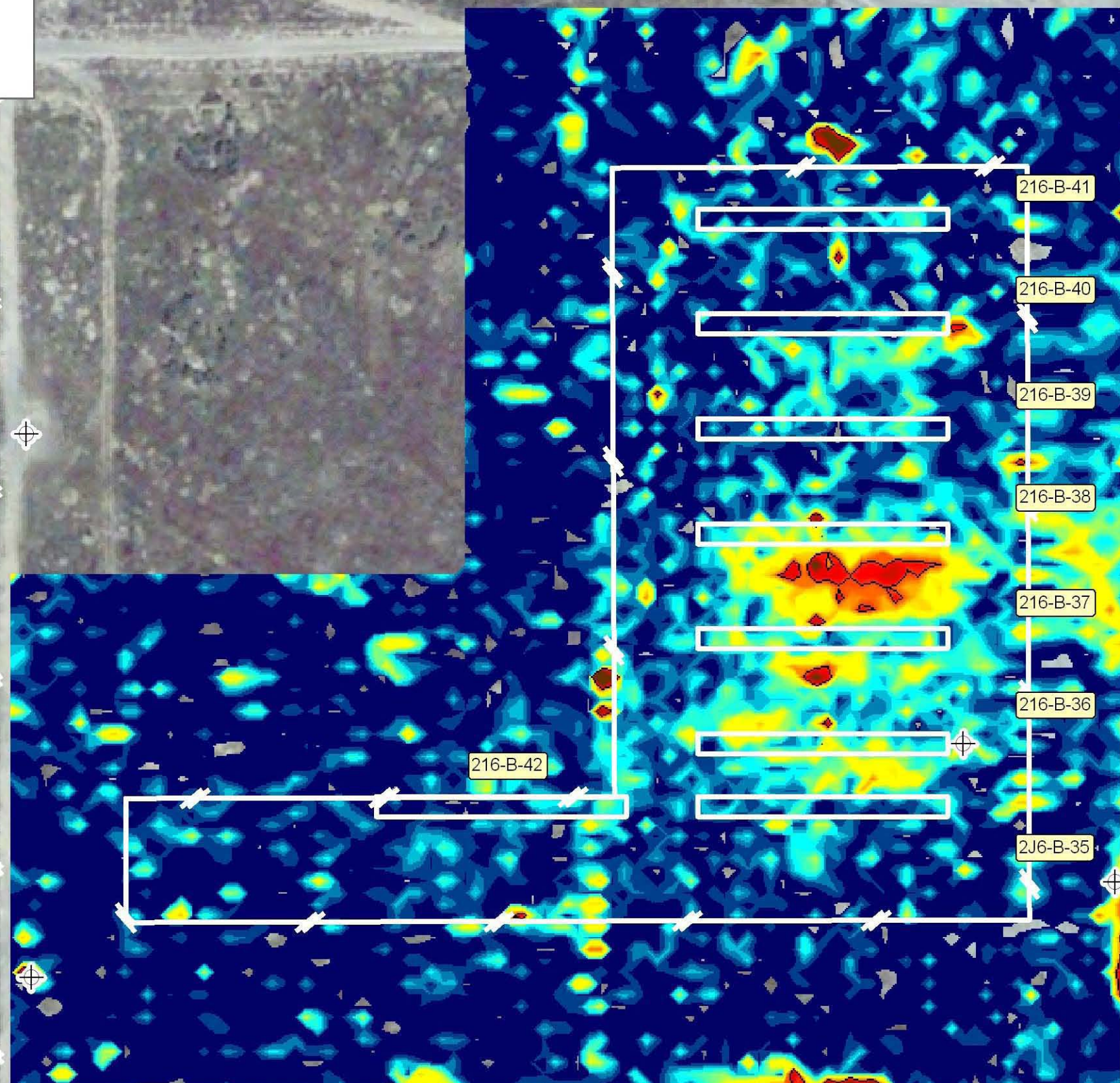


**Geophysical Survey**

Date: February 2007

Figure A-27

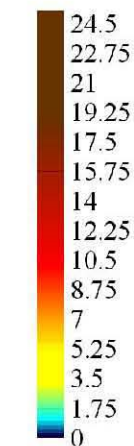
**In-Phase (5kHz) from  
Electromagnetic Induction  
216-B-35-42 Trenches  
B Complex**



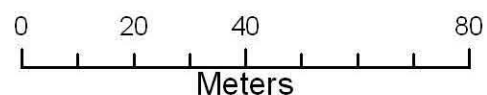
**241BY**

**241BX**

Electrical  
Conductivity  
(mS)



Well Locations



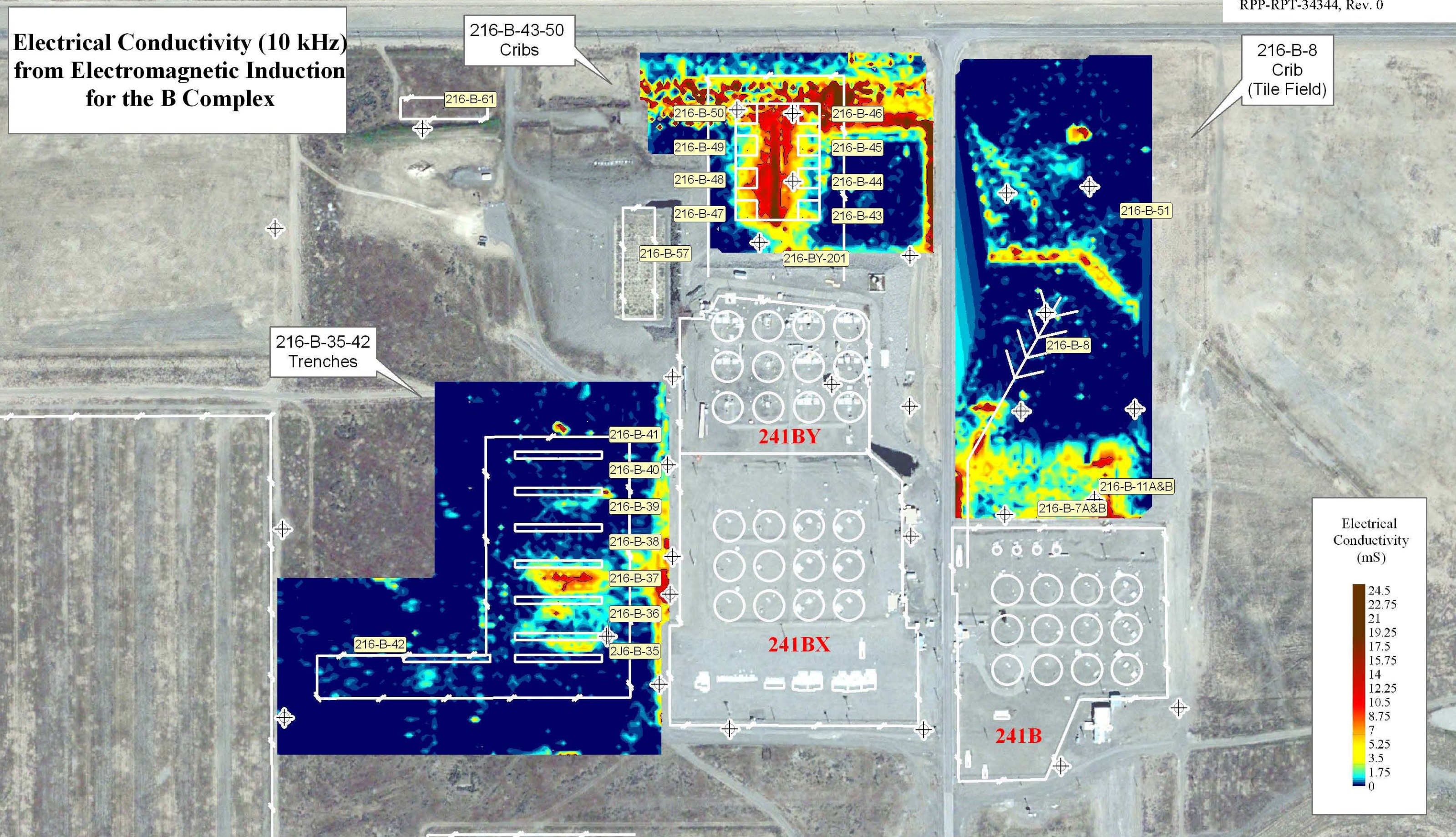
A-28

**Geophysical Survey**

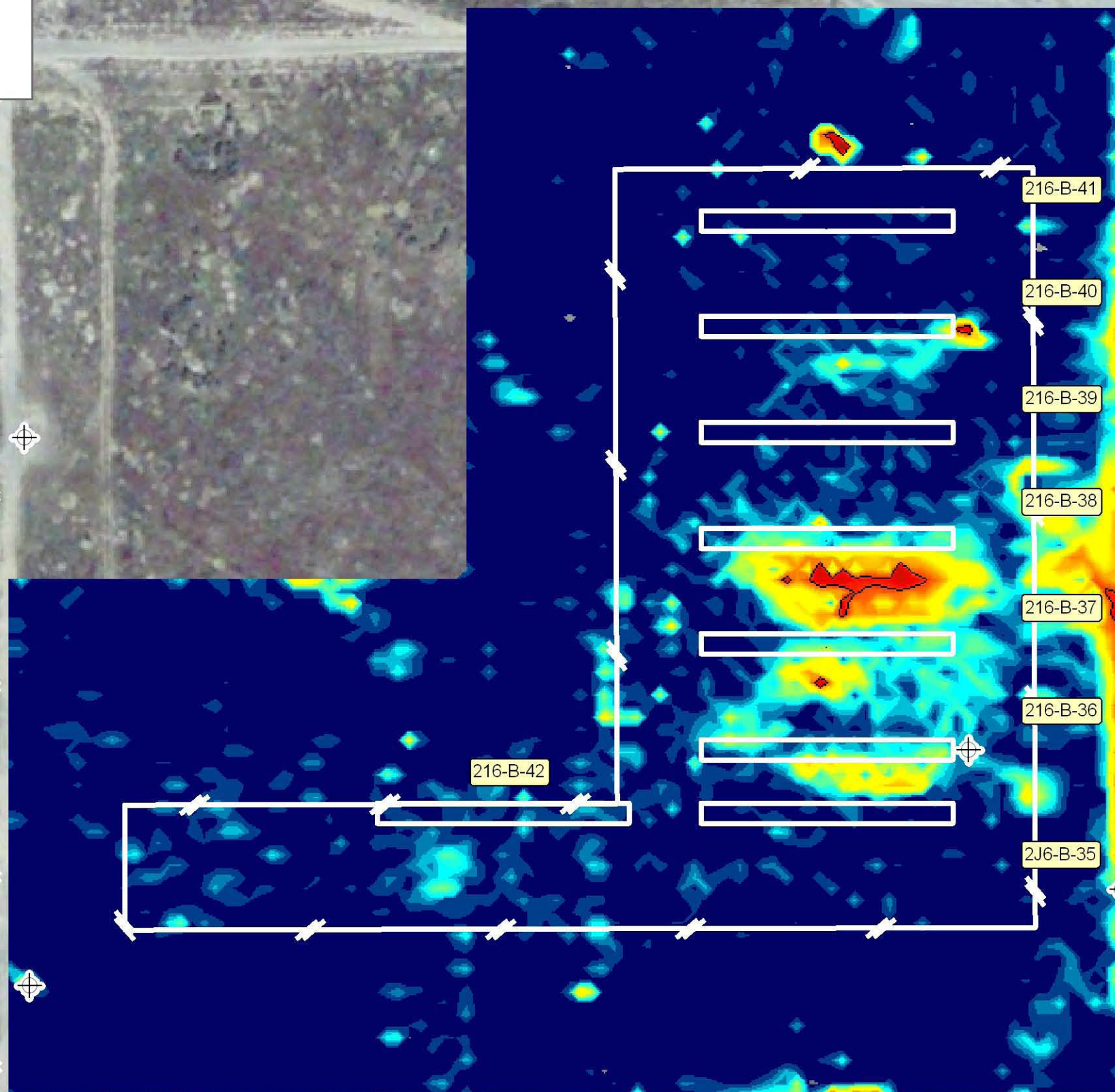
Date: February 2007

Figure A-28

# Electrical Conductivity (10 kHz) from Electromagnetic Induction for the B Complex



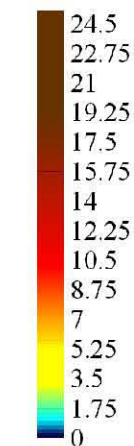
**In-Phase (10kHz) from  
Electromagnetic Induction  
216-B-35-42 Trenches  
B Complex**



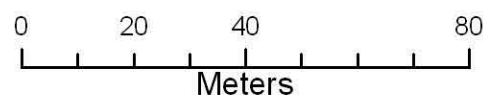
**241BY**

**241BX**

Electrical  
Conductivity  
(mS)



⊕ Well Locations



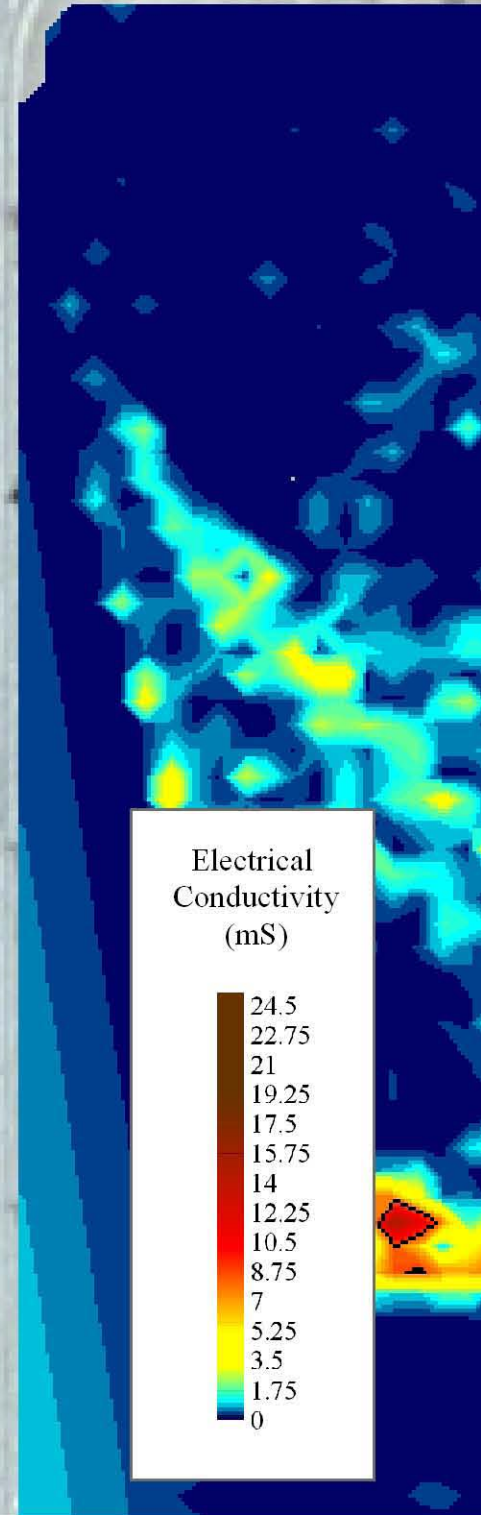
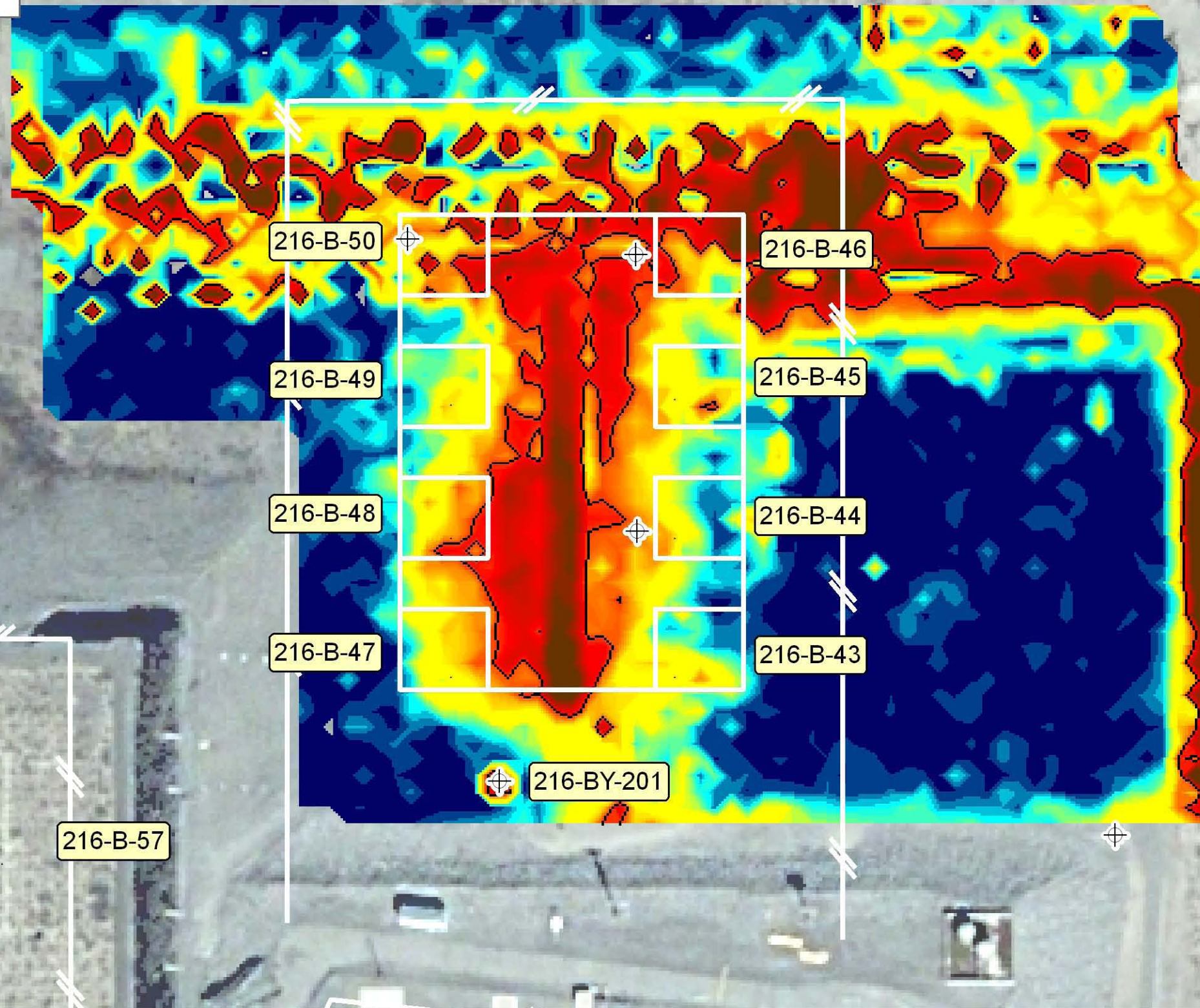
A-30

**Geophysical Survey**

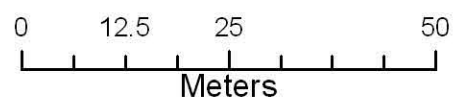
Date: February 2007

Figure A-30

**In-Phase (10kHz) from  
Electromagnetic Induction  
216-B-43-50 Cribs  
B Complex**



⊕ Well Locations

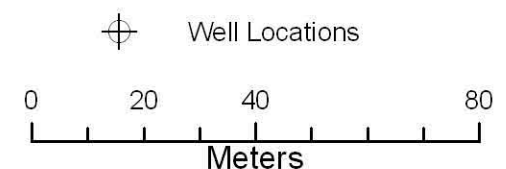
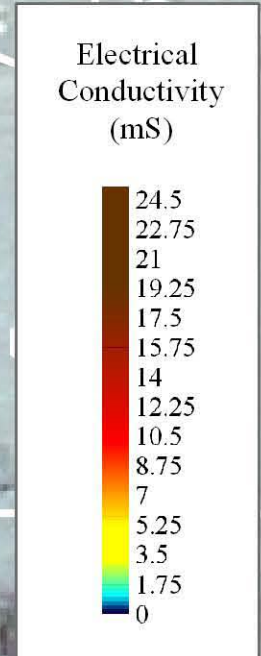
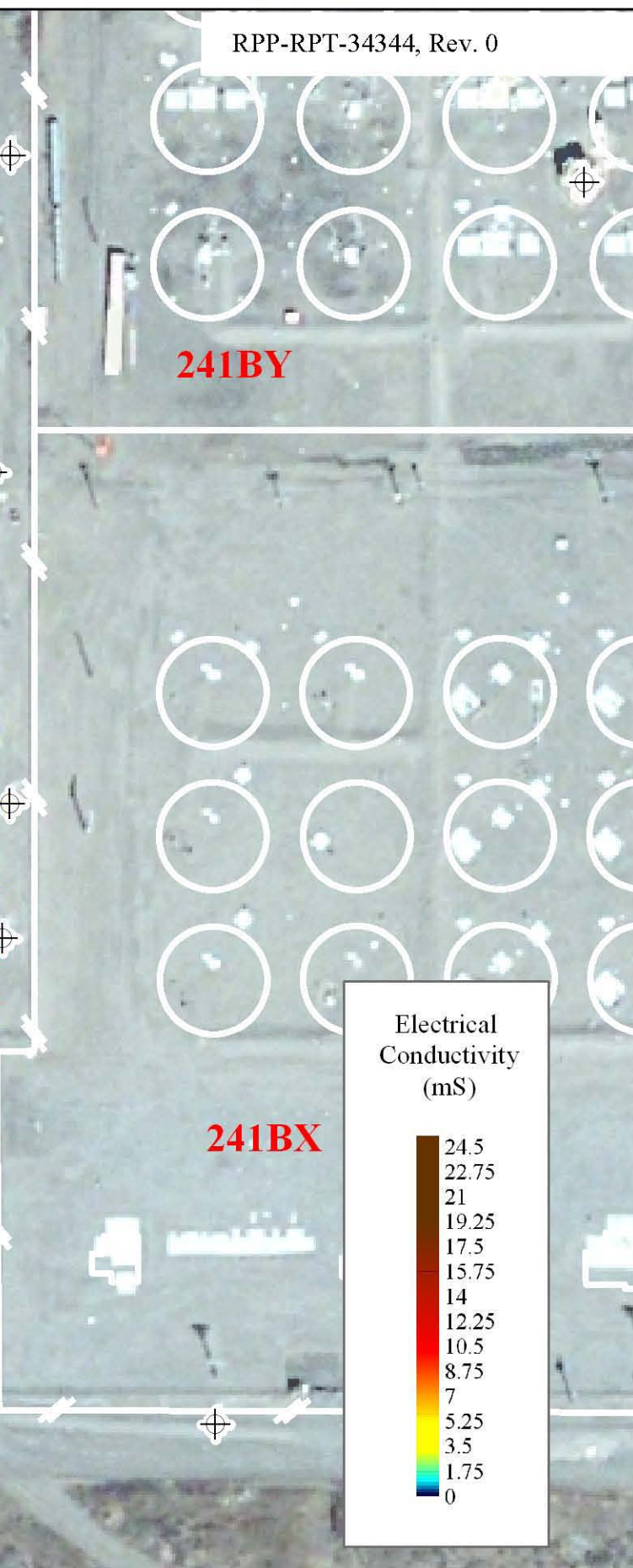
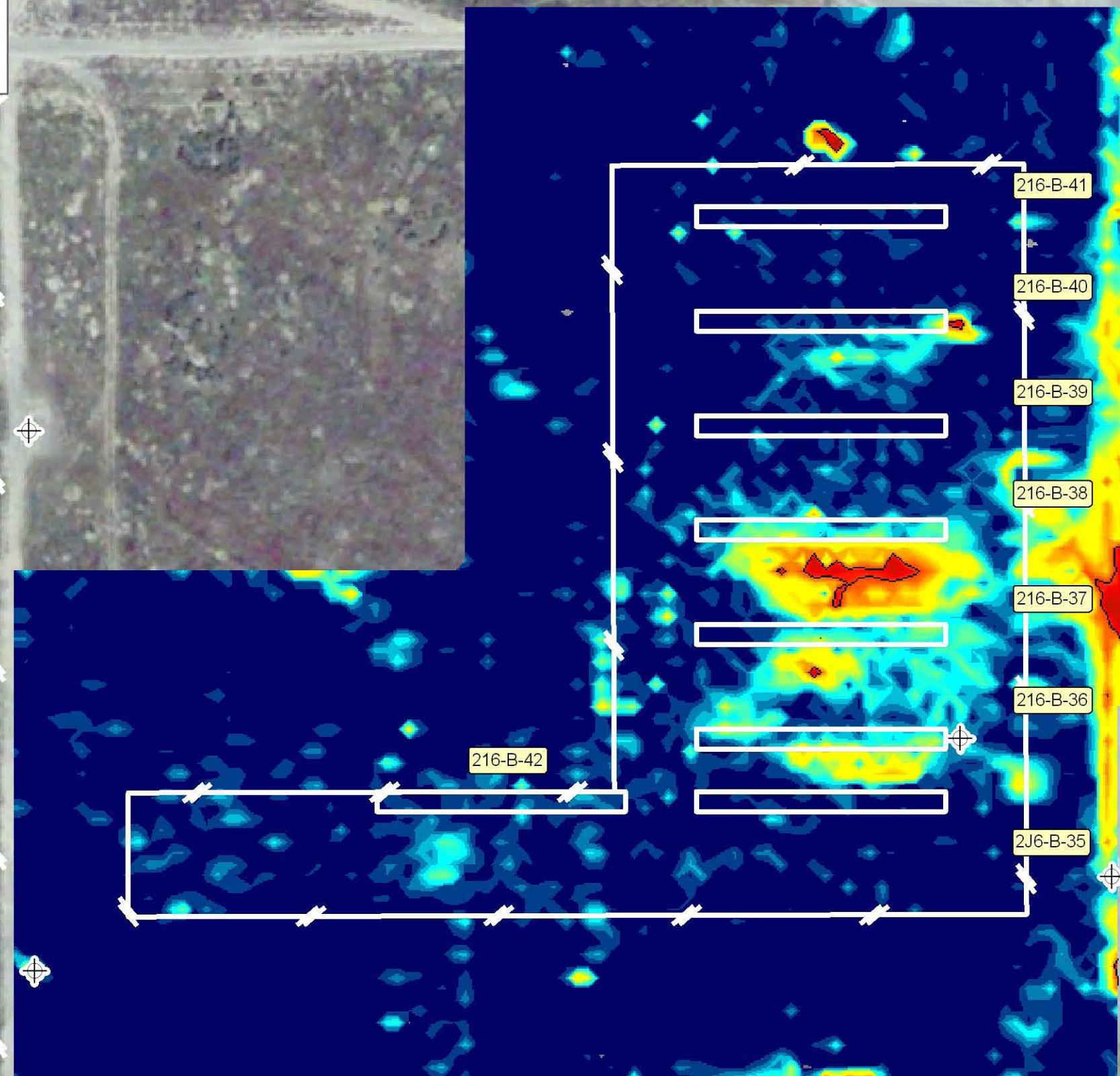


**Geophysical Survey**

Date: February 2007

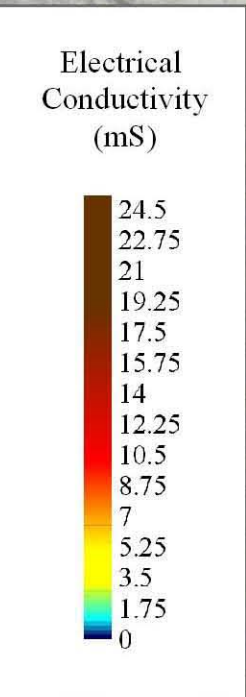
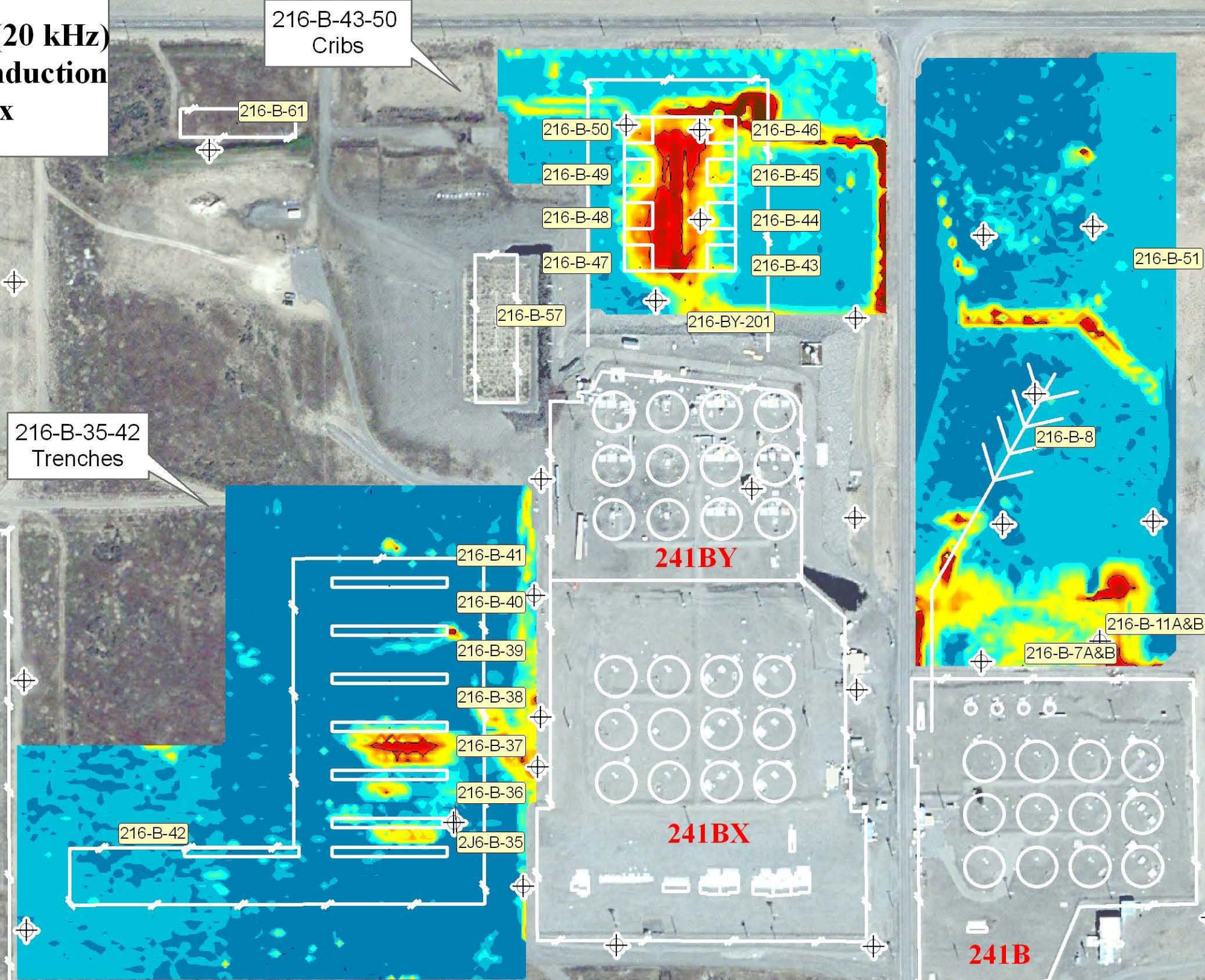
Figure A-31

**In-Phase (10kHz) from  
Electromagnetic Induction  
216-B-35-42 Trenches  
B Complex**



A-32

# Electrical Conductivity (20 kHz) from Electromagnetic Induction for the B Complex



216-B-35-42  
Trenches

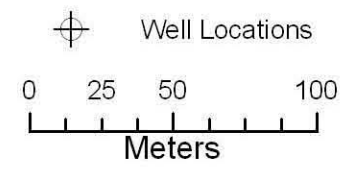
216-B-43-50  
Cribs

216-B-8  
Crib  
(Tile Field)

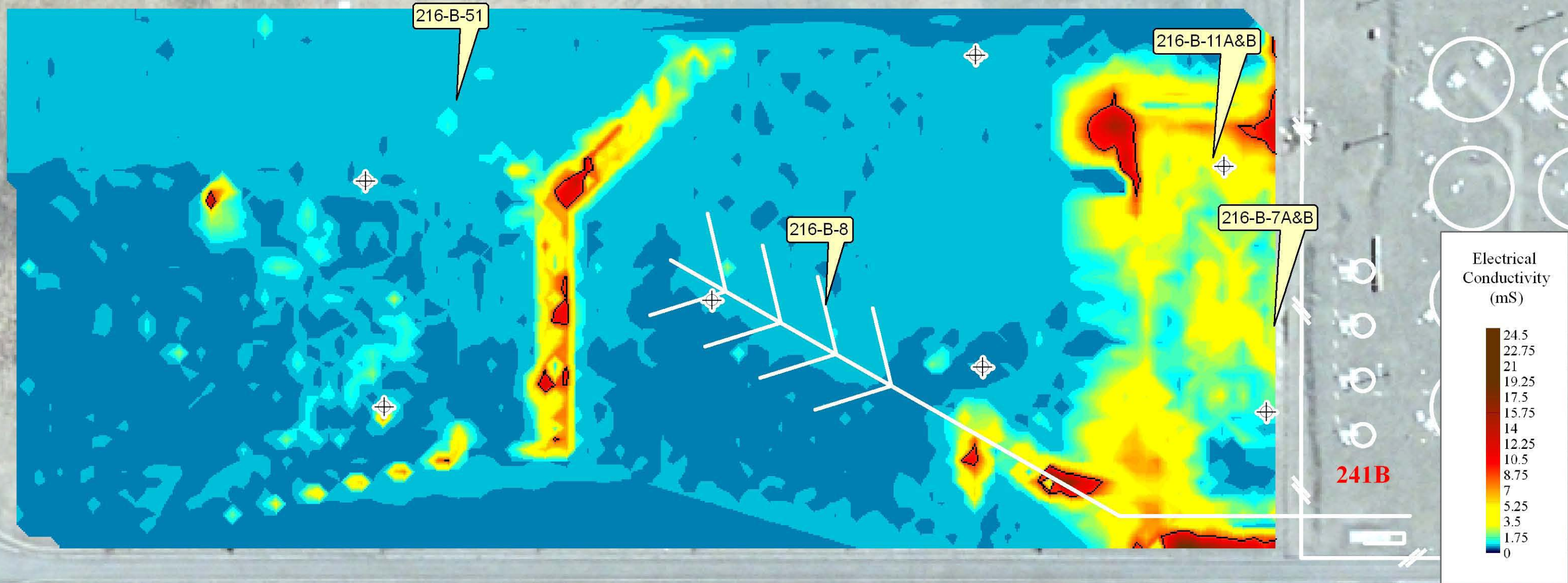
**241BY**

**241BX**

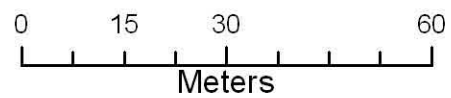
**241B**



**In-Phase (20kHz) from  
Electromagnetic Induction  
216-B-8 Crib (Tile Field)  
B Complex**



⊕ Well Locations

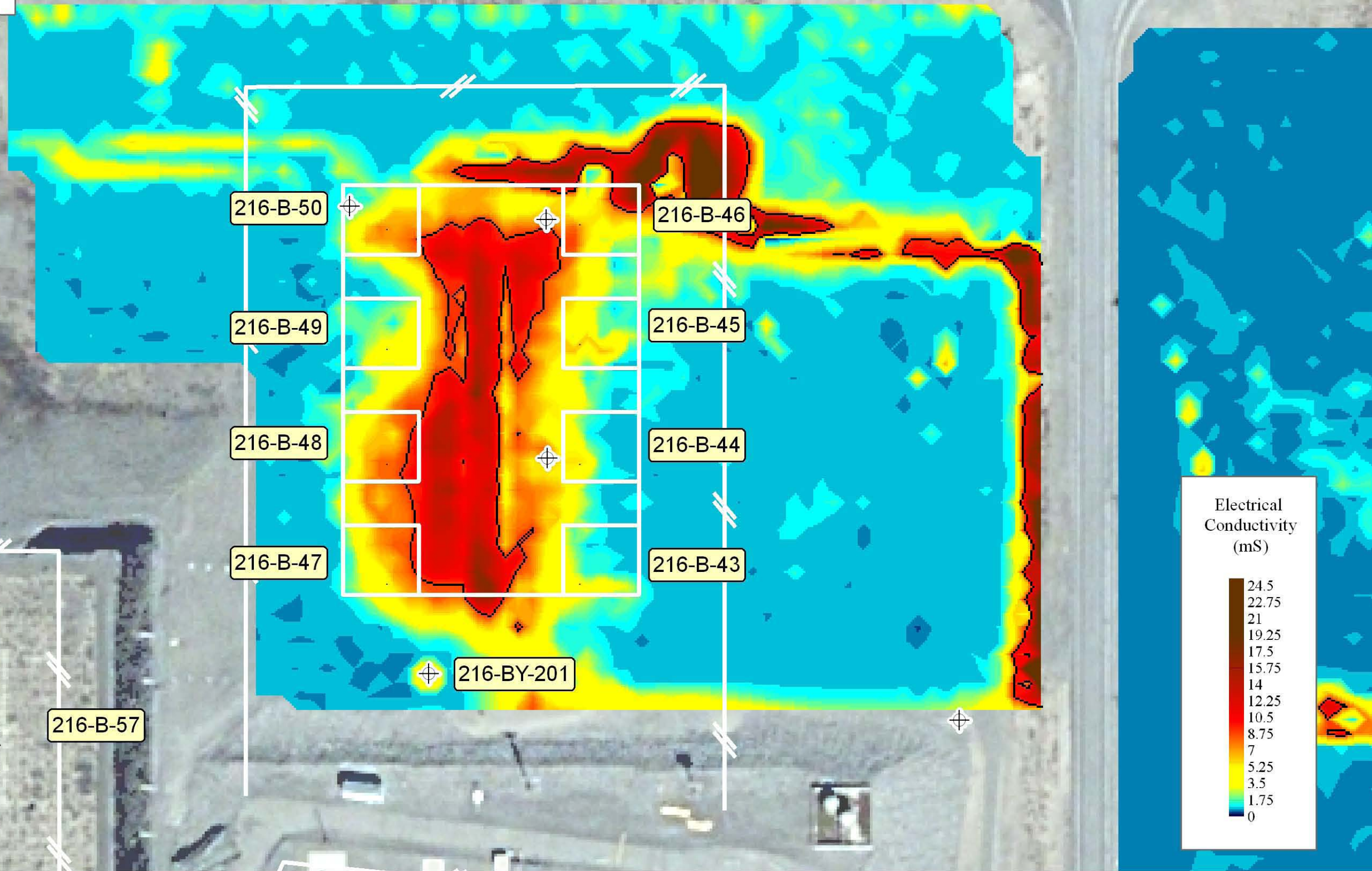


**Geophysical Survey**

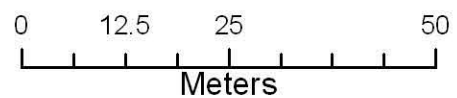
Date: February 2007

Figure A-34

**In-Phase (20kHz) from  
Electromagnetic Induction  
216-B-43-50 Cribs  
B Complex**



⊕ Well Locations



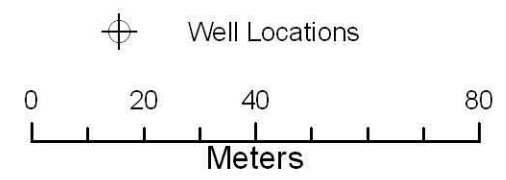
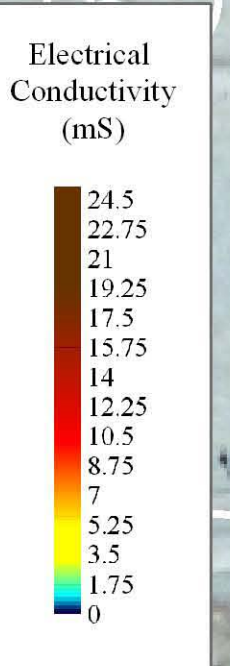
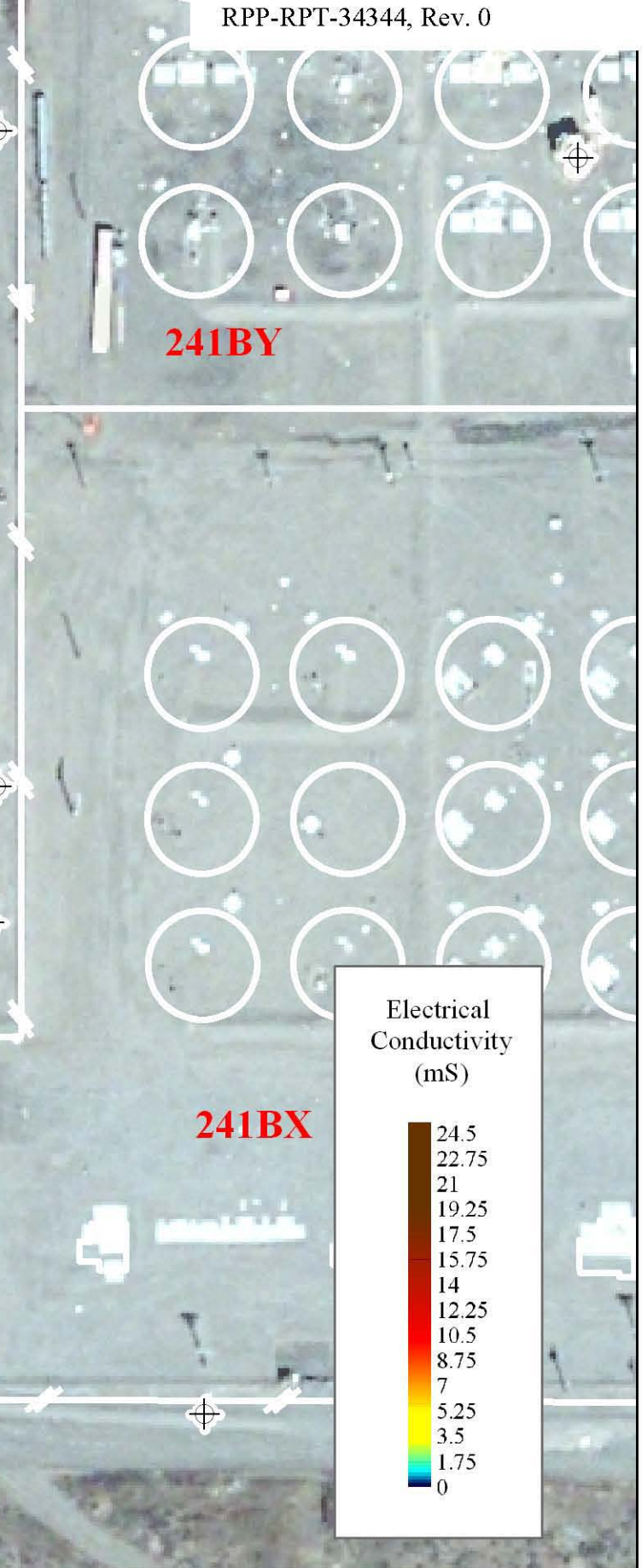
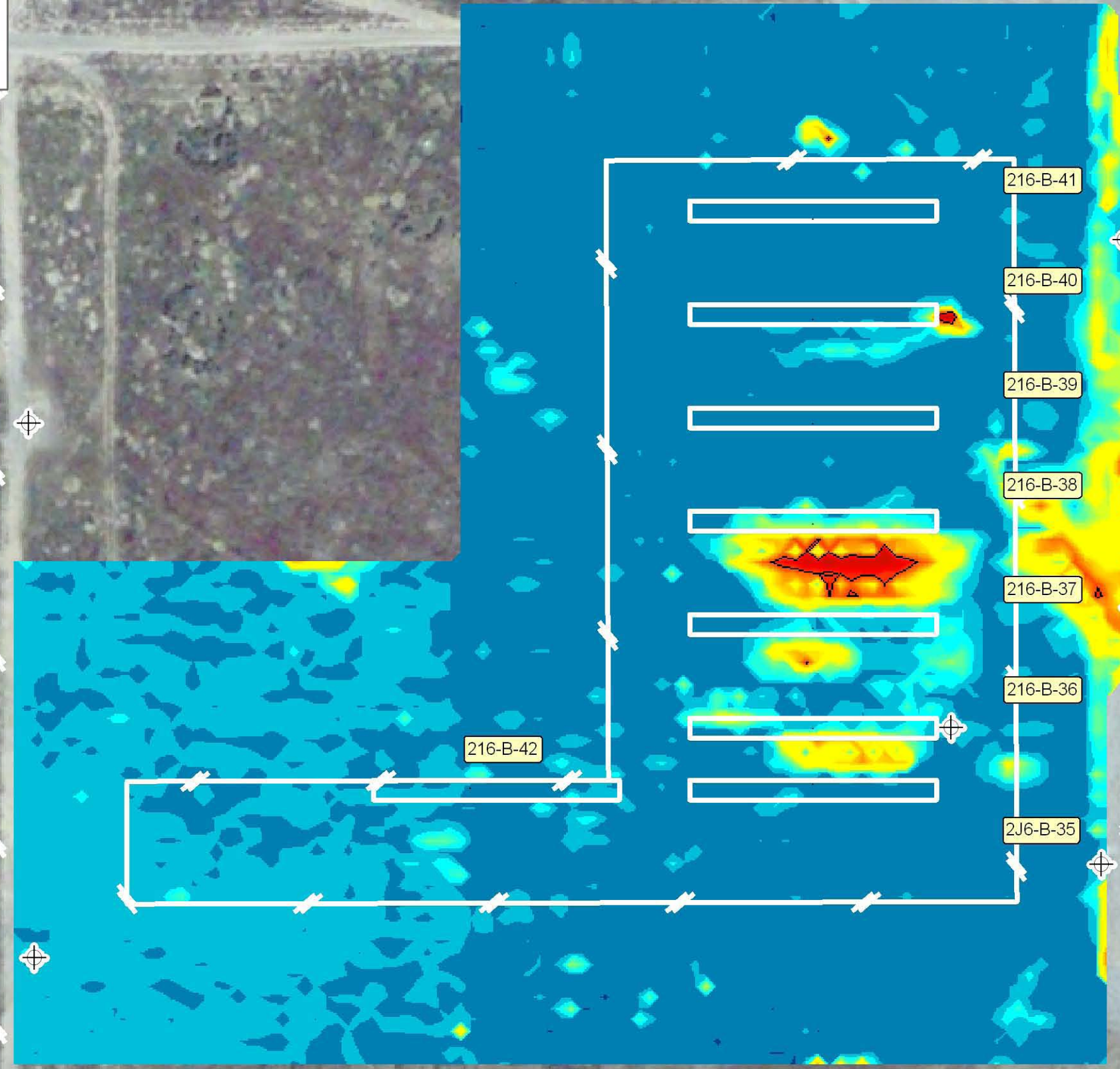
A-35

**Geophysical Survey**

Date: February 2007

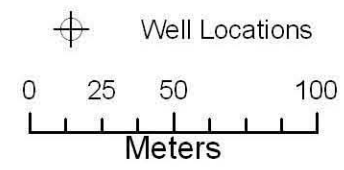
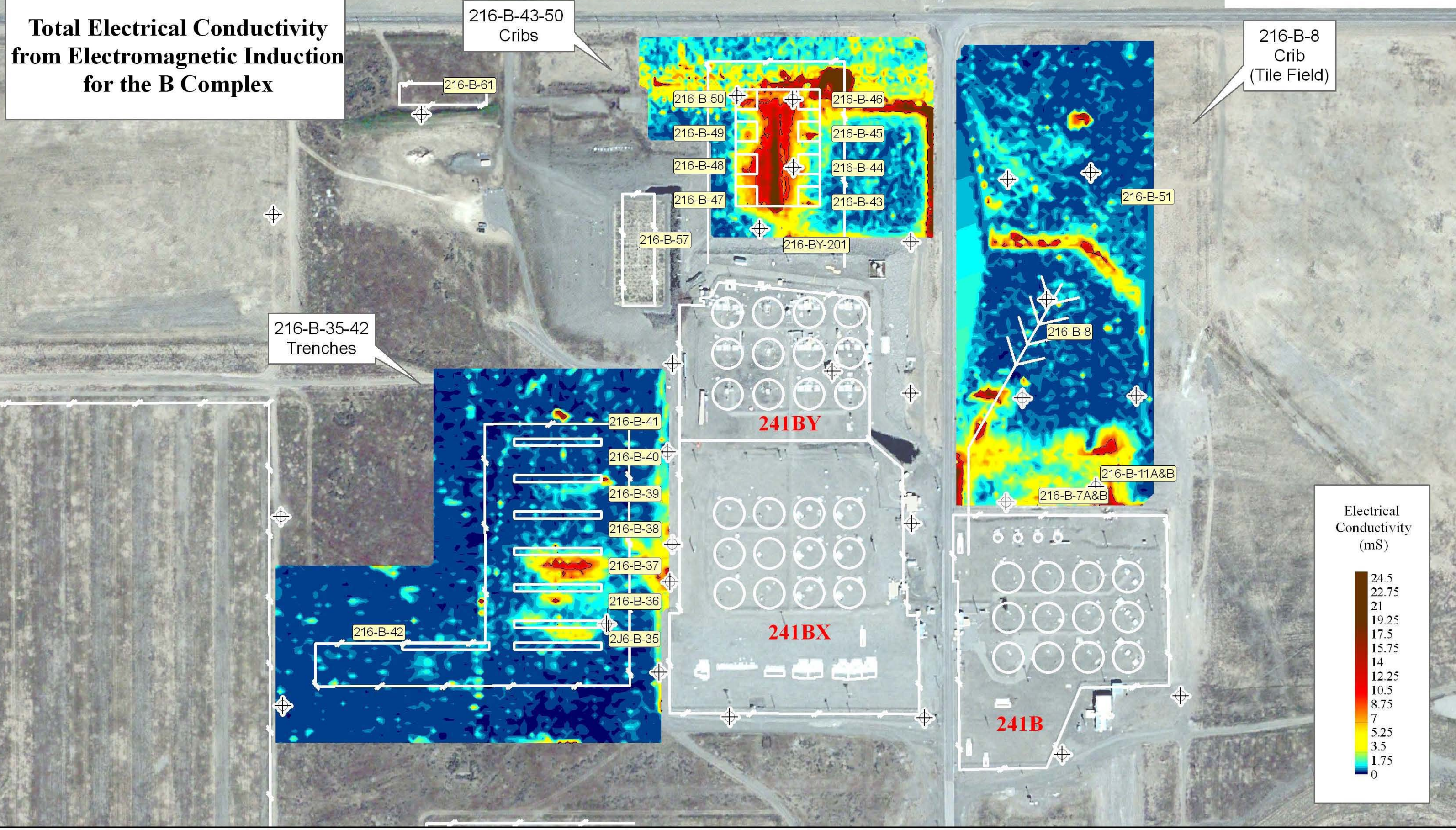
Figure A-35

**In-Phase (20kHz) from  
Electromagnetic Induction  
216-B-35-42 Trenches  
B Complex**

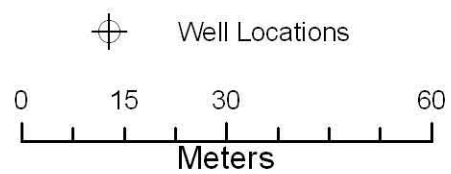
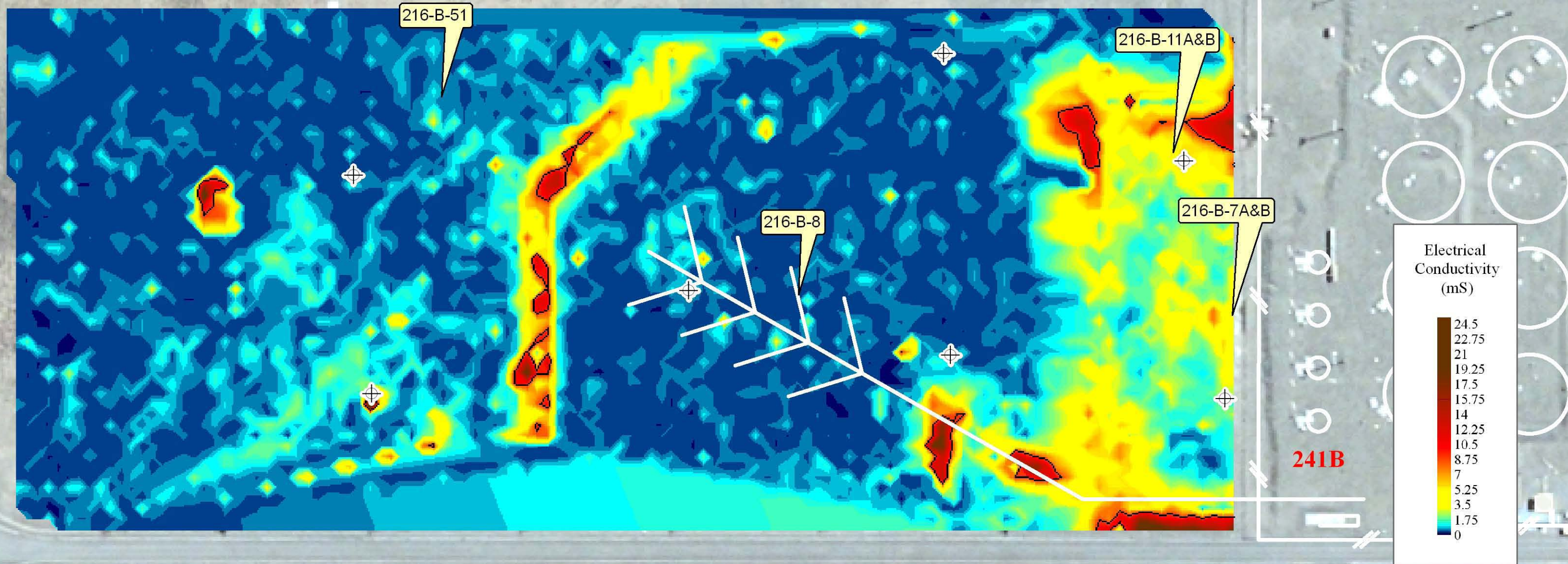


A-36

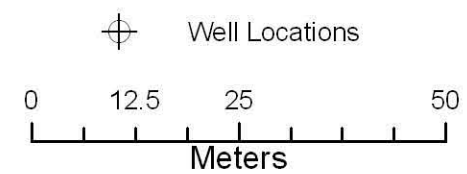
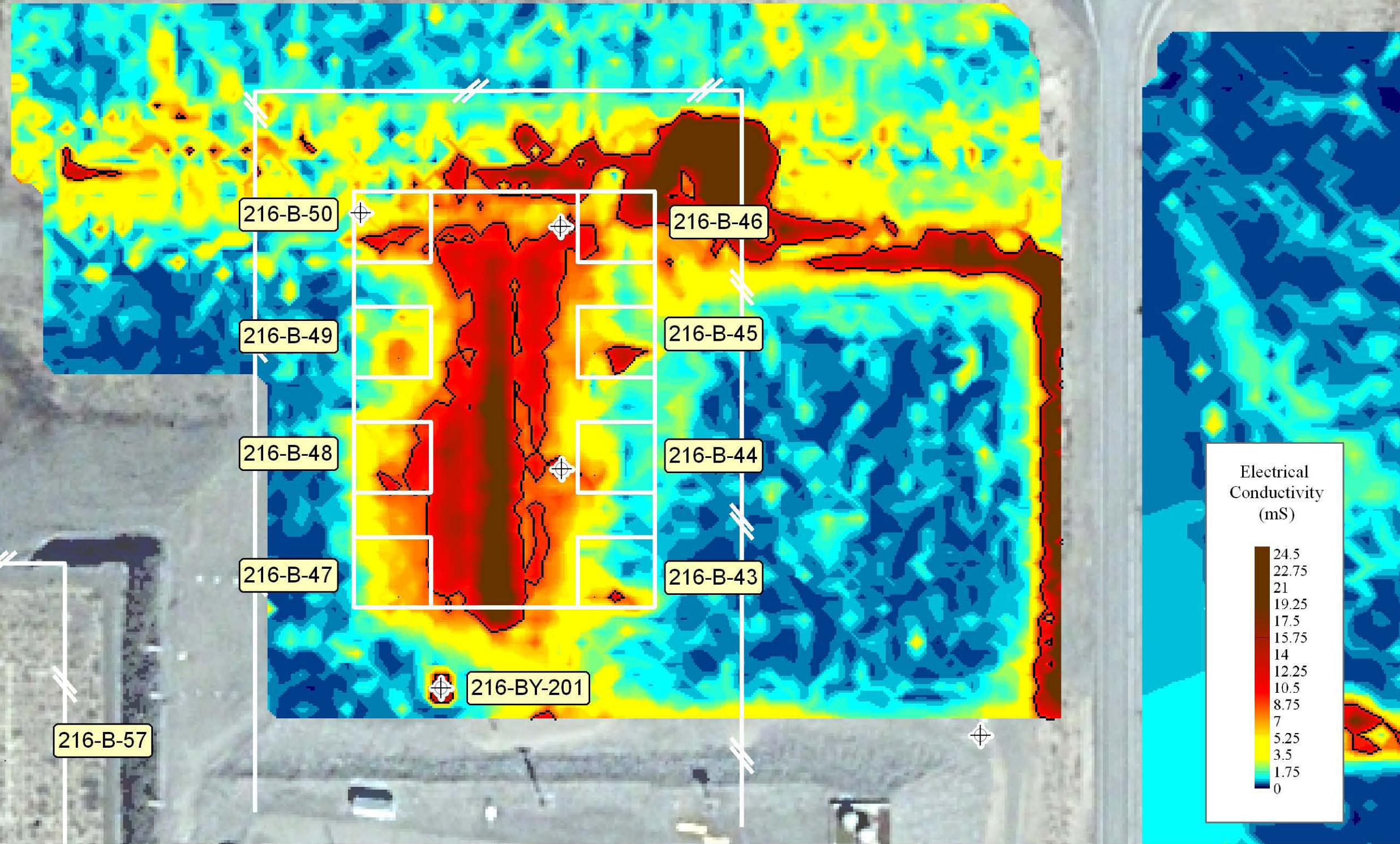
# Total Electrical Conductivity from Electromagnetic Induction for the B Complex



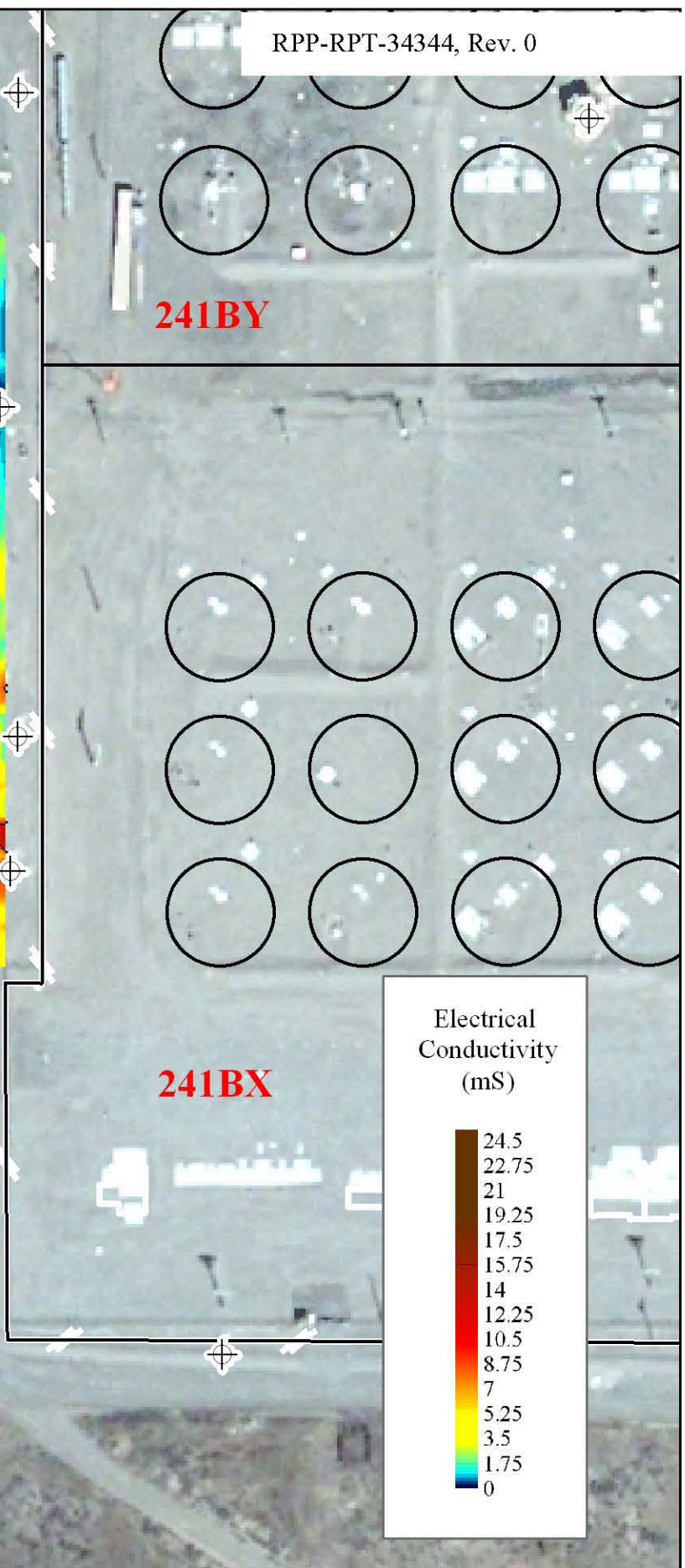
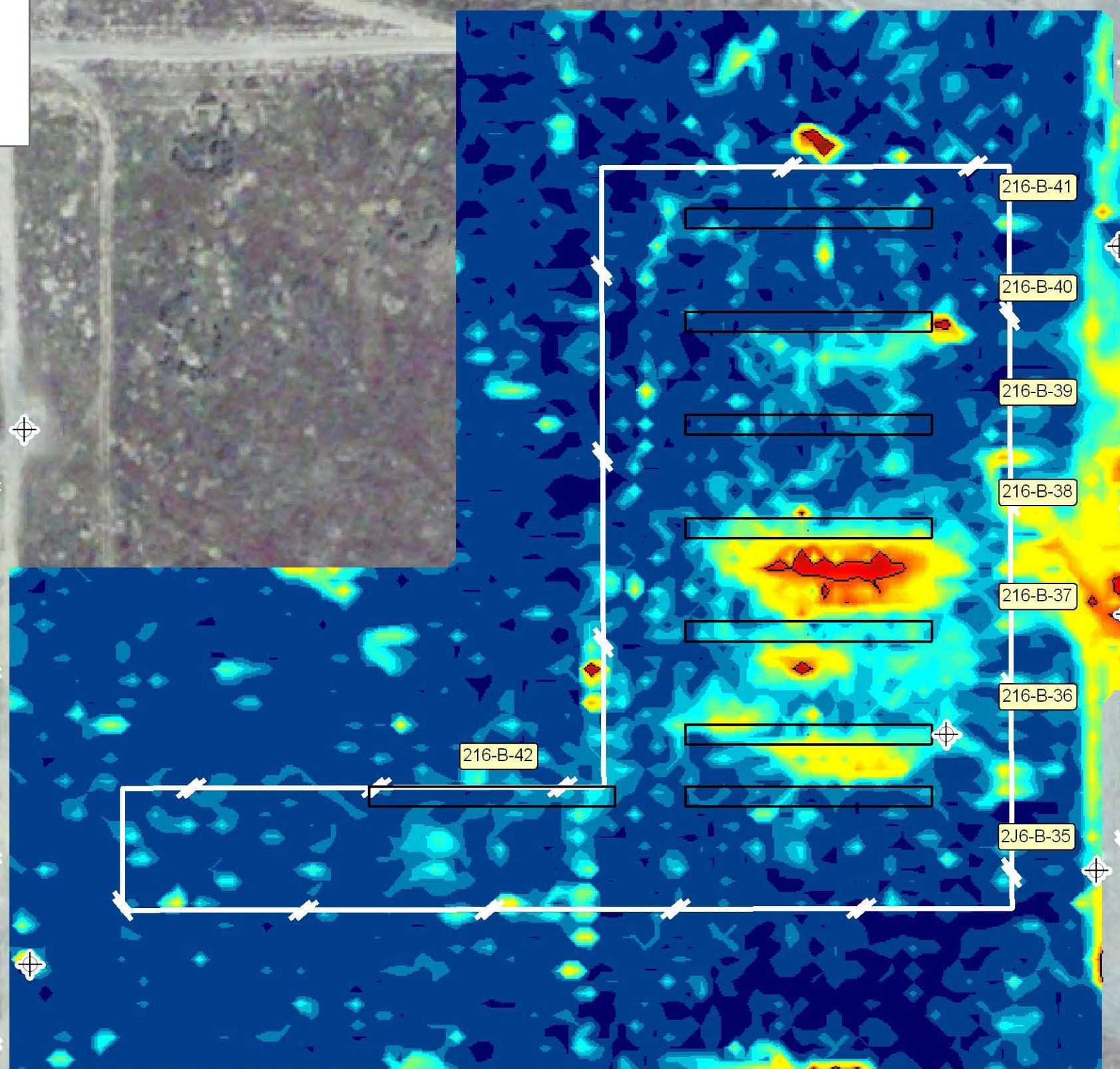
**Total Electrical Conductivity  
Electromagnetic Induction  
216-B-8 Crib (Tile Field)  
B Complex**



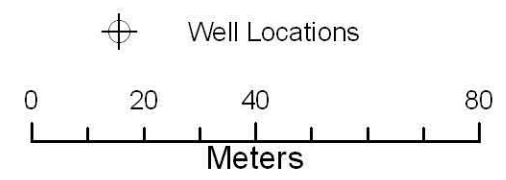
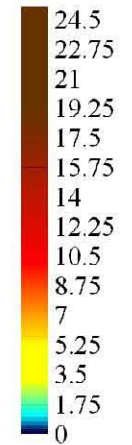
**Total Electrical Conductivity  
Electromagnetic Induction  
216-B-43-50 Cribs  
B Complex**



**Total Electrical Conductivity  
Electromagnetic Induction  
216-B-35-42 Trenches  
B Complex**



Electrical Conductivity (mS)



A-40